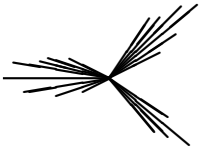

Instituto de Física Teórica
Universidade Estadual Paulista

TESE DE DOUTORAMENTO IFT–T.005/21

Quark and Gluon Distributions within Constituent Quarks and the Pion

Caroline Silva Rocha Costa

Supervisor

Prof. Gastão Inácio Krein

September 2021

Costa, Caroline Silva Rocha.
C837q Quark and gluon distributions within constituent quarks and the pion / Caroline Silva Rocha Costa. – São Paulo, 2021
116 f.: il. color.

Tese (doutorado) – Universidade Estadual Paulista (Unesp), Instituto de Física Teórica (IFT), São Paulo
Orientador: Gastão Inácio Krein

1. Cromodinâmica quântica. 2. Física nuclear. 3. Interações fortes (Física nuclear). I. Título

Sistema de geração automática de fichas catalográficas da Unesp. Biblioteca do Instituto de Física Teórica (IFT), São Paulo. Dados fornecidos pelo autor(a).

Quark and Gluon Distributions within Constituent Quarks and the Pion

Tese de doutorado apresentada ao Instituto de Física Teórica do Câmpus de São Paulo, da Universidade Estadual Paulista "Júlio de Mesquita Filho", como parte dos requisitos para obtenção do título Doutora em Física , especialidade Física Teórica.

Comissão Examinadora:

Prof. Dr. GASTÃO INÁCIO KREIN (Orientador)
Instituto de Física Teórica/UNESP

Prof. Dr. LAURO TOMIO
Instituto de Física Teórica/UNESP

Prof. Dr. TOBIAS FREDERICO
ITA/São José dos Campos - SP

Prof. Dr. KAZUO TSUSHIMA
Universidade Cruzeiro do Sul

Prof. Dr. ADEMIR EUGÊNIO DE SANTANA
Universidade de Brasília

Conceito: Aprovado

São Paulo, 11 de Outubro de 2021.

In memory of my grandmother, Zezé.

Acknowledgements

First and foremost, I would like to express my deep respect and admiration for my adviser, Professor Gastão Krein, both as a person and a scholar. His generous support, patience, and guidance over the years have been essential to my perseverance. I throughout enjoyed each of our individual and group meetings, from which I greatly benefited. These meetings were always full of his contagious enthusiasm and his great sense of humor. I never told him this, but at times when I felt discouraged by setbacks in the project, I would visit his office, and because of his enthusiasm I would always leave feeling motivated and with a renewed sense of purpose. I am continually amazed by his wisdom, and I am profoundly grateful for the opportunity to be his student and learn from him.

I would also like to express my gratitude to Ian Cloët for hosting me at Argonne National Lab and for his unwavering support throughout my stay. This work would not have been possible without his guidance. Ian is one of the kindest people I have ever met, making my time at Argonne an incredibly rewarding experience. I am deeply grateful to him for making this opportunity possible and for everything he taught me along the way

I would like also to thank Bruno El-Bennich for his constant support, encouragement, and the many insightful discussions we shared. His presence over the years has been invaluable.

I would also like to thank a lot Adam Freese for his patience, support and availability for answering "just one question". I learned a great deal from him, and his friendship,

along with our collaboration, was an unexpected but very welcome surprise during my time at Argonne.

I would also like to acknowledge my many friends from the Institute. I was incredibly lucky to share daily life with so many of you. First, I want to thank Fernando and Enzo, my very first friends at IFT. We not only shared our friendship but also our research, and each of you supported me in your own unique way. Vivian joined later, but she is equally part of this journey. It was wonderful having you all around. I am grateful to my dear friends Carlisson, Segundo, Carlitos, Victor César, José Luís, Gabriel, Johan, Vilson, Heliudsson, Jéssica, Ana Mizher, Daniel Wagner, Matheus Lise, Lucas Martins, Gabriel Lobo, Jogean, Derick, Ana, Nathaly, Dean, and Dennis for the countless moments we shared both in and out of the Institute. I hope I have not forgotten anyone, but you all know who you are. Of course I have also to acknowledge my amazing "aggregated" friends Rosane, Ivanita and Luiza. How life would have been without you? I also want to thank Dona Jô, not just for the daily bottle of coffees that kept me going through my PhD, but for her kindness, the conversations, and the laughs we shared. The same goes for my dear Sueli.

A special thank you to my roommate and lifelong friend, Camila Sugai, for her unwavering support, for welcoming me into her home, and for all the special moments we shared in daily life.

I must also express my deepest gratitude to my love, Max Guillen, for everything he means to me. No words will ever be enough to express my love and gratitude. His endless support, encouragement, and inspiration, both in physics and in life, have been beyond anything I could ask for. Sharing the wonders of the Universe with him has been an incredible experience.

Most importantly, I want to thank my entire family: my father, whose kindness and

love leave me speechless; my stepmother, Michele, for being a true friend and constant support; my little brother, Lorenzo, for bringing light into the darkest times; and my mom and all my siblings, Waltinho, Naty, Vitorinha, and Gabizinha—I love you all so much. Being close to you during the difficult pandemic period was incredibly important. Last, but certainly not least, my grandmother: It's all because of you.

This study was financed in part by the Coordenação de Aperfeiçoamento de Pessoal de Nível Superior – Brasil (CAPES) – Finance Code 001.

Abstract

The central goal of this thesis is to formulate a model that allows to include gluonic effects in parton distribution functions (PDFs) of constituent quarks and the pion. To this end, we construct a quark target model (QTM) to incorporate intrinsic glue into effective low-energy models of QCD, which often contain only quark degrees of freedom. This method guarantees the gauge invariance of observables order-by-order in the strong coupling. The quark and gluon PDFs for the constituent quarks are obtained in the QTM at leading order. The gauge invariance of the results is demonstrated by comparing both covariant and light cone gauges, with the former including an explicit Wilson line contribution that must be present in covariant PDF calculation. A key finding is that in covariant gauges the Wilson line can carry a significant amount of the light cone momentum. With coupling strength $\alpha_s = 0.5$ and dressed quark mass $M_q = 0.4\,\mathrm{GeV}$, we find quark and gluon momentum fractions of $\langle x \rangle_q = 0.81$ and $\langle x \rangle_g = 0.19$, where the Wilson line contribution to the quark momentum fraction is -0.18. We use the on-shell renormalization scheme and find that at one-loop this Wilson line contribution does not depend on the covariant gauge but does vanish in light cone gauge as expected. This result demonstrates that it is crucial to account for Wilson line contributions when calculating quantum correlation functions in covariant gauges. We also consider the impact of a gluon mass using the gauge invariant formalism proposed by Cornwall, and combine these QTM results with two quark-level models to obtain quark and gluon PDFs for the pion.

Key words: Quantum Chromodynamics; Parton Distributions; Wilson Lines; Low-Energy Effective Models

Areas: Particles and Fields, Nuclear Physics

Resumo

O objetivo central desta tese é formular um modelo que permita incorporar efeitos gluônicos em funções de distribuição de partons (PDFs) de quarks constituintes e pions. Para este fim, construímos um modelo que consiste de um quark como alvo (QTM) para incorporar glúons de maneira intrínseca a modelos de baixas energias da QCD, que geralmente contem apenas graus de liberdade de quark. Este método garante a invariância de calibre dos observáveis ordem a ordem na constante de acoplamento forte. As funções de distribuição de partons (FDP) do quark e do glúon no quark constituinte são obtidas no QTM em primeira ordem no acoplamento forte. A invariância por calibre dos resultados é demonstrada comparando ambos os resultados no calibre covariante e cone de luz, com o primeiro incluindo explicitamente a contribuição da Linha de Wilson que deve estar presente em cálculo de FDPs em calibres covariantes. Uma descoberta chave é que em calibres covariantes, a linha de Wilson pode carregar uma quantidade significativa de momento do cone de luz. Com a força de acoplamento $\alpha_s = 0.5$ e massa do quark constituinte $M_q = 0.4$ GeV, encontramos frações de momento do quark e do glúon de $\langle x \rangle_q = 0.81$ e $\langle x \rangle_g = 0.19$, onde a contribuição da linha de Wilson para a fração do momento carregado pelo quark é -0.18. Usamos o esquema de renormalização on-shell e descobrimos que em a um loop esta contribuição da linha de Wilson não depende do calibre covariante, mas desaparece, como esperado, no calibre do cone de luz. Este resultado demonstra que é crucial considerar as contribuições da linha de Wilson ao calcular funções de correlação quânticas em calibres covariantes. Também consideramos o impacto de uma massa de glúon usando o formalismo proposto por Cornwall que é invariante por calibre, e combinamos esses resultados MAQ com dois modelos de apenas quarks para obter FDPs do quark e glúon para o píon.

Palavras-chave: Cromodinâmica Quântica; Função de Distribuição de Partons; Linhas de Wilson; Modelos Efetivos;

Areas: Partículas e Campos, Física Nuclear

Contents

List of Figures

List of Tables

Chapter 1

Introduction

The development of a deep understanding of the rich and complex structure of Quantum Chromodynamics has been a long standing goal of the particle physics community. Although QCD is universally accepted to be the correct theory describing the strong force that binds quarks and gluons within hadrons, many problems are still to be addressed and resolved. In particular, unraveling the structure of hadrons in terms of the quarks and gluons is one of the most pressing contemporary issues in hadronic physics. After all, quarks are the building blocks of protons and neutrons (nucleons), which are the main components of atomic nuclei that make up most of the visible matter in the Universe. Quarks come in six flavors: up (u), down (d), strange (s), charm (c), bottom (b) and top (t). The u and d define the minimum quark content of the protons and neutrons, namely uud and ddu respectively; they are generated by the Higgs mechanism and their values are $m_u \approx m_d \sim 5$ MeV. They account to only 2% of the nucleon mass, $M_N \sim 1$ GeV. The gross of the nucleon mass is generated by the nonperturbative dynamics of quarks and gluons through the mechanism of dynamical chiral symmetry breaking (DCSB). This emergent phenomenon is associated with the QCD light-flavor sector (the quarks u and d, and to some extend the s quark), and

confers an effective mass to the quarks, $M_u \approx M_d \sim 300$ MeV. The DCSB generated massive quarks are known as "constituent quarks", or "dressed quarks", whereas those light quarks with Higgs generated masses are known as current quarks.

Although the existence of the quarks and gluons has been revealed through Deep Inelastic Scattering (DIS) experiments and electron-positron collisions [3, 4], quarks and gluons have never been observed in isolation in nature—they are permanently confined within hadrons and are only observed forming color-neutral bound states. Understanding this intriguing empirical finding, the so-called *confinement*, is a long-standing challenge, even though the formulation of QCD dates back to the 1970s. From the theoretical side, one perspective of confinement which has attracted considerable attention is that its realization in a physical theory would be related to dramatic changes in the QCD two-point and three-point correlation functions [5]—for a list of references, see Ref. [6]. In a nonconfining theory, a physical particle has a pole on the real axis at timelike momenta and the position of the pole is identified to be the physical mass. In a confining theory, however, the picture can get substantially more cumbersome with possible presence of complex mass poles and branch cuts in the propagators and vertex, besides positivity violation of the spectral functions [7–12]. Both confinement and DCSB are low-energy emergent phenomena, which render it difficult to tackle. Understanding such peculiar features from QCD first principles remains challenging.

At the high-energy domain, the coupling strength becomes small owing to asymptotic freedom of QCD [13, 14], and physical processes can be well described using perturbative methods based on an expansion of the coupling constant. This means that quantitative predictions can be made for hard scattering cross sections in hadronic interactions, for example. However, at low-energies, the coupling becomes large and one reaches the regime of QCD in which these aforementioned distinct features of the theory kick in, where the use of perturbation theory is no longer possible. Therefore, one can identify two regimes in QCD: a perturbative one for which there are precise

and systematic analytical methods to describe observables, and which can be accessed, tested, and explored through high energy collisions at high squared momentum transfer Q^2, and a nonperturbative for which there is no systematic perturbative approach based on the coupling constant of the theory.

The primary theoretical tool that has been used for studying nonperturbative QCD phenomena from first principles, where quarks and gluons are the fundamental degrees of freedom, is lattice QCD [15, 16]. In this approach, the theory is formulated in Euclidean space-time, discretized in a lattice, and quark-gluon correlation functions are computed using Monte-Carlo algorithms. This requires significant computational resources. Additionally, because PDFs are field theoretically defined in terms of matrix elements of bilocal operators depending on the light-cone coordinates, a direct computation on the lattice is not possible due to its Euclidean space formulation. Instead, lattice QCD calculates matrix elements of local operators, which in turn are directly related to the Mellin moments of the PDFs. The knowledge of a sufficiently high number of Mellin moments would, in principle, allow the PDFs to be reconstructed using the inverse Mellin transform. At present, however, calculation is limited to the lowest moments [17]. In recent years, an alternative approach has been proposed based on the so-called quasidistributions (quasi-PDFs), which are defined as matrix elements of equal-time correlators in the large momentum limit, through which the PDFs can be extracted via factorization and matching procedures [18–24]. This approach allows a direct implementation on lattice and has seen a rapid progress, but still has many systematic uncertainties and only recently it has become possible to extract gluon distributions [25].

An alternative approach to accessing the nonperturbative QCD regime, where PDFs reside, is through the quantum equations of motion of the quark and gluon fields correlation functions , the so-called Dyson-Schwinger equations (DSE) [26, 27]. In principle, all information about the theory could be obtained by solving these equations

of motion. In practice, however, these equations form an infinite system of coupled integrals, making them analytically impossible to solve. As a result, one most rely on truncation schemes to obtain a feasible tool to realistically describe a problem. Moreover, DSE calculations are also typically carried out in Euclidean space and therefore, in this formulation, PDFs must be reconstructed from its Mellin moments. *

A basic ingredient connecting in some way these two regimes of QCD is the universal *parton distribution function* (PDF), which contains information on how quarks and gluons momentum are distributed within a hadron. Strictly speaking, PDFs allow for a probabilistic interpretation in the infinite momentum frame and reflect the probability of finding a quark carrying a fraction x of the parent hadron's longitudinal momentum. Experimentally, PDFs are accessed in inclusive and semi-inclusive deep inelastic scattering processes. Factorization theorems in QCD allow to *factorize* a class of hard scattering cross sections into a short-distance part, which is process dependent, but determined perturbatively, and a long-distance part described by the PDFs, which has the advantage of being universal, but are intrinsically nonperturbative. Therefore, even at very high energies, the knowledge of the nonperturbative low-energy PDFs are needed to obtain a description of hadronic reactions. In general, the PDFs are obtained by global analysis of experimental data. Once these distributions are determined for a considerable high value of Q^2, the evolution equations of the PDFs are used to obtain predictions at other values of Q^2. Currently, a direct computation of PDFs from first principles remains elusive.

A shared attribute of effective field theories and model calculations is that the emphasis of calculation efforts has so far been on obtaining quark correlation functions and related quantities, such as electromagnetic form factors, quark PDFs, etc. In PDF calculations, gluon distribution is either inferred indirectly or is assumed to be

* It is worth mentioning that within the DSE approach, the formulation in either Euclidean or Minkowski spacetime is a matter of choice.

generated entirely perturbatively by DGLAP evolution equation [28–31]. In the former case, once the quark PDF is determined at the model scale, the gluon momentum fraction is inferred from the momemtum sum rule. In the latter, nonzero sea and gluon distributions are only generated after evolution to a high Q^2, assuming zero sea and gluon distributions at the low Q^2 input scale. However, since several of the major open questions in hadron physics — such as the origin of hadron mass, and the distribution of mass, momentum and spin in the proton — are believed to involve heavy gluonic contributions at all renormalization scales and, moreover, since a major focus of future experimental efforts such as at the Electron Ion Collider is the gluonic structure of hadrons [32], it is crucial to have gluonic observables directly calculated in effective models of QCD.

This thesis aims to devise a model framework that allows to incorporate gluonic effects in PDFs of constituent quarks and the pion [33]. For that purpose, we take the approach of incorporating intrinsic gluons to PDFs computed within an effective model of QCD build solely on quarks degrees of freedom. It is vital that such a model share many of the important QCD features. An ideal candidate is the Nambu-Jona-Lasinio model (NJL), a low-energy effective model that involves only quark degrees of freedom and manifests DCSB in a transparent way. Moreover, confinement can be emulated in the model by a proper choice of regularization scheme [34–36]. Since these models have been successful in the calculation of observables such as PDFs [37–39], form factors [36, 40], and GPDs [41, 42], this success can be carried over without constructing a new effective model whole cloth.

The simplest and most straightforward way of adding intrinsic glue to an effective model of quark degrees of freedom is to simply add gluonic substructure to the constituent quark degrees of freedom. A shared feature of low-energy effective models of QCD is the emergence through the DCSB phenomenon, as already mentioned, of

constituent quarks, which are massive quasi-particles with the same quantum numbers as the (nearly) massless quarks appearing in the QCD Lagrangian. These dressed quarks are made up of many quarks and antiquarks, and it seems reasonable to suppose that they would contain gluons, too, if the model were to incorporate explicit gluon degrees of freedom.

In this thesis we follow this approach and construct a quark target model (QTM) in which a quark and gluonic substructure is embedded within the constituent quark. In this way, we explicitly calculate the quark and gluon distributions in the constituent quark to leading order in the quark-gluon coupling strength. The PDFs are by definition gauge invariant. However, in general gauges, it is necessary to account for Wilson line contributions to the quark PDF in order to properly observe the momentum sum rule. This is important, because, for example, within the DSE approach PDFs have been calculated using Landau gauge [30, 31], however, these results neglect the Wilson line contributions that must be present in covariant gauges. The calculation here is done in covariant and light cone gauges to explicitly demonstrate gauge invariance of the QTM quark and gluon PDFs and explore the importance of the Wilson line contribution in covariant gauges. The quark and gluon fields appearing in the QTM are not the current quark and gluon fields appearing in the QCD Lagrangian. The former are dressed by the chiral symmetry breaking mechanism of some low-energy effective model, and the latter are postulated to be low-energy effective degrees of freedom as well. In particular, the gluons appearing within the dressed quarks may be massive [43]—a possibility we shall consider and derive the consequences of.

This thesis is organized as follows: In Chapter 2 we present an overview of Quantum Chromodynamics discussing some of its important symmetries, the chiral symmetry. The Nambu-Jona-Lasinio model as an effective model of QCD is introduced and it is shown the emergence of dynamical chiral symmetry breaking, and also the constrains imposed by chiral symmetry breaking on the solution of the pion bound

state Bethe-Salpeter equation, which will lead to the parameters that will be used to fully characterize the model. In Chapter 3 we review the formalism of inclusive deep inelastic scattering (DIS), with the historical facts that led to the formulation of the parton model. The leading twist quark and gluon distribution functions that will be used later in Chapter 4 are introduced. Chapter 4 is the scope of this thesis, where we construct the QTM and obtain analytical results for the quark and gluon PDFs of the quark target. Next, an explicit gluon mass is introduced and its impact on the QTM PDFs is studied under two scenarios, one where a naive mass term is added to the Lagrangian which directly breaks gauge invariance, and in the other scenario we use the formalism proposed by Cornwall [44] that maintains gauge invariance and the momentum sum rule via the introduction of an auxiliary field. In Chapter 5, numerical results for the QTM PDFs and their Mellin moments are presented for massive quarks and massless gluons. In the last part, we combine the QTM PDFs with two quark-only pion PDFs models, thereby obtaining quark and gluon PDFs for the pion at the model scale. DGLAP evolution is then performed and the PDFs are compared to data and an empirical PDF parameterization. Finally, in Chapter 6, we provide some conclusions and an outlook. The thesis also comprises three appendices, in which we state the notation and conventions we use throughout the thesis, and show details of lengthy derivations.

Chapter 2

Aspects of QCD

Quantum Chromodynamics (QCD) has long been established as the fundamental theory describing the strong force, from the most fundamental level of its basics degrees of freedom, the quarks and gluons, up to the hadronic and nuclear levels. The strong force is responsible for binding quarks and gluons inside subatomic particles, as the most familiar proton, neutron and pion, and many others. Describing these composite particles remains a great challenge as the coupling at the relevant energy scale becomes large, consenquently, not enabling the use of perturbation theory in the QCD coupling constant.

In this chapter, we provide a brief review of the aspects of QCD most relevant to this thesis. First, we introduce the QCD Lagrangian, discuss its path integral quantization, and define the noninteracting quark and gluon propagators in covariant and light-cone gauges. We then examine the approximate flavor and chiral symmetries in QCD and introduce the Nambu-Jona-Lasinio (NJL) model. Finally, we demonstrate how the NJL model mimics the QCD dynamical chiral symmetry breaking (DCSB), a phenomenon responsible for producing constituent quarks and pions, the latter being the (pseudo)-Goldstone bosons of DCSB.

2.1 QCD Lagrangian and QCD propagators

From a formal perspective of quantum field theory, QCD is a non-Abelian gauge theory with gauge group SU(3) coupled to quarks in the fundamental representation. The Lagrangian density characterizing QCD is given by

$$\mathcal{L}_{\rm QCD} = \sum_q \bar{\psi}_q^i (i\not{D}^{ij} - \delta^{ij} m_q)\psi_q^j - \frac{1}{4} G^a_{\mu\nu} G_a^{\mu\nu}\,, \tag{2.1}$$

where ψ_q and $\bar{\psi}_q$ are, respectively, the flavor-q current-quark and antiquark fields, with $q = u, d, s \cdots$, $a = 1, \cdots, 8$ is a color index of the SU(3) gauge group in the adjoint representation and $i, j = 1, 2, 3$ are color indices in the fundamental representation. Greek letters $\mu, \nu = 0, 1, 2, 3$ are used to denote Lorentz vectors indices. The gauge covariant derivative, necessary to obtain a color gauge invariant Lagrangian, is

$$D_\mu = \partial_\mu + igA_\mu, \tag{2.2}$$

where g is the strong coupling constant,

$$A_\mu(x) = \sum_{a=1}^{8} t^a A^a_\mu(x)\,, \tag{2.3}$$

with A^a_μ being the gluon gauge fields and t^a the generators of the SU(3), which in the fundamental representation are $t_a = \lambda_a/2$, where λ_a are the conventional eight Gell-Mann matrices. Hereafter, summation symbol is omitted, implying summation over repeated indices as usual. The antisymmetric gluon field strength tensor is constructed out of the gauge covariant derivative Eq. (2.2) and ensure gauge invariance of the gluon kinetic energy term describing gluon dynamics:

$$G_{\mu\nu} = t^a G^a_{\mu\nu} = -\frac{i}{g}[D_\mu, D_\nu] \tag{2.4}$$

$$= t^a \left(\partial_\mu A^a_\nu - \partial_\nu A^a_\mu - g f_{abc} A^b_\mu A^c_\nu\right)\,, \tag{2.5}$$

where f_{abc} is the structure constant of the $SU(3)$ and whose generators satisfy.

$$[t^a, t^b] = i f_{abc}\, t^c, \tag{2.6}$$

$$\mathrm{Tr}[t^a\, t^b] = T(R)\, \delta^{ab}, \tag{2.7}$$

$$\left[(t^a)^2\right]^{ij} = C(R)\, \delta_{ij}, \tag{2.8}$$

where R is a given representation. In the fundamental representation, $T(F) = 1/2$ and $C(F) \equiv C_F = (N^2 - 1)/2N$. Notice the appearance of self interactions amongst the gluons, generated by the last term on the L.H.S. of Eq. (2.5), a well distinct feature of QCD. Unlike the photon in Quantum Electrodynamics (QED), which lacks electric charge, gluons carry color charge which make them self-interacting. Under local gauge transformation

$$U(x) = \exp\left[i\theta_a(x) t_a\right], \tag{2.9}$$

the gluon field transform as

$$A_\mu(x) \to U(x) A_\mu(x) U^\dagger(x) - \frac{i}{g}\left((\partial_\mu U^\dagger(x)\right) U(x), \tag{2.10}$$

and the gluon strength tensor in Eq. (2.4) tensor as

$$G_{\mu\nu} \to U(x)\, G_{\mu\nu}\, U^\dagger(x), \tag{2.11}$$

since it is constructed such as to obtain a gauge invariant gluon kinetic term. It is worth pointing out that only the color trace of the contraction of two gluon field strength tensors is gauge invariant, which is the case of the Yang-Mills part of the Lagrangian density in Eq. (2.1). Notice that this term is equivalent to writing

$$\frac{1}{4} G^a_{\mu\nu} G^{\mu\nu}_a = \frac{1}{2}\, T_F\, \delta^{ab} G^a_{\mu\nu} G^{\mu\nu}_b = \frac{1}{2} \mathrm{Tr}\left[t_a t_b\right] G^a_{\mu\nu} G^{\mu\nu}_b = \frac{1}{2} \mathrm{Tr}\left[G_{\mu\nu} G^{\mu\nu}\right]. \tag{2.12}$$

The last term, on the other hand, owing to Eq. (2.11), can be written as

$$\frac{1}{2}\mathrm{Tr}\big[G_{\mu\nu}G^{\mu\nu}\big] = \mathrm{Tr}\big[U\,G_{\mu\nu}\,U^{\dagger}U\,G^{\mu\nu}\,U^{\dagger}\big] = \frac{1}{2}\mathrm{Tr}\big[G'_{\mu\nu}G'^{\mu\nu}\big]. \tag{2.13}$$

Based upon this discussion, a gluon mass term $\sim m_g^2 A_\mu A^\mu$ is not allowed as it would violate local gauge invariance. Therefore, gluons must be massless. Nevertheless, results from both Lattice QCD [45–47] and Dyson-Schwinger equations [48–50] suggest that gluons acquire a dynamical and momentum dependent effective mass, which poses the question of how a finite gluon mass can be introduced at the Lagrangian level while preserving gauge invariance. We will come back to this point in later sections.

Having introduced the QCD classical Lagrangian, we proceed to the path integral quantization of the theory. The quantum field theory associated with the QCD classical Lagrangian Eq. (2.1) can be described using the path-integral approach, in which the partition function is the main object of interest:

$$Z[\Phi] = \int \mathcal{D}[\Phi]\, e^{i\mathcal{S}_{\mathrm{QCD}}[\Phi]} \;: \qquad \mathcal{S}_{\mathrm{QCD}} = \int \mathrm{d}^4x\, \mathcal{L}_{\mathrm{QCD}}, \tag{2.14}$$

where $\Phi = \big\{\psi, \bar{\psi}, A\big\}$ denotes all fields of the theory and $\mathcal{D}[\Phi] = \big\{\mathcal{D}\psi\mathcal{D}\bar{\psi}\mathcal{D}A\big\}$ is the functional measure of the fields of the theory.

Nonetheless, a noninteracting gluon propagator cannot be read off from Eq. (2.1) because the term quadratic in the gluon field (the kinetic part) cannot be inverted. This can be seen by writing the Yang-Mills part of the QCD action explicitly in terms of the gluon fields

$$\begin{aligned} S_{\mathrm{YM}} &= -\frac{1}{4}\int \mathrm{d}^4x\, G^a_{\mu\nu}G^{\mu\nu}_a \\ &= \int \mathrm{d}^4x \left[\frac{1}{2}A^a_\mu\left(\partial^2 g^{\mu\nu} - \partial^\mu\partial^\nu\right)A^a_\nu + \frac{g}{2}f^{abc}\left(\partial_\mu A^a_\nu - \partial_\nu A^a_\mu\right)A^{\mu b}A^{\nu c}\right. \\ &\qquad \left. - \frac{1}{4}f^{abc}f^{cde}A^a_\mu A^b_\nu A^{\mu c}A^{\nu d}\right]. \end{aligned} \tag{2.15}$$

The quadratic part has zero eigenvalues: $(\partial^2 g^{\mu\nu} - \partial^\mu \partial^\nu) A^a_\nu(x) = 0$. More explicitly, writing the Fourier transform of the gluon fiels, the inverse of the gluon propagator is obtained in momentum space, $(D^{-1}(p))_{\mu\nu} = p^2 P^T_{\mu\nu}$, where $P^T_{\mu\nu} = (g_{\mu\nu} - p_\mu p_\nu / p^2)$ is a transverse projector. Therefore, the inverse of the gluon propagator is proportional to a transverse projector which implies that the four-momentum is an autovector of the inverse of the gluon propagator with zero eigenvalue and, therefore, cannot be inverted. This, in turn, entails the lack of a gluon propagator. This traces back to the multiple counting of equivalent gauge field configurations due to gauge transformation invariance of the fields, which the path integral formalism entails.

This difficulty can be overcome by using the Faddeev-Popov procedure [51, 52], which consists of redefining the integration measure and requires a gauge fixing Lagrangian term as well as a ghost term to be added to the classical Lagrangian:

$$\mathcal{L}^{\text{cov}}_{\text{g.f.+ghost}} := \mathcal{L}^{\text{cov}}_{\text{g.f.}} = -\frac{1}{2\xi}(\partial \cdot A)^2 + \partial^\mu \bar{c}^a D^{ab}_\mu c^b, \ \text{(covariant gauges, } \partial \cdot A^a = 0) \tag{2.16}$$

$$\mathcal{L}^{\text{axial}}_{\text{g.f.}} = -\frac{1}{2\xi}(n \cdot A)^2, \qquad \text{(axial gauges, } n \cdot A^a = 0) \tag{2.17}$$

where ξ is a gauge fixing parameter and D^{ab}_μ is the covariant derivative in the adjoint representation. In the axial gauge, ghosts need not be considered as they do not couple to the gauge field and can be simply integrated out. With the change in the gluon quadratic term, we are now able to obtain the corresponding gluon propagators

$$D^{ab}_{\mu\nu}(p) = \left[-g_{\mu\nu} + (1-\xi)\frac{p_\mu p_\nu}{p^2}\right]\delta^{ab} D(p^2), \qquad \text{(covariant gauges)} \tag{2.18}$$

$$D^{ab}_{\mu\nu}(p) = \left[-g_{\mu\nu} + \frac{n_\mu p_\nu + n_\nu p_\mu}{n \cdot p} - (n^2 + \xi p^2)\frac{p_\mu p_\nu}{(n \cdot p)^2}\right]\delta^{ab} D(p^2), \quad \text{(axial gauges)} \tag{2.19}$$

with

$$D(p^2) = \frac{1}{p^2 + i\epsilon}. \tag{2.20}$$

In the limit $\xi \to 0$ and the special case $n^2 = 0$, the axial gauge propagator reduces to the light-cone gauge propagator:

$$D^{ab}_{\mu\nu}(p) = \left[-g_{\mu\nu} + \frac{n_\mu p_\nu + n_\nu p_\mu}{n \cdot p} \right] \delta^{ab} D(p^2) \qquad \text{(light cone gauge)}. \tag{2.21}$$

The adoption of the light-cone propagator requires a carefull treatment of the spurious singularity $(p \cdot n)^{-1}$. These singularities must be regularized using some regularization prescription. The simplest one is the *principle value* (PV) prescription [53],

$$\frac{1}{p \cdot n} \Longrightarrow P\frac{1}{p \cdot n} = \lim_{\zeta \to 0} \frac{1}{2} \left(\frac{1}{p \cdot n + i\zeta} + \frac{1}{p \cdot n - i\zeta} \right). \tag{2.22}$$

Another popular prescription is the *Mandelstam-Leibbrandt* (ML) prescription [54, 55],

$$\frac{1}{p \cdot n} = \lim_{\zeta \to 0} \frac{p \cdot \bar{n}}{(n \cdot p)(p \cdot \bar{n}) + i\zeta}. \tag{2.23}$$

where $\bar{n}$ is another null vector and such that $n \cdot \bar{n} = 1$. In principal, how it is regularized should not matter, as these unphysical singularities must cancel out at the end when calculating observables, such as the parton distribution functions (PDFs).

For covariant gauges, the most prominent choices for the gauge fixing parameter have been the Feynman gauge ($\xi = 1$) and Landau gauge ($\xi = 0$). For practical calculations, the Feynman gauge has been proven to be the most popular in perturbative calculations, whilst the Landau gauge has been the choice for fixed-gauge calculations of Lattice QCD and DSE communities [56]. Throughout this thesis both covariant and light-cone gauges (within the PV prescription) will be employed.

By introducing sources terms to each of the fields, the partition function takes the form

$$Z[J] = \int \mathcal{D}\Phi \, e^{i\left(\mathcal{S}_{\rm QCD}[A,\psi,\bar{\psi}]+\mathcal{S}_{\rm q.f.}[A,c,\bar{c}]+S_c[J]\right)}, \tag{2.24}$$

where $J = \{J^\mu,\, \bar{\eta},\, \eta,\, \bar{\sigma},\, \sigma\}$ are the sources for the gluon, quark and ghost fields, and the source action is

$$S_{\rm c}[J] = -\int {\rm d}^4x \, \left(\bar{\eta}\,\psi + \bar{\psi}\,\eta + \bar{c}\,\sigma + \bar{\sigma}\,c + J_\mu A^\mu\right), \tag{2.25}$$

and $D[\Phi] = \left\{\mathcal{D}A\,\mathcal{D}\psi\,\mathcal{D}\bar{\psi}\,\mathcal{D}c\,\mathcal{D}\bar{c}\right\}$ is the functional measure. Correlation functions and partition function are related to one another by functional derivatives of the latter [57]. More specifically, correlation functions are obtained by taking functional derivatives of the partition function with respect to the sources and then setting the sources to zero at the end. The quark propagator, for instance, is obtained by

$$iS_{\alpha\beta}(x-y) \equiv \langle 0|T\left[\psi_\alpha(x)\bar{\psi}_\beta(y)\right]|0\rangle = \frac{1}{Z[0]}\left(-i\frac{\delta}{\delta\bar{\eta}_\alpha(x)}\right)\left(i\frac{\delta}{\delta\eta_\beta(x)}\right) Z[J]\Big|_{J=0}. \tag{2.26}$$

On the left hand side, in the language of canonical quantization, the quark propagator is obtained as a vacuum expectation value of a time ordered product of the quark and antiquarks fields, where now the fields are operators in the Heinsenberg picture. It is equivalent to the functional formalism, where the corresponding correlation function is obtained by taking functional derivatives of the partition function as stated on the right hand side of Eq. (2.26). The partition function is also called generating functional as it generates all the Greens functions of a QFT. It is possible and convenient to define a new generating functional:

$$W[J] \equiv i \ln Z[J]. \tag{2.27}$$

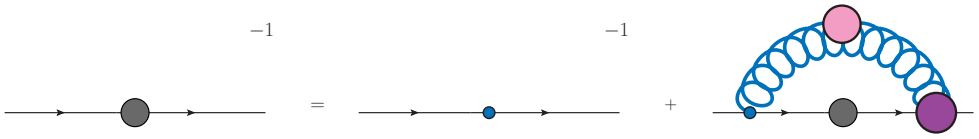

FIGURE 2.1 — Diagrammatic representation of the Dyson-Schwinger equation of the quark propagator, where the filled grey circle represents the full quark propagator, the purple cirle is the full vertex and the pink circle is the full gluon propagator.

This generating functional generates Green functions that contains only connected diagrams in contrast to $Z[J]$ that generates both connected and disconnected ones.

Another generating functional that is often of more interest goes under the name of *effective action* $\Gamma[\varphi_i]$ and can be defined by performing a Legendre transformation of $W[J]$:

$$\Gamma_{\text{eff}}[\varphi] \equiv -W[J] - \int \mathrm{d}^4x\, J^i(x) \cdot \varphi_i(x), \tag{2.28}$$

where $\varphi_i = \langle \phi_i(x) \rangle = \langle \Omega | \phi_i(x) | \Omega \rangle_{\text{J}}$ is the vacuum expectation value of the field $\phi_i(x)$ in the presence of the source J. From Eq. (2.28) it can be shown that

$$\frac{\delta}{\delta \varphi_i} \Gamma_{\text{eff}}[\varphi] = -J^i(x). \tag{2.29}$$

We are generally interested in this generating functional as it generates the one-particle irreducible (1PI) Green functions, i.e., diagrams that cannot be split into two other disconnected pieces by cutting one intermal line. Taking the functional derivative of the effective action with respect to the antiquark and quark fields and setting to zero at the end $\left(\dfrac{\delta^2 \Gamma \text{eff}}{\delta \bar{\psi} \delta \psi} \right) \Big|_{\bar{\psi}=\psi=0}$ leads to the well known quark DSE (quark gap equation) [26, 58]:

$$S^{-1}(p) = S_0^{-1}(p) - ig^2 \int \frac{d^4k}{(2\pi)^4} S(p-k) \gamma^\mu D_{\mu\nu}(k) \Gamma^\nu(k,p), \tag{2.30}$$

where

$$S_0^{-1}(p) = \not{p} + m_q \tag{2.31}$$

is the inverse of the free quark propagator, m_q denotes the bare quark mass appearing in the Lagrangian, $S(p-k)$ and $D_{\mu\nu}(k)$ are respectively the full (dressed) quark and gluon propagators, and $\Gamma^\nu(k,p)$ is the full vertex. Here, the quark gap equation is written in its *unrenormalized* form.

Because correlation functions are ultraviolent divergent, it is necessary first to introduce a regularization scheme in order to render divergent integrals finite. A second step is to redefine the fields, mass parameters and coupling constant appearing in the QCD Lagrangian in terms of renormalized quantities. Denoting the bare fields and parameters in the Lagrangian with the subscript "0" to distinguish it from its renormalized counterparts,

$$\psi_0 = Z_2^{1/2}\psi, \qquad A_0^{a\nu} = Z_3^{1/2}A^{a\nu}, \qquad c_0^a = \tilde{Z}^{1/2}c^a, \qquad m_{0q} = Z_m m_q, \qquad g_0 = Z_g g,$$

the QCD lagrangian becomes:

$$\begin{aligned}\mathcal{L} = {} & Z_2\bar{\psi}(i\not{\partial} - Z_m m_q)\psi - \frac{Z_3}{4}(\partial_\mu A_\nu^a - \partial_\nu A_\mu^a)^2 - \frac{Z_3}{2\xi_0}(\partial\cdot A^a)^2 + \tilde{Z}\partial_\nu\bar{c}^a\partial^\nu c^a \\ & - Z_g g Z_2 Z_3^{1/2}\bar{\psi}t^a \not{A}^a\psi + Z_g g Z^{3/2} f_{abc}A_\mu^b A_\nu^c \partial^\mu A^{\nu,a} - \frac{1}{4}Z_3(Z_g g f_{abc}A_\mu^b A_\nu^c)^2 \\ & + Z_g\tilde{Z}Z_3^{1/2} g f_{abc}\partial_\mu\bar{c}^c A^{\mu,b}c^a,\end{aligned} \tag{2.32}$$

which can also be written as

$$\begin{aligned}\mathcal{L} \; = {} & \bar{\psi}(i\not{\partial} - m_q)\psi - \tfrac{1}{4}(\partial_\mu A_\nu^a - \partial_\nu A_\mu^a)^2 - \frac{1}{2\xi}(\partial\cdot A^a)^2 + \partial_\nu\bar{c}^a\partial^\nu c^a \\ & - g\bar{\psi}t^a\not{A}^a\psi + g f_{abc}A_\mu^b A_\nu^c\partial^\mu A^{\nu,a} - \tfrac{1}{4}(g f_{abc}A_\mu^b A_\nu^c)^2 \\ & + g f_{abc}\partial_\mu\bar{c}^c A^{\mu,b}c^a + \mathcal{L}_{\text{c.t.}},\end{aligned} \tag{2.33}$$

where the counterterm Lagrangian has the same form as the free and interaction Lagrangian terms in Eq. (2.33) and whose coefficients are obtained as differences between Eqs. (2.33) and (2.32)[1].

Because the regularization introduces a scale, the masses and couplings are scale-dependent. The way these parameters are related at different scales are governed by the renormalization group (RG) equations [61, 62], whose particular form will depend on the choice of the renormalization scheme. The evolution of a generic renormalized n-point correlation function, for instance, $G_n(\{p_i\}, g, m_q, \mu)$, which depends on a set of momenta, on the renormalized coupling and mass parameters and on the renormalization scale μ, is described by the Callan-Symanzik equation [63, 64]:

$$\left[\mu\frac{\partial}{\partial\mu} + \mu\frac{dg}{d\mu}\frac{\partial}{\partial g} + \mu\frac{dm}{d\mu}\frac{\partial}{\partial m}\right] G_n(\{p_i\}, g, m, \mu) = n\gamma(g)\, G_n(\{p_i\}, g, m, \mu). \quad (2.34)$$

We focus on the second term, which describes the change of the coupling constant with a change of the renormalization scale. In the $\overline{\text{MS}}$ renormalization scheme, it takes the form:

$$\beta(g) = \mu\frac{dg}{d\mu} = -b_0\, g^3 + O(g^5), \qquad \text{where} \qquad b_0 = \frac{33 - 2N_f}{12\pi}. \quad (2.35)$$

Or, in terms of the coupling $\alpha_s = g^2/4\pi$,

$$\beta(\alpha_s) = \mu^2\frac{d\alpha_s(\mu)}{d\mu^2} = -b_0\, \alpha_s^2(\mu) + O(\alpha_s^3). \quad (2.36)$$

This can be integrated from a scale μ_0 to μ to give

$$\frac{1}{\alpha_s(\mu)} = \frac{1}{\alpha_s(\mu_0)} + b_0 \ln\left(\frac{\mu^2}{\mu_0}\right). \quad (2.37)$$

[1] A remark about $\xi_0 = Z_3\xi$: it is nontrivial that we can choose the same Z_3 as for A^a_ν. The reason why this relation holds follows from BRST invariance and generalized Ward-Takahashi and Slavnov-Taylor identities. [59, 60]

It is a common practice to introduce a dimensionful parameter, the so called $\Lambda_{\rm QCD}$, in the definition of $\alpha_s(\mu)$:

$$\frac{1}{\alpha_s(\mu)} - b_0 \ln\left(\frac{\mu^2}{\Lambda^2_{\rm QCD}}\right) = \frac{1}{\alpha_s(\mu_0)} - b_0 \ln\left(\frac{\mu_0^2}{\Lambda^2_{\rm QCD}}\right). \tag{2.38}$$

This leads to the leading order (LO) QCD running coupling constant:

$$\alpha_s(\mu) = \frac{1}{b_0 \ln\left(\mu^2/\Lambda^2_{\rm QCD}\right)}, \tag{2.39}$$

which is one of the most important results in QCD history, as it reveals the asymptotic freedom of QCD, a discovery that led to the 2004 Nobel Prize in Physics [13].

Perturbative QCD (pQCD) only tells us how the coupling changes with the scale. In calculations, one needs to fix μ at a convenient reference scale. Of course this reference scale should belong to a region where pQCD can be applied. That is, in processes involving large momentum transfer, so that the coupling is small. On the other hand, the coupling increases at small momenta and, in particular, when the μ scale is of the order of $\Lambda_{\rm QCD}$, nonperturbative effects arise and QCD becomes nonperturbative. At such scale, QCD models and effective theories become fundamental tools to obtain a description of hadronic processes and nonperturbative phenomena. It is important that these models hold as many similarities as possible to the real theory, exhibiting some of its distinct features and symmetries. We shall discuss next one of these important symmetries and features of QCD.

2.2 Flavor and Chiral Symmetry

In the last section, we have focused on the SU(3) color gauge group of QCD. However, QCD has yet other important symmetries which play a fundamental role in our understanding of the theory and its realization in nature, being the flavor symmetry the most important example, as it is connected to the chiral symmetry breaking (CSB), which we shall discuss hereafter. Since this section is devoted to features related to flavor symmetry and gluons are flavor independent, we disregard the Yang-Mills part of the Lagrangian density in Eq. (2.1) and focus on the quark part of the Lagrangian density:

$$\mathcal{L} = \sum_q \bar{\psi}_q (i\not{D} - m_q)\psi_q, \tag{2.40}$$

where color label is omitted.

In the limit where all quark masses are equal and non-vanishing, the Lagrangian density in Eq. (2.40) is invariant under the global transformation

$$\psi'(x) = e^{it_a\theta^a_{\mathrm{V}}}\psi(x), \tag{2.41}$$

where "V" stands for vector, indicating that this transformation will induce vector currents and t_a are the generators of the $\mathrm{SU}(N_f)_{\mathrm{V}}$ group in the N flavor case. For two flavors, $\tau_a = \tau_a/2$ with $a = 1, 2, 3$, are the generators of the $\mathrm{SU}(2)_V$, where τ are the Pauli matrices. It is also invariant under a global phase transformation, $\mathrm{U}(1)_{\mathrm{V}}$. Furthermore, if all quark masses are zero, Eq. (2.40) is also invariant under the transformation

$$\psi'(x) = e^{i\gamma_5 t_a\theta^a_A}\psi(x). \tag{2.42}$$

According to Noether's theorem, to each of these symmetries, there will be an associated

conserved current, as well as a conserved charge – A vector current (and vector charge) for the former transformation, Eq. (2.41),

$$J_a^\mu(x) = \bar{\psi}(x)\gamma^\mu t_a \psi(x), \quad Q_a^\mu(t) = \int \mathrm{d}^3x\, J_a^0(x),$$

and an axial vector current (and axial vector charge) for the latter, Eq. (2.42),

$$J_{5a}^\mu(x) = \bar{\psi}(x)\gamma^\mu\gamma_5 t_a \psi(x), \quad Q_{5a}^\mu(t) = \int \mathrm{d}^3x\, J_{5a}^0(x).$$

In the limit of equal masses, the vector current is conserved, whereas the axial vector current is not. This can be seen seen by computing their divergences with the help of the Dirac equations for the quark and antiquark fields :

$$\partial_\mu J_a^\mu(x) = i\bar{\psi}\,[m\mathbb{1}, t_a]\,\psi = 0, \qquad \partial_\mu J_{5a}^\mu = i\bar{\psi}\,\{m\mathbb{1}, t_a\}\,\gamma_5\,\psi. \tag{2.43}$$

Were the quark masses distinct, the mass matrix would spoil vector current conservation.*

In the axial vector current case, the mere presence of non-vanishing mass terms in the Lagrangian density spoils the invariance, leading to non-conservation of the current. Moreover, the presence of non-vanishing mass terms is responsible for spoiling another symmetry of the Lagrangian density. This can be seen by using the chiral projectors,

$$P_{R,L} = \frac{1 \pm \gamma_5}{2},$$

to project the left and right-handed counterparts out of the quark field

$$\psi_L = P_L\psi, \qquad \psi_R = P_R\psi, \tag{2.44}$$

$$\bar{\psi}_L = \bar{\psi}\,P_R, \qquad \bar{\psi}_R = \bar{\psi}\,P_L. \tag{2.45}$$

*Additional U(1) symmetries will not be discussed in this thesis.

Therefore, Lagrangian density in Eq. (2.40) takes the form

$$\mathcal{L} = \bar{\psi}_L(i\not{D} - m)\psi_L + \bar{\psi}_R(i\not{D} - m)\psi_R - \bar{\psi}_L m\psi_R - \bar{\psi}_R m\psi_L.$$

Notice that, for vanishing quark masses, the Lagrangian density decouples into two independent terms in the same form as in Eq. (2.40):

$$\mathcal{L} = \bar{\psi}_L i\not{D}\psi_L + \bar{\psi}_R i\not{D}\psi_R.$$

Consequently, it is invariant under $\mathrm{SU}(N_f)_L \times \mathrm{SU}(N_f)_R$. The mass matrix $m\mathbf{1}$ breaks chiral symmetry by mixing left-handed and right-handed quarks. This means that, in the limit of massless quarks, the particle spin is either aligned or anti-aligned with the particle momentum, meaning that the quark has a well defined handedness in all reference frames. A massless right-handed particle, for instance, cannot be turned into a left-handed particle, otherwise there would exist a reference frame with respect to which the particle would travel above the speed of light.

As it is realized in nature, all quarks have distinct and non-zero masses, meaning they do not remain invariant under the global unitary transformation $\mathrm{SU(6)_A \times SU(6)_V}$ described by Eqs. (2.41) and (2.42), and which is equivalent to the symmetry $\mathrm{SU}(6)_L \times \mathrm{SU}(6)_R$. However, since the *up* and *down* quark masses are nearly identical and very small when compared to the Λ_{QCD} scale:

$$m_u \approx 2.16 \text{ MeV}, \quad m_d \approx 4.67 \text{ MeV} : \quad m_u \approx m_d, \tag{2.46}$$

there is an approximate $\mathrm{SU}(2)_L \times \mathrm{SU}(2)_R = \mathrm{SU}(2)_A \times \mathrm{SU}(2)_V$ chiral flavor symmetry. In fact, even when the *strange* quark is considered

$$m_s \approx 93 \text{ MeV}, \tag{2.47}$$

the chiral flavor symmetry $\mathrm{SU}(3)_A \times \mathrm{SU}(3)_V$ remains approximately valid. In the

heavy quark sector (*charm*, *top* and *bottom*), however, chiral flavor symmetry is severely broken by the mass terms correponding to the heavy quarks:

$$m_c \approx 1.25 \text{ GeV}, \quad m_c \approx 4.18 \text{ GeV}, \quad m_t \approx 170 \text{ GeV}. \tag{2.48}$$

The (approximate) chiral symmetry of the QCD Lagrangian is not realized in nature in the usual way symmetries are realized, through (approximate) degeneracy of the spectrum of the theory—the Wigner way. Just to mention one example, if this (approximate) symmetry were realized in the normal way, one would have a particle with a mass (almost) equal to the proton, but of opposite parity to that of the proton; such a particle does not exist. The symmetry is thought to be realized in the Nambu-Goldstone way, in which it is spontaneously broken by the interactions of the theory. This has major outcomes. A consequence resulting from the breaking of a continuous symmetry is stated in the well known Goldstone theorem. According to the Goldstone theorem, to each continuous symmetry which is spontaneously broken, there exists a zero mass boson, a Goldstone boson, with the same quantum numbers of the generator of the broken symmetry. In QCD, since chiral symmetry is only approximate, the realization of the Goldstone theorem, in the two-flavor case, takes place through the appearance not of massless bosons in the spectrum of the theory, but of three bosons with very small mass and odd parity, the neutral and charged pions $\pi^0, \pi^\pm$ (here we are neglecting the electromagnetic interaction). If chiral symmetry were an exact symmetry of QCD, pions would be massless. If the strange quark is also regarded as light, that is, in the three-flavor case, there are eight generators corresponding to the broken chiral symmetry. Therefore, there are eight Nambu-Goldstone bosons in the spectrum, which, in the chiral limit, are identified to be the eight light pseudoscalar mesons, $\pi^0, \pi^\pm, K^0, K^\pm, \bar{K}^0$ and η (here we will not discuss the $U(1)$ axial anomaly). As previously discussed, to treat nonperturbative phenomena, such as it is the case of dynamical chiral symmetry breaking, effective theories play an important role. In the

next section, we will explore these topics within the Nambu–Jona-Lasinio model.

2.3 The Nambu-Jona-Lasinio model

The Nambu-Jona-Lasinio (NJL) model was originally developed by Nambu and Jona-Lasinio [65, 66] in the pre-QCD era as an effective theory to describe dynamical mass generation of nucleons and pions in analogy to the Bardeen–Cooper–Schrieffer (BCS) theory of superconductivity. Nowadays, the NJL model has been reinterpreted in terms of quark degrees of freedom and has become a quite successful and popular low-energy QCD model, and an important phenomenological tool. The model has been used to study different aspects of DCSB in vacuum, at finite temperature and baryon density [67–70], in constrained geometries [71, 72], in heavy-flavor hadrons [73–75], and under strong magnetic fields [76].

The starting point is to consider an interaction Lagrangian density which has the desired feature, the chiral symmetry. The two-flavor NJL model is described by a four-point quark interaction Lagrangian density which has the form:

$$\mathcal{L}_{\rm NJL} = \bar{\psi}(i\partial\!\!\!/ - m_q)\psi + G_\pi[(\bar{\psi}\psi)^2 + (i\bar{\psi}\gamma_5\tau\psi)^2] \tag{2.49}$$

$$= \mathcal{L}_0 + \mathcal{L}_{\rm int}, \tag{2.50}$$

where $m_q = \mathrm{diag}(m_u, m_d)$, with $m_u = m_d = m$, τ are the Pauli matrices and G_π is the coupling constant. The free Lagrangian is identical to that of the pure quark sector of QCD. As previously discussed in Sec. (2.2), the free Lagrangian density is chiral invariant as long as $m = 0$. While the two terms in the interacting Lagrangian are not chiral invariant individually, their sum is, as can be easily verified using the chiral projectors introduced in Eq. (2.44).

A straightforward approach to analyze whether the interaction might generate mass for the quarks is to compute the quark self-energy via perturbation theory in the coupling constant G_π and check if it generates a mass in the quark propagator. From the general theory of quantum fields, one can already anticipate the result – Since the quark self-energy to all orders in perturbation theory is proportional to the mass appearing in the Lagrangian, starting with $m = 0$ in the Lagrangian, there will be no corrections to the quark self-energy, and thus no mass pole in the quark propagator arises and a quark mass cannot be generated perturbatively. Alternatively, starting with a non-zero quark mass, the mass must remain small relative to the hadronic scale to preserve approximate chiral symmetry, as discussed in Sec. (2.2). However the smallness of the mass would not be sizeable enough to obtain the values of some measured quantities such as, *e.g.*, the pion decay constant.

The NJL nonperturbative approach that resembles that of perturbation theory consists of adding and subtracting a self-energy term to the NJL Lagrangian. Explicitly, the lagragian is written as

$$\begin{aligned}\mathcal{L}_{\text{NJL}} &= \bar{\psi}(i\partial\!\!\!/ - m)\psi - \bar{\psi}\Sigma_0\psi + G_\pi[(\bar{\psi}\psi)^2 + (i\bar{\psi}\gamma_5\tau\psi)^2] + \bar{\psi}\Sigma_0\psi \\ &= \hat{\mathcal{L}}_0 + \hat{\mathcal{L}}_{\text{int}},\end{aligned} \tag{2.51}$$

where now

$$\hat{\mathcal{L}}_0 = \bar{\psi}(i\partial\!\!\!/ - M)\psi, \tag{2.52}$$

with $M \equiv m + \Sigma_0$ and

$$\hat{\mathcal{L}}_{\text{int}} = G_\pi[(\bar{\psi}\psi)^2 + (i\bar{\psi}\gamma_5\tau\psi)^2] + \bar{\psi}\Sigma_0\psi.$$

If Σ_0 is assumed to completely capture the effect of the original interacting Lagrangian

$\mathcal{L}_{\rm int}$, then $\hat{\mathcal{L}}_{\rm int}$ can be treated perturbatively and Σ_0 can be determined from the requirement that $\hat{\mathcal{L}}_{int}$ does not lead to additional self-energy terms. At leading order, this means taking $\Sigma^{(1)} = 0$:

$$\begin{aligned}\Sigma^{(1)}(p) &= 2iG_\pi \int \frac{d^4k}{(2\pi)^4}\Big[\mathrm{Tr}\,[\,\hat{S}_0(k)\,] - \hat{S}_0(k) - \gamma_5 \mathrm{Tr}\,[\,\hat{S}_0(k)\gamma_5\,] + \gamma_5 \hat{S}_0(k)\gamma_5\Big] - \Sigma_0 \\ &= 0\,, \end{aligned} \tag{2.53}$$

where

$$\hat{S}_0(p) = \frac{1}{\not{p} - M + i\epsilon} \tag{2.54}$$

is the propagator corresponding to the Lagrangian $\hat{\mathcal{L}}_0$. Eq. (2.53) leads to the well known gap equation:

$$M = m + 8iG_\pi \left(N_c N_f + \frac{1}{2}\right) \int \frac{d^4k}{(2\pi^4)} \frac{M}{p^2 - M^2 + i\epsilon}. \tag{2.55}$$

The 1/2 term is commonly neglected[2]. In terms of the quark condensate $\langle\bar{\psi}\psi\rangle$, the dressed quark mass can be expressed as:

$$M = m - 4G_\pi \langle\bar{\psi}\psi\rangle, \tag{2.56}$$

where [68]

$$\langle\bar{\psi}\psi\rangle = -i \int \frac{d^4p}{(2\pi)^4} \mathrm{Tr}\,\hat{S}_0(p) = -12i \int \frac{d^4p}{(2\pi)^4} \frac{M}{p^2 - M^2 + i\epsilon}. \tag{2.57}$$

Because the NJL model is a non-renormalizable quantum field theory, the model is regularization scheme-dependent and will have a dependence on an additional parameter that has to be introduced in order to render the loop integrals finite. Several regularization schemes are possible, such as the three momentum cutoff, Pauli-Villars

[*2] This term is $1/N_c$ suppressed.

regularization and the proper-time regularization (PTR) [67–69]. The scheme that shall be used in this work is the PTR. In the PTR scheme the gap equation evaluates to

$$M = m + \frac{3G_\pi M}{\pi^2}\int_{\tau_{\rm UV}}^{\tau_{\rm IR}} d\tau\, \frac{e^{-\tau M^2}}{\tau^2}, \tag{2.58}$$

where $\tau_{\rm UV(IR)} = 1/\Lambda^2_{\rm UV(IR)}$ and $\Lambda_{\rm UV(IR)}$ are the ultraviolet (UV) and infrared (IR) cutoffs. The PTR scheme only requires a UV cutoff to regularize the UV divergence ($\tau = 0$). Nevertheless, an infrared cutoff has been used to simulate confinement in the model [34, 35, 73, 77, 78]. Besides the trivial solution, Eq. (2.58) also allows a non-trivial solution as long as the coupling G_π is sufficiently large, that is, if $G_\pi > G^c_\pi$, where G^c_π is a critical value given by $G^c_\pi = \frac{\pi}{3}(\Lambda^2_{\rm UV} - \Lambda^2_{\rm IR})^{-1}$. A dynamical mass is generated even if $m = 0$. This is illustrated in Fig. 2.2. Since the interaction is the source of mass generation, M is said to be dynamically generated.

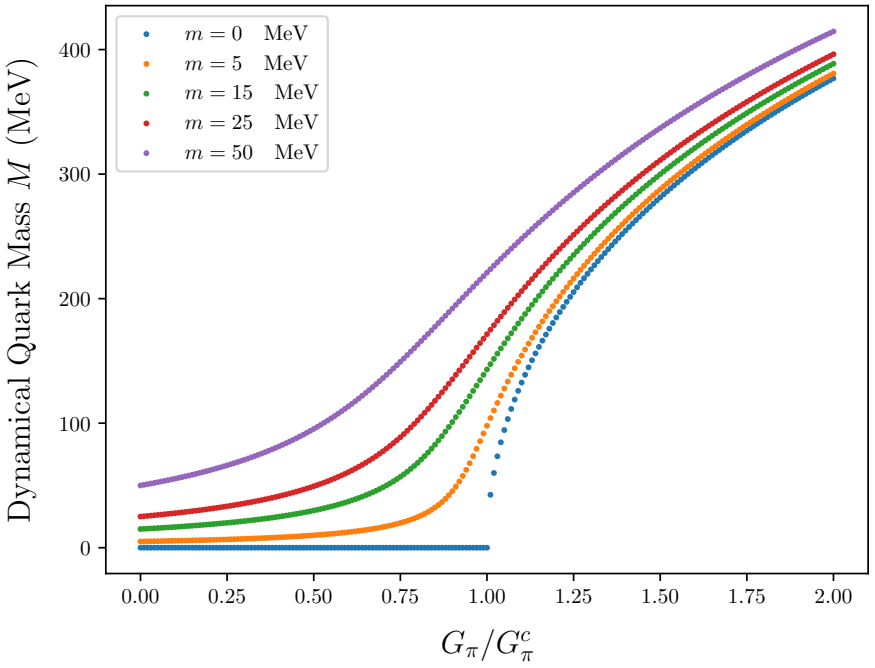

FIGURE 2.2 — Dynamical mass generation as a function of the ratio G_π/G^c_π.

So far, we have illustrated the mechanism of dynamical chiral symmetry breaking emerging from the NJL model. In the next section, we shall sketch the description of mesons in the NJL model, in particular, the pion.

2.4 Pion in the NJL Model

In a relativistic quantum field theory, bound states are described by the Bethe-Salpeter equation (BSE). For a more detailed and general discussion, see [79, 80]. In the NJL model, the BSE for mesons is given by [81]

$$\mathcal{T}(q) = \mathcal{K} + \int \frac{d^4k}{(2\pi)^4}\, \mathcal{K}\, S(k+q)\, \mathcal{T}(q), \tag{2.59}$$

where $\mathcal{T}$ is the two-body t-matrix, S is the quark propagator and $\mathcal{K}$ is the interaction kernel. Since we are interested only in the pion channel, corresponding to the NJL Lagrangian given in Eq. (2.49), the interaction kernel has the form

$$\mathcal{K}_{\alpha\beta,\delta\gamma} = -2iG_\pi(\gamma_5\,\tau_i)_{\alpha\beta}(\gamma_5\,\tau_i)_{\delta\gamma}. \tag{2.60}$$

Eq. (2.59) has solution

$$\mathcal{T}_{\alpha\beta,\delta\gamma(k)} = (\gamma_5\,\tau_i)_{\alpha\beta}\,\tau_\pi(k)(\gamma_5\,\tau_i)_{\delta\gamma}, \tag{2.61}$$

with

$$\tau_\pi(k) = \frac{-2\,i\,G_\pi}{1 + 2G_\pi\Pi_\pi(k^2)}, \tag{2.62}$$

where $\Pi_\pi(k^2)$ is the polarization propagator given by

$$\Pi_\pi(k^2) = 6i \int \frac{d^4k}{(2\pi)^2} \mathrm{Tr}\left[\gamma_5\,\hat{S}_0(q)\,\gamma_5\,\hat{S}_0(k+q)\right], \tag{2.63}$$

with $\hat{S}_0$ given in Eq. (2.54). Solving Eq. (2.63), the result can be plugged in Eq. (2.62) to find the mass of the pion. The mass of the pion is obtained as the pole of Eq. (2.62), that is, setting $[1 + 2G_\pi \Pi_\pi(k^2 = m_\pi^2)] = 0$, one obtains a transcendental equation, whose solution leads to the pion mass [68]:

$$m_\pi^2 = -\frac{m}{M} \frac{1}{4iG_\pi N_c N_f I(m_\pi^2)}\,, \tag{2.64}$$

where

$$I(k^2) = \int \frac{d^4p}{(2\pi)^4} \frac{1}{[(p + k/2)^2 - M^2]\,[(p - k/2)^2 - M^2]}. \tag{2.65}$$

One then sees in Eq. (2.64) that in the chiral limit, $m = 0$, the pion mass vanishes, which is the realization of Goldstone's theorem.

The residue at the pole,

$$Z_\pi^{-1} = -\left.\frac{\partial \Pi_\pi(k^2)}{\partial k^2}\right|_{k^2 = m_\pi^2}\,, \tag{2.66}$$

determines what is interpreted as the quark-pion coupling constant $\sqrt{Z_\pi}$. The parameters of the model are then $\Lambda_{\rm UV}^2, \Lambda_{\rm IR}^2, m$ and G_π. The infrared cutoff incorporates confinement and is commonly chosen to have the value $\Lambda_{\rm IR} = 240$ MeV. The UV cutoff as well as the coupling strength G_π are constrained to reproduce the physical pion mass and the pion decay constant with a dressed quark mass given by $M_q = 400$ MeV. This leads to $\Lambda_{\rm UV} = 640$ MeV. We use these parameters results obtained in [40] for the pion dressed quark PDF that will be used in Chapter 4.

Chapter 3

Deep Inelastic Scattering

Inclusive deep inelastic scattering has been long the conventional process for probing the inner structure of hadrons. In a series of inelastic scattering experiments in the 1960s, it has provided the most compelling evidences of the existence of quarks and also a first hint pointing to the existence of gluons, which would later be experimentally verified to exist [82–85]. The experimental findings revealed that quarks carried only approximately 50% of the proton's momentum. The remaining missing momentum fraction was subsequently attributed to electrically neutral constituents known as gluons. This discovery played a pivotal role in the establishment of Quantum Chromodynamics as the correct theory to describe the strong interactions.

This chapter addresses various aspects of DIS. The formalism of DIS is briefly reviewed by first introducing the DIS kinematics, cross-section and the corresponding structure functions. The discussion covers the key points that led to the formulation of the parton model.

3.1 Kinematics and Cross Section

Deep inelastic scattering is characterized by the process in which a lepton is scattered off a target via the exchange of a virtual boson transferring large amounts of four-momentum to the target, which typically shatters producing many new particles. To set the general notation, we consider the scattering of a lepton of momentum ℓ^μ on a hadron H of momentum P to an outgoing lepton of momentum ℓ'^μ and a hadronic final state X,

$$l(\ell) + H(P) \longrightarrow l'(\ell) + X(P_X).$$

In general this notation holds for inclusive ineslastic scattering, where only the scat-

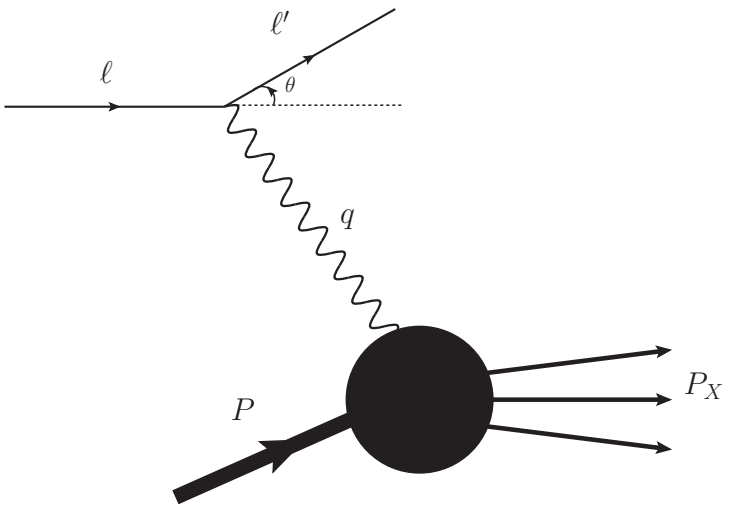

FIGURE 3.1 — Deep Inelastic scattering.

tered lepton is detected, meaning that there is a sum and integral over all possible states for X. For large momentum transfer to the target, $q^\mu = \ell^\mu - \ell'^\mu$, one can capture the microscopic structure of the initial hadron state H. In the target rest frame, $P^\mu = (M_H, 0, 0, 0)$, the DIS kinematics is fully determined by three Lorentz invariants, which are commonly chosen to be: the centre-of-mass energy squared s,

the mass squared of the produced hadronic system and the negative of the time-like four-momentum squared transfered to the target, respectively given by:

$$s \equiv (\ell + P)^2 = M_H^2 + 2M_H E, \tag{3.1}$$

$$W^2 \equiv P_X^2 = M_X^2 = (P + q)^2, \tag{3.2}$$

$$Q^2 \equiv -q^2 = (\ell' - \ell)^2 = 4EE' \sin^2\left(\frac{\theta}{2}\right), \tag{3.3}$$

where E and E' are, respectively, the energies of the incident and scattered lepton and where lepton masses have been neglected ($m_l = m_{l'} = 0$). The kinematics variables can also be chosen among the following invariants:

$$\nu = \frac{P \cdot q}{M_H} = E - E', \tag{3.4}$$

$$x = \frac{Q^2}{2P \cdot q} = \frac{Q^2}{2M_H \nu}, \qquad (0 \leq x \leqslant 1) \tag{3.5}$$

$$y = \frac{q \cdot P}{l \cdot P} = \frac{\nu}{E}, \qquad (0 \leq y \leqslant 1) \tag{3.6}$$

where ν is the energy transfered from the lepton to the target, the Bjorken x is the momentum fraction of the hadron carried by the struck quark and y is the energy fraction of the incident lepton carried by the exchanged particle (γ, Z^0 or $W^{\pm}$), that is, the fractional energy loss of the lepton in the rest frame of the nucleon. A reaction is said to be deep inelastic when both the momentum transfer q and the mass of the produced hadronic system M_X are large compared to a typical hadron mass, $Q^2 \gg M_H^2$ and $W^2 = M_X^2 \gg M_H^2$. The elastic scattering occurs when $W^2 = M_X^2 = M_H^2$ ($x = 1$), that is to say the hadron target remains intact, while the inelastic scattering correponds to $W = M_X^2 > M_H^2$ ($x < 1$). In inclusive DIS, since only the scattered lepton is detected, the quantities that are measured experimentally are the scattering angle θ of the final lepton and the energy of the scattered lepton E'. From these quantities, the squared momentum transfer Q^2 can be determined. Therefore, the cross section can expressed in terms of two independent variables, typically in terms of (x, Q^2) or (ν, Q^2).

In the one-photon exchange approximation, the cross-section for inclusive deep ineslatic scattering can be separated in a leptonic term $L^{\mu\nu}$ and a hadronic tensor $W^{\mu\nu}$

$$d\sigma \sim |M|^2 \sim L^{\mu\nu} W_{\mu\nu}, \tag{3.7}$$

where the unpolarized leptonic tensor is

$$\begin{aligned} L_{\mu\nu} &= \frac{1}{2} \sum_{s',\, s} \bar{u}(\ell', s') \gamma_\mu u(\ell, s) \bar{u}(\ell, s) \gamma_\nu u(\ell, s') \\ &= 2 \left(\ell_\mu \ell'_\nu + \ell_\nu \ell'_\mu - g_{\mu\nu} \left(\ell \cdot \ell' - m^2 \right) \right), \end{aligned} \tag{3.8}$$

where here m is the lepton mass and the factor of 2 comes from averaging over the inital spins and the hadronic tensor is given by

$$\begin{aligned} W_{\mu\nu} &= \frac{1}{4\pi} \sum_{X_k} \prod_{k=1}^{n_X} \frac{d^3 p_k}{(2\pi)^3 2E_k} \langle P | \, J_\mu \, | X_k \rangle \langle X_k | \, J_\nu \, | P \rangle (2\pi)^4 \delta^4 (P + q - P_X) \\ &= \frac{1}{4\pi} \int d^4 z \, e^{iqz} \langle P | \left[J^\dagger_\mu(z), J_\nu(0) \right] | P \rangle. \end{aligned} \tag{3.9}$$

The leptonic tensor is well known and can be directly calculated using perturbation theory. On the other hand, the hadronic tensor involves nonperturbative QCD dynamics and therefore is not calculable within perturbative QCD. However, symmetry properties of QCD can shed light on the general structure of the hadronic tensor. By imposing current conservation and parity symmetry, the unpolarized hadronic tensor can be parametrized in terms of two independent inelastic form factors,

$$W^{\mu\nu}(q, P) = \left(-g^{\mu\nu} + \frac{q^\mu q^\nu}{q^2} \right) W_1(\nu, Q^2) + \frac{\hat{P}^\mu \hat{P}^\nu}{M_H^2} W_2(\nu, Q^2), \tag{3.10}$$

where $\hat{P}^\mu = \left(P^\mu - \frac{q \cdot P}{q^2} q^\mu \right)$ and $\hat{P}^\nu = \left(P^\nu - \frac{q \cdot P}{q^2} q^\nu \right)$ and scalar functions $W_1(\nu, Q^2)$ and $W_2(\nu, Q^2)$ are referred as the unpolarized structure functions. When contracting the leptonic tensor and the hadronic tensor, only the terms contracted to $\sim g_{\mu\nu}$ and $P_\mu P_\nu$ in the hadronic tensor survive due to leptonic current conservation (implying in

$q_\mu W^{\mu\nu} = 0$):

$$L_{\mu\nu}J^{\mu\nu} = 4\ell\cdot\ell'\,W_1(\nu,Q^2) - \frac{2}{M_H^2}\left[M_H^2\ell\cdot\ell' - 2(\ell\cdot P)(\ell'\cdot P)\right]W_2(\nu,Q^2). \tag{3.11}$$

In the Lab frame,

$$\ell\cdot\ell' = 2EE'\sin^2\frac{\theta}{2}, \tag{3.12}$$

$$P\cdot\ell = EM_H, \qquad P\cdot\ell' = E'M_H, \tag{3.13}$$

yielding

$$d\sigma \sim L_{\mu\nu}J^{\mu\nu} = 4EE'\left(2W_1(\nu,Q^2)\sin^2\frac{\theta}{2} + W_2(\nu,Q^2)\cos^2\frac{\theta}{2}\right). \tag{3.14}$$

In the 1960s these structure functions were predicted to become independent of Q^2 in the limit Q^2, $\nu\to\infty$ with fixed x, the so called *Bjorken scaling* [86]. This behavior was in sharp contrast with the falling of the electromagnetic form factors as functions of Q^2 observed in elastic electron-nucleon scattering and could be explained if the inelastic electron-nucleon were due to the incoherently elastic scattering of the lepton from individual point-like spin 1/2 constituents within the nucleon since in this case the structure functions exhibit scaling. For comparison, the cross section of a lepton scattering elastically off a point-like target as the muon, for instance, has the form:

$$d\sigma \sim 4EE'\left[\cos^2\frac{\theta}{2} + \frac{Q^2}{2M^2}\sin^2\frac{\theta}{2}\right]\delta\left(\nu - \frac{Q^2}{2M}\right). \tag{3.15}$$

Therefore, by comparing to Eq. (3.14), the structure functions become

$$F_1(x,Q^2) \equiv MW_1(\nu,Q^2) = \frac{Q^2}{4M\nu}\delta\left(1-\frac{Q^2}{2M\nu}\right) \xrightarrow{Q^2\to\infty} F_1(\omega), \tag{3.16}$$

$$F_2(x,Q^2) \equiv \nu W_2(\nu,Q^2) = \delta\left(1-\frac{Q^2}{2M\nu}\right) \xrightarrow{Q^2\to\infty} F_2(\omega), \tag{3.17}$$

and we can see they are only functions of the dimensionless ratio $\frac{1}{\omega}\equiv Q^2/2M\nu$. The experimental obervation of approximate scaling at SLAC-MIT [3, 4, 87–91] right after

Bjorken prediction paved the way to the discoverement of the composite nature of the nucleon in terms of point-like constituents and has led to the formulation of the *Parton Model* [92, 93]. Around the same time Callan and Gross suggested that these scaling functions were not independent, implying $2xF_1(x) = F_2(x)$, what became known as the *Callan-Gross relation* [94]. This relation entails that the nucleon constituents are spin 1/2 particles[3].

3.2 Parton Model

In the parton model, hadrons are viewed as made up of point-like quasi-free constituents called partons. These partons would be later identified to be the quarks and gluons. Recall that this assumption allows to explain the Bjorken scaling that were observed in scattering experiments. Feynman interpreted it as an indication of the existence of constituents inside the nucleon [93]. In the parton model, the inelastic lepton-hadron scattering is viewed as a superposition of incoherent elastic scattering of the partons inside the nucleon from a highly virtual photon and the partons are assumed to move collinearly to the target each carrying a momentum fraction ξ_k of the total target momentum $P = p_k$, where p_k is the four-momentum of a single parton ($p_k = \sum_k \xi_k P$, with $\sum \xi_k = 1$). The hadronic tensor $W^{\mu\nu}$ in the parton model is represented by the handbag diagram given in Fig. (3.2), where the lower blob is parametrized through a bilocal matrix element that is related to the Parton Distributions. The infinite momentum frame is often used when discussing the parton model. In this frame, the nucleon moves with a very large momentum[4] and the transverse momentum and mass of the parton can be neglected.

[3] $F_1(x) = 0$ if the constituents were spin-0 particles.

[4] The target moves in the z direction with $P_\mu = (\sqrt{P^2 + M^2}, 0, 0, -P) \xrightarrow{P\to\infty} \left(P + \frac{M^2}{2P}, 0, 0, -P\right)$.

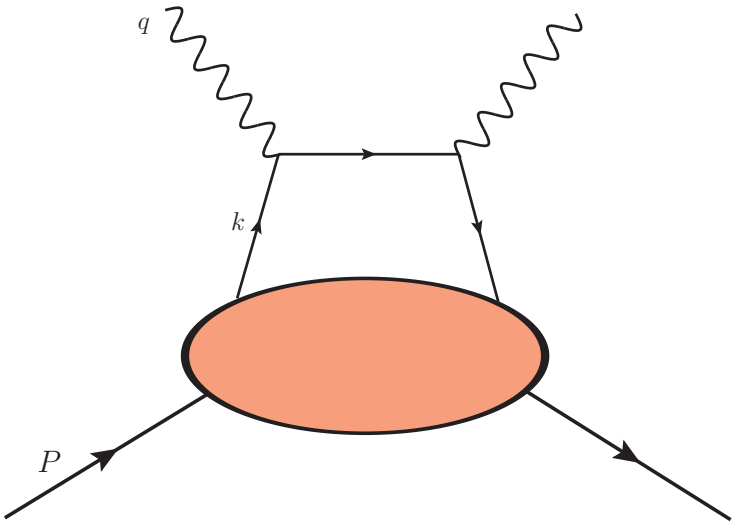

FIGURE 3.2 — The handbag diagram for inclusive deep inelastic scattering off a hadronic target.

The structure functions are expressed in terms of the *parton distributions function*, $f_k(\xi)$, that describes the probability that the struck parton carries a longitudinal momentum fraction ξ of the target momentum. Then, for each parton k,

$$\int d\xi f_k(\xi) = 1, \tag{3.18}$$

and momentum conservation implies:

$$\sum_k \int d\xi \, \xi f_k(\xi) = 1. \tag{3.19}$$

Now looking back at the structure functions in Eqs. (3.16) and (3.17) and writing $x_k = x/\xi_k$ and $m_k = \xi_k M$[5], the structure functions $F_i^{(k)}$ with $i = 1, 2$ for a parton k

[5] Partons cannot have a mass that changes with its momentum fraction. A nucleon can only emit a parton moving parallel to it if $m = M = 0$. However this can be justified in a reference frame in which both the parton mass and the hadron target mass can be neglected [95].

become

$$F_1^{(k)} = \frac{M}{m_k}\frac{Q^2}{4m_k\nu}\delta\left(1-\frac{Q^2}{2m_k\nu}\right) = \frac{1}{2}\frac{x}{\xi_k}\delta\left(\xi_k - x\right), \tag{3.20}$$

$$F_2^{(k)} = \delta\left(1-\frac{x}{\xi}\right) = \xi_k\delta\left(\xi_k - x\right). \tag{3.21}$$

These results are integrated over all partons

$$F_i = \sum_k e_k^2 \int d\xi f_k(\xi) F_i^{(k)}(x,\xi_k), \tag{3.22}$$

leading to the unpolarized structure functions in the parton model:

$$F_1(x) = \frac{1}{2}\sum_k e_k^2 f_k(x), \tag{3.23}$$

$$F_2(x) = x\sum_k e_k^2 f_k(x), \tag{3.24}$$

with

$$x = \frac{1}{\omega} = \xi_k. \tag{3.25}$$

The structure funtions in the parton model depend only on the dimensionless variable x, the Bjorken x, and, in the infinite momentum frame, this can be identified as the longitudinal momentum fraction carried by the struck parton. Moreover, the Callan-Gross relation can be seen to hold in the parton model.

3.3 Light-cone dominance in DIS

In order to analyze the region of dominance of the hadronic tensor in DIS, it is convenient to adopt light-cone coordinates (A.1). Take the argument of the exponential in

Eq. (3.9) in light-cone coordinates (See App. A.1 for definitions)

$$q \cdot z = q^+ z^- + q^- z^+ - \mathbf{q}_\perp \cdot \mathbf{z}_\perp. \tag{3.26}$$

In the lab frame,

$$q_\pm = \frac{1}{\sqrt{2}}(q_0 \pm q_3) = \frac{1}{\sqrt{2}}\left(\nu^2 \pm \sqrt{\nu^2 - q^2}\right), \tag{3.27}$$

and taking the Bjorken limit, $\nu \to \infty$ with fixed x,

$$q_\pm = \frac{1}{\sqrt{2}} \times \begin{cases} 2\nu + Mx, \\ -Mx, \end{cases} \tag{3.28}$$

we see that $q_+ \to \infty$, while q^- is finite. According to the Riemann-Lebesgue lemma, the integral in Eq. (3.9) is dominated by the region where $|q \cdot z|$ is finite: $z^- \sim 0$ and $z^+ \sim 1/Mx$. Now notice that the commutator $\left[J_\mu(z)^\dagger, J_\nu(0)\right]$ vanishes unless $z^2 = 2z^+z^- - \mathbf{z}_\perp^2 \geqslant 0$ due to causality. This inequality together with the fact that $z^- \sim 0$ implies that $\mathbf{z}_\perp \to 0$, which leads to $z^2 \sim 0$, the light-cone region. Therefore, the Bjorken limit of DIS is dominated by the region near the light-cone. This allows to arrange bilocal operators, *e.g.*, the current commutators appearing in the DIS hadronic tensor in Eq. (3.9), in terms of the degree of their light-cone singularity. This is formally done using the Operator Product Expansion (OPE) and leads to the definition of *twist*, that determines which operators are most important as $Q^2 \to \infty$ [60, 62, 96, 97]. An informal definition of twist that is often used is that it is the order M/Q at which an operator contributes to a DIS process. In this thesis, we are interested in the leading twist quark and gluon distributions, which are defined in the next section.

3.4 Parton Distributions

At leading twist, the (unpolarized) distribution of a flavor-q quark in a given hadron is defined as the lightcone Fourier transform of the expectation value of a bilocal operator:

$$f_{q/H}(x) = \int \frac{d\xi^-}{4\pi}\, e^{ixP^+\xi^-} \langle P|\bar{\psi}_f(0)\gamma^+ W[0,\xi^-]\psi_f(0,\mathbf{0}_\perp,\xi^-)|P\rangle_c.$$

The operator $W[0,\xi]$ is the *Wilson link* (or Wilson line) along the light-like line connecting the quark and antiquark fields that has to be introduced in order to ensure gauge invariance of the PDF. It is defined by

$$W[0,\xi^-] = Pe^{-ig\int_{\xi^-}^{0} d\eta^- A^+(\eta^-)}, \tag{3.29}$$

where P denotes the path-ordering operator and A^+ is the plus component of the gluon field. In the light-cone gauge, $A^+ = 0$, and therefore the Wilson line reduces to unity, such that one does not have to deal with its contributions. In a general covariant gauge, however, the Wilson line makes non-trivial contributions to the PDF as we shall see.

The gluon distribution in a hadron is defined in terms of the gluon field strength tensor

$$f_{g/H}(x) = \int \frac{d\xi^-}{2\pi P^+ x} e^{ixP^+\xi^-} \langle P|G^+_\mu(0)W[0,\xi^-]G^{\mu+}(\xi^-)|P\rangle. \tag{3.30}$$

The ultraviolet divergence of the PDFs introduces a scale dependence due to the required renormalization at some energy resolution scale μ. In this work, a variant of on-shell subtraction is employed, where the ultraviolet regulator is kept finite, eliminating the need for counterterms and thus no actual 'subtraction' is performed. However, the renormalized mass is still defined by the pole mass. The variation of the PDFs with respect to the scale is described by a renormalization group equation, which is introduced in the next section.

3.5 DGLAP evolution equations

In the parton model, where interactions between partons are neglected, we have seen that the structure functions (and therefore the quark PDF) do not depend on Q^2. In QCD, however, this scaling will not manifest. In fact, the scaling functions have a weak logarithmic Q^2 dependence $\sim \alpha_s \log(Q^2)$ arising from processes of gluon radiation and formation of quark-antiquarks pairs in QCD, and such violations can be described perturbatively by the so-called DGLAP evolution equations (Dokshizer-Gribov Lipatov-Altarelli-Parisi equations) that introduces the necessary logarithimic Q^2 dependence into the PDF.

The DGLAP equations are coupled integro-differential equations that describes the Q^2 dependence of the parton distributions[6]. They can be written as

$$\frac{\partial f_{i/H}(x,Q^2)}{\partial \log Q^2} = \frac{\alpha_s(Q^2)}{2\pi} \sum_{j=q,\bar{q},g} \int_x^1 \frac{dy}{y} P_{ij}\left(\frac{x}{y}\right) f_{j/H}(y,Q^2), \tag{3.31}$$

where $\alpha_s(Q^2)$ is the QCD running coupling, $f_{j/H}(y,Q^2)$ is a parton (quark, antiquark or gluon) distribution in a hadron at a scale Q^2 and $P_{ij}(x/y)$ are the splitting functions characterizing the probability of a parton of type j with a momentum fraction y to emit a quark or gluon and become a parton of type i with a momentum fraction x. Here, Q^2 represents the hard scale of the process, which determines the resolving power of the probe. As Q^2 increases, one can probe deeper into the hadron, revealing more partons.

It is convenient to split the quark PDF into two classes of linear combinations of quark and antiquark distributions, the non-singlet quark distribution[7] and the singlet

[6] Similar to the β function that governs the dependence of the running coupling on Q^2.

[7] A non-singlet distribution is defined as a linear combination of quark distributions orthogonal to the singlet quark distribution.

quark distribution. The latter does not mix with the gluon distribution and evolves indepently. It has the form

$$q^{NS}(x) = q(x) - \bar{q}(x), \tag{3.32}$$

and evolves according to

$$\frac{\partial q^{NS}(x,Q^2)}{\partial \log Q^2} = \frac{\alpha_s(Q)^2}{2\pi} P_{qq}(x) \otimes q^{NS}(x,Q^2), \tag{3.33}$$

where the symbol $\otimes$ represents the convolution product defined by

$$(f \otimes g)(x) = \int_x^1 \frac{dy}{y} f(y) g\left(\frac{x}{y}\right). \tag{3.34}$$

The singlet combination, defined by

$$\Sigma(x) = q(x) + \bar{q}(x), \tag{3.35}$$

does mix with the gluon distribution. Therefore, the singlet quark distribution and gluon distribution DGLAP equations are coupled and have the form:

$$\begin{pmatrix} \Sigma(x,Q^2) \\ g(x,Q^2) \end{pmatrix} = \frac{\alpha_s(Q^2)}{2\pi} \begin{pmatrix} P_{qq}(x) & P_{qg}(x) \\ P_{gq}(x) & P_{gg}(x) \end{pmatrix} \otimes \begin{pmatrix} \Sigma(x,Q^2) \\ g(x,Q^2) \end{pmatrix}. \tag{3.36}$$

The splitting functions themselves are calculated in perturbative QCD as a series expansion in $\alpha_s(Q^2)/2\pi$. Results for the splitting functions have been found up to NNLO. At leading order they were found to be [98–100]:

$$P_{qq} = C_F \left[\frac{1+z^2}{(1-z)_+} + \frac{3}{2}\delta(1-z) \right], \tag{3.37}$$

$$P_{qg} = T_F \left[z^2 + (1-z)^2 \right], \tag{3.38}$$

$$P_{gq} = C_F \left[\frac{1+(1-z)^2}{z} \right], \tag{3.39}$$

$$P_{gg} = 2C_A \left[\frac{z}{(1-z)_+} + \frac{1-z}{z} + z(1-z) \right] + \delta(1-z) \left[\frac{11}{6} C_A - \frac{2}{3} T_F N_f \right], \tag{3.40}$$

where $C_F = \frac{N_c^2-1}{2N_c} = 4/3$, $C_A = N_c$ and $T_R = 1/2$ are the QCD Casimir invariants. N_f is the number of active flavors, *i.e.*, the number of quarks for which $Q^2 \geq m_q^2$. Given a sufficiently smooth test function $f(z)$, the "plus" distribution $1/(1-z)_+$ is defined so that its integral with $f(z)$ is

$$\int_0^1 dz \, \frac{f(z)}{(1-z)_+} = \int_0^1 dz \frac{f(z) - f(1)}{1-z}. \tag{3.41}$$

To solve the DGLAP equations, it is also necessary to determine the strong coupling strength up to the order one is working with. At NLO, the running coupling $\alpha_s(Q^2)$ can be determined numerically for a given value of Λ via

$$\frac{1}{\alpha_s(Q^2)} + b' \ln \left(\frac{b' \alpha_s(Q^2)}{1 + b' \alpha_s(Q^2)} \right) = b \ln \left(\frac{Q^2}{\Lambda^2} \right). \tag{3.42}$$

Here, $b = (11 - 2N_f/3)/(4\pi)$ and $b' = (102 - 24N_f/3)/(16\pi^2 b)$, Λ is the $\Lambda_{\rm QCD}$ parameter and N_f is the number of active quark flavors mentioned earlier. The running coupling depends on the number of active flavors. For example, in a region where Q^2 is smaller than the square of the *charm* mass, $Q^2 < (1.275 \text{ GeV})^2$, the number of active flavors is $N_f = 3$. For Q^2 in the range between the square of the *charm* and the square of the *bottom* quark masses, $(1.275 \text{ GeV})^2 < Q^2 < (4.18 \text{ GeV})^2$, the number of active flavors becomes $N_f = 4$. As Q^2 increases, more quark flavors become active.

Alternatively, one can start out of a given value of $\alpha_s(Q^2)$ to obtain the corresponding Λ for a given flavor number, as Λ depends on the number of active flavors. Using the quark mass values given in the 2018 Particle Data [101], the requirement of continuity of the running coupling $\alpha_s(Q^2)$ across the thresholds yields the following $\Lambda_{\rm QCD}$ values:

$$\begin{aligned} N_f &= 3, \qquad & \Lambda_{\rm QCD} &= 0.370 \text{ GeV}, \\ N_f &= 4, \qquad & \Lambda_{\rm QCD} &= 0.228 \text{ GeV}, \\ N_f &= 5, \qquad & \Lambda_{\rm QCD} &= 0.092 \text{ GeV}, \end{aligned} \tag{3.43}$$

in the $\overline{\rm MS}$ scheme.

Exact analytic solutions of the evolution equations are not known, except for the LO non-singlet equation. Hence the evolution equations are solved numerically. Several codes are available for solving these equations. Here we use the so-called brute-force method [102].

Chapter 4

Quark Target Model

In this Chapter, we construct the quark target model [33]. Instead of having a hadron as a target, in the QTM the target is taken to be a dressed quark. As discussed in the Introduction, the dressed quarks themselves are seen as embedding a substructure that contains both quarks and gluons. With this in mind, we start presenting the formalism for calculating the PDFs of a quark target at leading order in $\alpha_s = g^2/(4\pi)$. We compute the quark and gluon distributions in the dressed quark at one-loop in perturbative QCD. Then, we discuss an extension of the model to incorporate a gluon mass in a gauge invariant way. In the last part of this chapter, we present the convolution formalism, which combines the results obtained with the NJL model and another valence quark model to obtain the quark and gluon PDFs of the pion.

4.1 General formalism

In this sectiom, we formulate the QTM and present the definitions of the PDFs of interest. To formulate the QTM, we begin with an effective quark-gluon Lagrangian,

which is identical in form to the QCD Lagrangian:

$$\mathcal{L} = \sum_q \bar{\psi}_q (i\not{D} - m_q)\psi_q - \frac{1}{4} G^a_{\mu\nu} G^{\mu\nu}_a + \mathcal{L}_{\text{GF}} \,. \tag{4.1}$$

Here, ψ_q denotes a quark field and m_q its mass. Although this lagrangian has the same form of the QCD lagrangian, we call it effective because ψ_q will be a quark dressed by the interactions of an underlying low-energy effective model of QCD rather than QCD itself, and thus the quark mass m_q will not be the true current quark mass. However, within the context of the QTM, we shall refer to ψ_q and m_q as the "bare quark field" and "bare quark mass," respectively. We additionally include a gauge-fixing Lagrangian $\mathcal{L}_{\text{GF}}$, which is necessary to quantize the theory and fully define the perturbative gluon propagator as discussed in Chapter 2. Since we restrict ourselves to $O(g^2)$ within the QTM—and since gluons only appear attached to quark vertices along with a factor g—no gluon self-interactions appear in this work; the leading-order QTM is effectively abelian.

A quark target of flavor Q (where we use capital letters to signify dressed quark targets in order to distinguish them from bare quarks), whose state is denoted by $|Q(P)\rangle$, has an unpolarized quark distribution $f_{q/Q}(x)$, defined by:

$$f_{q/Q}(x) = \int \frac{d\lambda}{4\pi}\, e^{ix(P\cdot n)\lambda} \langle \mathrm{Q}(P)|\bar{\psi}_q(0) \not{n} W(0, n\lambda)\psi_q(n\lambda)|\mathrm{Q(P)}\rangle \tag{4.2}$$

where n is a light-like vector defining the light cone and $x = k\cdot n/P\cdot n$ is the longitudinal momentum fraction carried by the struck bare quark. We choose to write the PDFs using a light-vector n instead of the form appearing in Eq. (3.4) because it proves more convenient for our purposes. Here, $W(0, n\lambda)$ is the Wilson line operator connecting the quark and antiquark fields introduced in order to ensure color gauge invariance of the

PDF:

$$W(0,n\lambda) = \mathrm{P}\,\exp\left(-ig\int_{\lambda}^{0} d\xi\, n\cdot A(n\xi)\right)\,, \tag{4.3}$$

with P denoting the path-ordering operator. The unpolarized gluon distribution in the quark is defined as

$$x f_{g/Q}(x) = \int \frac{d\lambda}{2\pi}\frac{1}{P\cdot n} e^{ix(P\cdot n)\lambda}\langle Q(P)|G^{+}_{\mu}(0)W(0,n\lambda)G^{\mu+}(n\lambda)|Q(P)\rangle. \tag{4.4}$$

The quark and gluon PDFs within the quark target can be calculated by evaluating Feynman diagrams. The momentum space Feynman rules for the operator defining the PDFs are given below in Eqs. (4.5),(4.6) and (4.7). In these diagrams, the red dot represents the operator insertion. The operator insertion can be on the quark legs, on the gluon legs or on the quark-quark-gluon vertex. The latter of which arises from the Wilson line.

$$= \frac{\not{n}}{2}\delta\left(n\left[xP - \frac{k_1+k_2}{2}\right]\right)\,, \tag{4.5}$$

$$= \frac{-1}{(P\cdot n)}\left[(nk_1)g^{\rho\mu_1} - k_1^{\rho}n^{\mu_1}\right]\delta_{a_1a_2}\left[(nk_2)g_{\rho}^{\mu_2} - k_{2\rho}n^{\mu_2}\right]$$
$$\times\left\{\delta\left(n\left[xP - \frac{k_1+k_2}{2}\right]\right) + \delta\left(n\left[xP + \frac{k_1+k_2}{2}\right]\right)\right\} \tag{4.6}$$

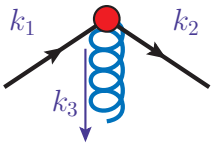

$$= \frac{g n^{\mu_3}}{(k_3 n)} \frac{\not{n} t^{a_3}}{2} \left\{ \delta \left(n \left[xP - \frac{k_1 + k_2 + k_3}{2} \right] \right) + \delta \left(n \left[xP - \frac{k_1 + k_2 - k_3}{2} \right] \right) \right\}. \quad (4.7)$$

Eq. (4.7) is the momentum space rule for the Wilson line, and it can be derived by first splitting the Wilson line appearing in Eq. (4.2) into a Wilson line going to infinity and then back to the endpoint

$$W(x, y) = W(x, +\infty) W(+\infty, y) = [W(+\infty, x)]^\dagger W(+\infty, y), \quad (4.8)$$

and then expanding each of the Wilson lines above to first order in g (since reattachment of the gluon to the quark target will introduce another factor of g). This means we approximate the Wilson line as:

$$[W(+\infty, x)]^\dagger W(+\infty, y) \approx 1 + ig \int_x^\infty d\xi \, n \cdot A(\xi) - ig \int_y^\infty d\xi \, n \cdot A(\xi) + O(g^2) \,. \quad (4.9)$$

When this expansion is inserted in Eq. (4.2), the first term gives rise to the diagram in Eq. (4.5) while the g-order terms are responsible for the two terms contained in the Wilson line diagram in Eq. (4.7).

The one-loop diagrams contributing to the quark PDF of the quark target are depicted in Fig. 4.1, while the quark target gluon PDF is represented by a single diagram, which is depicted in Fig. (4.2). In every diagram, the quark field renormalization constant Z_2 is implicitly present, since the operator defining the PDFs is defined in terms of the unrenormalized fields [59]. However, Z_2 can also be expanded as a series in g, with the leading order form

$$Z_2 = 1 + g^2 Z_2^{(2)} + O(g^3). \quad (4.10)$$

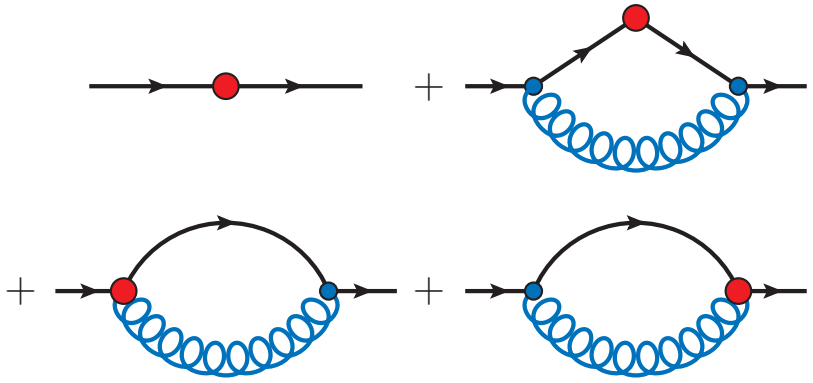

FIGURE 4.1 — Leading order diagrams contributing to the quark PDF in the quark target model.

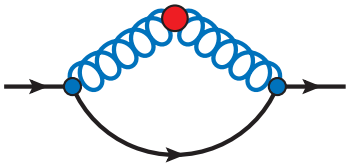

FIGURE 4.2 — Leading order diagram contributing to the gluon PDF in the quark target model.

At leading-order, Z_2 only effectively contributes to the first diagram of Fig. 4.1.

The PDF definitions given in Eqs. (4.2) and (4.4) are gauge invariant, but the individual diagrams in Fig. 4.1 are not. As an extreme example of this, the diagram in Eq. (4.7) is zero in light cone gauge because $n \cdot A = 0$—and thus, the Wilson line is unity. This is not true in general. The Wilson line carries momentum in covariant gauges as we shall see. To study the gauge dependence of the various contributions to the quark PDF of the quark target, given by the diagrams in Figs. 4.1, we will explicitly consider general covariant and light cone gauges.

4.2 Quark and Gluon Distributions

Because the quark propagator gets dressed at order g^2, before evaluating the various diagrams in Fig. 4.1 and 4.2, we first consider the quark self-energy. The physical dressed quark mass and quark field renormalization constant can be understood by considering the gap equation for the *unrenormalized* quark propagator:

$$S_0^{-1}(p) = \not{p} - m_q - \Sigma(p), \tag{4.11}$$

where $S_0(p)$ is the unrenormalized dressed quark propagator, m_q is the bare quark mass, and $\Sigma(p)$ is the self-energy, where at leading order it is given by

$$\Sigma^{(1)}(p) = ig^2 C_F \int \frac{d^4k}{(2\pi)^4} \gamma^\mu S(p-k) \gamma^\nu D_{\mu\nu}(k)\,, \tag{4.12}$$

and takes the general form

$$\Sigma(p) = A(p^2)\not{p} + B(p^2) + C(p^2)\not{n}, \tag{4.13}$$

where in covariant gauges $C(p^2) = 0$. We emphasize that dressing and renormalization are distinct procedures. Dressing accounts for the incorporation of interactions in the calculation of Green's functions, whereas renormalization rescales the fields through factors such as Z_2. These procedures are often done in tandem since—when an infinite UV regulator is taken—the dressing produces UV divergences that must be contained by renormalization. The unrenormalized and renormalized propagator are both dressed: they are defined respectively as time-ordered two-point Green's functions of the unrenormalized and renormalized quark fields and differ by a factor Z_2, i.e., $S_0(p) = Z_2\, S(p)$.

At order g^2 in the QTM the gluon propagator does not get dressed, therefore, in a general covariant gauge and in light cone gauge the gluon propagators take the

standard form:

$$D^{\rm cov}_{\mu\nu}(k) = \frac{-1}{k^2+i0}\left[g_{\mu\nu} - (1-\xi)\frac{k_\mu k_\nu}{k^2+i0}\right], \tag{4.14a}$$

$$D^{\rm LC}_{\mu\nu}(k) = \frac{-1}{k^2+i0}\left[g_{\mu\nu} - \frac{k_\mu n_\nu + n_\mu k_\nu}{(k\cdot n)}\right]. \tag{4.14b}$$

The self-energy accounts for changes in the quark propagator due to the quark and gluon interactions shifting the pole of the propagator to what is identified to be the physical mass M_q:

$$M_q = m_q + \Sigma(\not{p} = M_q). \tag{4.15}$$

The shift of the quark mass also causes the residue of the propagator to change. Near the physical pole $\not{p} \simeq M_q$,

$$S_0(p) = \frac{1}{\not{p} - m_q - \Sigma(p)} \simeq \frac{Z_2}{\not{p} - M_q}, \tag{4.16}$$

where Z_2 is the field renormalization constant, obtained by

$$Z_2^{-1} = 1 - \left.\frac{d\Sigma(p)}{d\not{p}}\right|_{\not{p}=M_q}. \tag{4.17}$$

Using Eqs. (4.12) and (4.17) the quark self-energy and field renormalization constant are found to be:

$$\Sigma^{\rm cov}(p) = -g^2 C_F \int_0^1 dx\,(4\,M_q - 2\,x\,\not{p})I_2(\Delta_q(x)) \tag{4.18a}$$

$$Z_2^{\rm cov} = 1 + g^2 C_F \int_0^1 dx\left[2\,x\,I_2(\Delta_q(x)) + 8\,M_q^2\,(x-2)(x-1)\,x\,I_3(\Delta_q(x))\right], \tag{4.18b}$$

where the Feynman mass parameter is given by

$$\Delta_q(x) = (1-x)^2 M_q^2\,, \tag{4.19}$$

with the 2- and 3- propagator integrals defined in a regularization scheme independent manner:

$$I_n(\Delta) \equiv i \int \frac{\mathrm{d}^4k}{(2\pi)^4} \frac{1}{(k^2 - \Delta + i\epsilon)^n}, \tag{4.20}$$

Details of the calculations are given in Appendix A.5. Throughout this thesis we shall employ the proper-time regularization (PTR). In the context of PTR, first Feynman parametrization is used to combine a product of propagators into a single propagator, then Wick rotating to Euclidean space and finally using:

$$\frac{1}{A^n} = \frac{1}{(n-1)!} \int_0^\infty d\tau\, e^{-\tau\Delta} \longrightarrow \frac{1}{(n-1)!} \int_{1/{\Lambda_{\mathrm{UV}}}^2}^{1/{\Lambda_{\mathrm{IR}}}^2} d\tau\, \tau^{n-1}\, e^{\tau\Delta}. \tag{4.21}$$

For completeness, we quote here the basic integrals and their results in the PTR scheme that will appear throughout this thesis:

$$I_2(\Delta) = -\frac{1}{16\pi^2} \int \mathrm{d}\tau\, \frac{1}{\tau}\, e^{-\tau\Delta} = -\frac{1}{16\pi^2}\, \Gamma\left(0, \Delta/\Lambda_{\mathrm{UV}}^2, \Delta/\Lambda_{\mathrm{IR}}^2\right), \tag{4.22}$$

$$I_3(\Delta) = \frac{1}{16\pi^2} \int \mathrm{d}\tau\, \frac{1}{2}\, e^{-\tau\Delta} = \frac{1}{32\pi^2} \frac{1}{\Delta} \left(e^{-\Delta/\Lambda_{\mathrm{UV}}^2} - e^{-\Delta/\Lambda_{\mathrm{IR}}^2} \right). \tag{4.23}$$

where $\Gamma(s, a, b) = \int_a^b \mathrm{d}t\, t^{s-1}\, e^{-t}$ is the generalized incomplete gamma function.

Because we are using the on-shell renormalization scheme Z_2^{cov} is independent of the choice of covariant gauge [103].

The two diagrams in the second line of Fig. 4.1 are the Wilson line diagrams. Its explicit form, and likewise the triangle diagram form, can be deduced from the definition of the unpolarized quark PDF given by Eq. (4.2). We start by the bilocal operator defining the unpolarized quark PDF:

$$\hat{O}_q(0, n\lambda) = \bar{\psi}_q(0)\, \not{n}\, W(0, n\lambda)\, \psi_q(n\lambda), \tag{4.24}$$

where $W(0, n\lambda)$ is the Wilson line defined in Eq. (4.3). In order to derive the corrections to the quark PDF, we start from the off-diagonal matrix element

$$\langle \mathrm{Q}(p_2)|\, \hat{O}_q(y,z)\, |\mathrm{Q}(p_1)\rangle_c, \tag{4.25}$$

where at the end we take $p_1 = p_2 = P$, $y = 0$ and $z = n\lambda$, and the result is inserted in the PDF definition in Eq. (4.2). The Lehmann, Symanzik and Zimmermann (LSZ) formalism is used to write the transition amplitude in terms of time-ordered products of the interacting theory [104]:

$$\begin{aligned}\langle \mathrm{Q}(p_2)|\, \hat{O}_{q/g}(y,z)\, |\mathrm{Q}(p_1)\rangle_c = (-i)^2 \int \mathrm{d}^4x_1 \int \mathrm{d}^4x_2\, e^{ip_2x_2}\, \bar{u}(p_2)\, [i\overrightarrow{\not\partial}_{x_2} - m] \\ \times \langle \Omega|\, T\left[\psi(x_2)\hat{O}_{q/g}(y,z)\bar{\psi}(x_1)\right]|\,\Omega\rangle [-i\overleftarrow{\not\partial}_{x_1} - m]\, u(p_1)\, e^{-ip_1x_1},\end{aligned} \tag{4.26}$$

where $|\Omega\rangle$ is the interacting vacuum state. The vacuum expectation value is:

$$\begin{aligned}\langle \Omega|\, T\left[\psi(x_2)\hat{O}_{q/g}(y,z)\bar{\psi}(x_1)\right]|\,\Omega\rangle &= \langle 0|\, T\left[\psi(x_2)\hat{O}_{q/g}(y,z)\bar{\psi}(x_1)\, e^{iS_{\mathrm{int}}}\right]|\,0\rangle \\ &= \langle 0|\, T\left[\psi(x_2)\hat{O}_{q/g}(y,z)\bar{\psi}(x_1)\left(1 + iS_{\mathrm{int}} + \frac{1}{2!}\,(iS_{\mathrm{int}})\,(iS_{\mathrm{int}}) + \cdots\right)\right]|\,0\rangle,\end{aligned} \tag{4.27}$$

and

$$S_{\mathrm{int}} = -g \int \mathrm{d}^4x\ \bar{\psi}(x)\gamma^\mu\psi(x)A_\mu(x) \tag{4.28}$$

is the quark-gluon interaction part of the QCD action. The operator $\hat{O}_{q/g}$ can be either the quark or gluon bilocal operators defining the PDFs. Notice that the Wilson line should also be expanded in powers of the coupling "g". The first term in Eq. (4.27) gives the vacuum expectation value at zeroth order in the strong coupling. This term when inserted in Eq. (4.26) and then in quark PDF definition will lead to the zeroth order quark PDF illustrated in the first diagram in Fig. 4.1,

$$f^{(0)}_{q/Q} = \delta(1-x), \tag{4.29}$$

where there is an implicit Z_2 factor multiplying this contribution as stated earlier. Following the same logic, the next term in Eq. (4.27) of order g in the interaction will give rise to the Wilson line contribution given by the diagrams in the second line of Fig. (4.1), where the Wilson line is expanded to $O(g)$ according to Eq. (4.9). These two diagrams give the same contribution. Together they give:

$$f^W_{q/Q}(x) = g^2 \frac{C_F}{(P\cdot n)} n^\nu \int \frac{d^4k}{(2\pi)^4} \left[\delta\left(x - \frac{k\cdot n}{P\cdot n}\right) - \delta(1-x)\right] \times \bar{u}(P) \frac{i}{n\cdot(P-k)+i0} \gamma^\mu S(k) \not{n} D_{\mu\nu}(P-k) u(p). \tag{4.30}$$

In practice, this integral is evaluated by calculating Mellin moments to eliminate the delta function, and then taking the inverse Mellin transform. This means evaluating the PDFs using the moments where

$$A_n = \int_0^1 dx\, x^{n-1} f_{i/J}(x). \tag{4.31}$$

A proper calculation is shown in App. C. Using this approach, we find for the Wilson line contribution:

$$f^W_{q/Q}(x) = g^2 C_F \left[\frac{4x}{1-x} I_2(\Delta_q(x)) - \delta(1-x)\int_0^1 dy \frac{4y}{1-y} I_2(\Delta_q(y))\right], \tag{4.32}$$

where this result is independent of ξ. The appearance of a delta term corresponds to the so-called virtual diagram that appears in the cut diagram approach [59]. It has the same divergent behavior necessary to cancel the divergence in the first term.

Another common approach to evaluate such integrals is to employ light-cone coordinates. In this case the delta function selects the +-component of the momentum carried by the quarks, therefore it can be trivially integrated in k^+. The k^- integral is then calculated using the residue theorem and one end up with a quadratic integral in $\mathbf{k}_\perp$.

The second diagram in the fisrt line of Fig. 4.1 is the triangle diagram, its contribution comes from expanding the interacting vacuum to second order in the strong coupling g, i.e., from the third term in Eq. (4.27) that when inserted back in the PDF definition in Eq. (4.2), gives:

$$f_{q/Q}^{\text{tri}}(x) = \frac{ig^2}{2}\frac{C_F}{P\cdot n}\int\frac{\mathrm{d}^4k}{(2\pi)^4}\,\delta\left(x-\frac{k\cdot n}{P\cdot n}\right)\bar{u}(P)\,\gamma^\mu\,S(k)\,\not{n}\,S(k)\,\gamma^\nu\,D_{\mu\nu}(P-k)\,u(P). \tag{4.33}$$

The derivations are all shown in App. C. In a covariant gauge, we find the result to be:

$$f_{q/Q}^{\text{tri,cov}}(x) = g^2C_F\left[2(x-1)I_2(\Delta_q(x)) + 8x(x-1)M_q^2I_3(\Delta_q(x))\right]. \tag{4.34}$$

Adding all the contributions, the quark PDF can be written as

$$f_{q/Q}(x) = Z_2\delta(1-x) + f_{q/Q}^{\text{tri}}(x) + f_{q/Q}^{W}(x). \tag{4.35}$$

The gluon PDF for the QTM does not have a Wilson line contribution at leading order. The only diagram contributing to the gluon PDF in Fig. 4.2 is given by:

$$\begin{aligned} xf_{g/Q}(x) &= -ig^2C_F\int\frac{d^4k}{(2\pi)^4}\,\bar{u}(P)\gamma^{\mu_1}S(P-k)\gamma^{\mu_2}u(P) \\ &\times\frac{1}{P\cdot n}\left[(n\cdot k)g_{\rho\mu_1}-k_\rho n_{\mu_1}\right]\left[(n\cdot k)g^\rho_{\ \mu_2}-k^\rho n_{\mu_2}\right]\left\{\delta\left(n\left[xP-k\right]\right)+\delta\left(n\left[xP+k\right]\right)\right\} \end{aligned} \tag{4.36}$$

and evaluates to:

$$xf_{g/Q}(x) = -g^2C_F\left\{2\left[1+(1-x)^2\right]I_2(\Delta_g(x)) + 8x^2(1-x)M_q^2I_3(\Delta_g(x))\right\}, \tag{4.37}$$

where here the Feynman mass parameter is given by

$$\Delta_g(x) = x^2M_q^2 = \Delta_q(1-x)\,. \tag{4.38}$$

4.2.1 Individual diagrams in light cone gauge

In light cone gauge, we find the quark renormalization factor to be:

$$Z_2^{\mathrm{LC}} = Z_2^{\mathrm{cov}} + g^2 C_F \int_0^1 \mathrm{d}x \left\{ \frac{4x}{1-x} I_2\big(\Delta_q(x)\big) \right\}, \tag{4.39}$$

where the "extra" term relative to the covariant gauge appears due to the "extra" term (the n-dependent) in the light cone gauge gluon propagator. We find the triangle diagram to be:

$$f_{q/Q}^{\mathrm{tri,LC}}(x) = f_{q/Q}^{\mathrm{tri,cov}}(x) - g^2 C_F \frac{4x}{1-x} I_2(\Delta_q(x)) \,. \tag{4.40}$$

Clearly, the Wilson line contribution is zero since it reduces to unity in this gauge,

$$f_{q/Q}^{W,\mathrm{LC}}(x) \;\; = 0. \tag{4.41}$$

One may compare these results to Eq. (4.35) and find that:

$$Z_2^{\mathrm{LC}} \delta(1-x) + f_{q/Q}^{\mathrm{tri,LC}}(x) = Z_2^{\mathrm{cov}} \delta(1-x) + f_{q/Q}^{\mathrm{tri,cov}}(x) + f_{q/Q}^{W,\mathrm{cov}}(x) \,, \tag{4.42}$$

as expected from gauge invariance of the PDF. Although there is no Wilson line diagram in light cone gauge, the contributions from the Wilson line in the covariant gauge are split into Z_2 and the triangle diagram in this gauge.

4.2.2 Sum Rules

Here we discuss a relevant aspect of the analytical resuls obtained. The quark number and momentum sum rules for the QTM can be stated as:

$$\int_0^1 \mathrm{d}x\, f_{q/Q}(x) = 1, \tag{4.43}$$

$$\int_0^1 \mathrm{d}x \left[x\, f_{q/Q}(x) + x\, f_{g/Q}(x)\right] = 1. \tag{4.44}$$

With a little calculus, it is possible to analytically show that the quark PDF in Eq. (4.35) satisfies the quark number sum rule:

$$\begin{aligned}\int_0^1 \mathrm{d}x\, f_{q/Q}(x) &= Z_2^{\mathrm{cov}} + \int_0^1 \mathrm{d}x \left[f_{q/Q}^{\mathrm{tri,\,cov}}(x) + f_{q/Q}^{\mathrm{W,\,cov}}(x)\right] \\ &= 1 + 2\, g^2\, C_F \int_0^1 \mathrm{d}x \,\frac{\mathrm{d}}{\mathrm{d}x}\left[x(x-1) I_2\big(w_q(x)\big)\right] = 1,\end{aligned} \tag{4.45}$$

Notice from Eq. (4.32) that the Wilson line does not contribute to the quark number sum rule. Upon integration over x the two terms cancel exactly. The same is not true for the momentum sum rule: In general, in covariant gauge, the Wilson line does in fact carry momentum as will be shown explicitly in the next Chapter when we present our numerical results. Indeed, one may note that only when the Wilson line contribution is included in the quark PDF do we find

$$f_{q/Q}(1-x) = f_{g/Q}(x) + \{\delta(x) \text{ terms}\} \tag{4.46}$$

This symmetry ensures the momentum sum rule is satisfied once the quark number rule is already satisfied, as it entails:

$$\int_0^1 dx\, x \left[f_{q/Q}(x) + f_{g/Q}(x)\right] = \int_0^1 dx\, f_{q/Q}(x) = 1\,. \tag{4.47}$$

The fact that the Wilson line contributes to the momentum sum rule has important implications for the calculation of partonic correlation functions in QCD effective theories.

4.3 Quark Target Model with a Gluon Mass

In this section we extend the QTM to incorporate a gluon mass and study its impact on the QTM PDFs. As mentioned earlier in Sec. 2.1, the gluon propagator appears to be described by a momentum-dependent mass function that saturates at a finite value in the IR. The mass is generated nonperturbatively by the full structure of QCD, including gluon self-interactions to all orders in α_s. It thus isn't possible to reproduce gluon mass generation in an effective model of gluons at order α. Nonetheless, the effect of gluon mass can be incorporated in the model by placing an explicit gluon mass in the Lagrangian. This is notoriously at odds with the QCD symmetries. However, this approach has been sucessfully used to obtain the two-point ghost and gluon correlation functions in great agreement with lattice results already at one-loop [105, 106], which is a quite remarkable result given the simplicity of the approach. Therefore, we proceed to explore the implications of incorporating a finite gluon mass to the QTM PDFs.

A naive gluon mass Lagrangian that has been used to describe lattice QCD results has the form:

$$\mathcal{L}_{\text{mass}}^{(\text{naive})} = m_g^2 \text{Tr}\left[A_\mu(x)A^\mu(x)\right] , \tag{4.48}$$

but this notoriously violates gauge invariance. Not surprisingly, using this Lagrangian to calculate PDFs in the quark target model explicitly violates the momentum sum rule—as we shall see below. This occurs because a gauge transformation can always be

used to introduce explicit dependence on spacetime coordinates x into the Lagrangian, nullifying conservation of the energy-momentum tensor.

Using the Lagrangian in Eq. (4.54) leads to a gluon propagator with a gluon mass. Explicitly, the covariant and light cone gauge propagators obtained are respectively:

$$D^{\text{cov}}_{\mu\nu}(k) = \frac{-1}{k^2 - m_g^2 + i0}\left[g_{\mu\nu} + \frac{(\xi-1)k_\mu k_\nu}{k^2 - \xi m_g^2}\right], \tag{4.49a}$$

$$D^{\text{LC}}_{\mu\nu}(k) = \frac{-1}{k^2 - m_g^2 + i0}\left[g_{\mu\nu} - \frac{k_\mu n_\nu + n_\mu k_\nu}{(kn)}\right]. \tag{4.49b}$$

It is worth noting that in the Landau gauge ($\xi = 0$), the gluon propagator remains transverse, even with the introduction of gluon mass. For the QTM calculations carried out in the last section, the only effect of introducing a gluon mass is to change the massless gluon propagators appearing in the PDF calculations to their massive counterparts above. This will, certainly, bring terms $\sim m_g^2$. The presence of a gluon mass in the propagator changes the Feynman mass parameters used in the previous section to:

$$\Delta_q(x) = x m_g^2 + (1-x)^2 M_q^2, \tag{4.50}$$

$$\Delta_g(x) = (1-x)m_g^2 + x^2 M_q^2 = \Delta_q(1-x)\,. \tag{4.51}$$

Using the massive gluon propagator to calculate the quark and gluon QTM PDFs gives the following result

$$f_{q/Q}(x; m_g) = f_{q/Q}(x) - g^2 C_F\, 4x(1-x)m_g^2\, I_3\big(\Delta_q(x)\big), \tag{4.52}$$

and

$$x\, f^{\text{naive}}_{g/Q}(x;m_g) = x\, f_{g/Q}(x) - g^2 C_F \Big\{ 4x^2(1-x)m_g^2 + 8(1-x)^2 m_g^2 \Big\} I_3\big(\Delta_g(x)\big)\,. \tag{4.53}$$

The functions $f_{q/Q}(x)$ and $f_{g/Q}(x)$ are the same functions obtained in Eqs. (4.35) and (4.36) in the last section, except for the new Feynman mass parameters that includes a gluon mass in the basic integrals. The quark field renormalization constant, Z_2 from Eqs. (4.18b) and (4.39), is also updated accordingly. The quark PDF in Eq. (4.52) with the Z_2 modified exactly satisfies quark number sum rule for any m_g. However, the momentum sum rule is violated for the quark and gluon PDFs given in Eq. (4.52) and (4.53). Crucially, we do not observe the expected symmetry $f_{q/Q}(x;m_g) = f^{\text{naive}}_{g/Q}(1-x;m_g)$, which would have guaranteed the momentum sum rule. Instead, the symmetry is violated by an amount

$$f_{q/Q}(x;m_g) - f^{\text{naive}}_{g/Q}(1-x;m_g) = g^2 C_F \Big\{ 8m_g^2 \frac{x^2}{(1-x)}\, I_3\big(W_g(x)\big) \Big\}\,,$$

which is proportional to m_g^2.

Nevertheless, this can be resolved by using a gauge-invariant Lagrangian incorporating gluon mass which has been suggested by Cornwall [44]. This gauge-invariant lagrangian contains two terms, one which is exactly equal to the "naive" lagrangian just discussed above and the other is constructed by introducing a new color octet scalar field. It is given by:

$$\mathcal{L}_{\text{mass}} = m_g^2 \text{Tr}\left[\left(A_\mu(x) - \frac{1}{ig}\Big(\partial_\mu V(\theta(x))\Big) V^{-1}(\theta(x)) \right)^2 \right]\,, \tag{4.54}$$

where the field $V(\theta(x)) = \exp\{i\theta(x)\}$ transforms under the fundamental representation of the color group, so that its covariant derivative is

$$D_\mu V\left(\theta(x)\right) = \partial_\mu V\left(\theta(x)\right) - igA_\mu(x)V\left(\theta(x)\right), \tag{4.55}$$

allowing the mass Lagrangian (4.54) to be written in terms of the covariant derivative:

$$\mathcal{L}_{\text{mass}} = -\frac{m_g^2}{g^2}\text{Tr}\left[\left\{\left(D_\mu V\left(\theta(x)\right)\right) V^{-1}\left(\theta(x)\right)\right\}^2\right]. \tag{4.56}$$

This Lagrangian is non-renormalizable, but since the calculations in this work are done at one loop, non-renormalizability is not an issue.

If the change in the gluon propagator were the only effect of introducing gluon mass—as is the case when the naive Lagrangian of Eq. (4.48) is used—then we would observe violation of the momentum sum rule. However, the Cornwall Lagrangian ends up saving the momentum sum rule, as we shall presently see. Using the Lagrangian in Eq. (4.54) or Eq. (4.56) has two primary effects on the calculation of PDFs in the quark target model. One of these is that the gluon propagators will also be massive and have the same form as given in Eqs. (4.49a) and (4.49b), and the other effect is that the Cornwall lagrangian will give additional terms to the PDF. Because the Cornwall lagrangian introduces new fields, these fields can also carry momentum since they will contribute to the energy-momentum tensor (EMT). The contribution of the mass Lagrangian to the EMT is found to be:

$$T^\theta_{\mu\nu} = \frac{{m_g}^2}{g^2}\Big\{-2\text{Tr}\Big[\left(D_\mu V\right) V^{-1}\left(D_\nu V\right) V^{-1}\Big] + g_{\mu\nu}\text{Tr}\Big[\left(D^\alpha V\right) V^{-1}\left(D_\alpha V\right) V^{-1}\Big]\Big\}. \tag{4.57}$$

Here, for the sake of simplifying the notation we have omitted the dependence of the fields $V \equiv V(\theta(x))$. Like the gluon light-cone correlator, the bilocal light cone correlator defining the theta-field PDF is defined such as that its first Mellin moment gives the

++ component of the ETM. Therefore, we find the bilocal light cone correlator defining the theta-field PDF to be:

$$x\, f_{\theta/Q}(x) = -\frac{2\, m_g^2}{g^2}\, \frac{n^\mu n^\nu}{P\cdot n} \int \frac{\mathrm{d}\lambda}{2\pi}\, e^{ix\lambda\, P\cdot n} \\ \Big\langle Q(P)\Big|\, \big[D_\mu V\big(\theta(0)\big)\big]\, V^{-1}\big(\theta(0)\big)\, W_A(0,n\lambda)\, \big[D_\nu V\big(\theta(n\lambda)\big)\big]\, V^{-1}\big(\theta(n\lambda)\big)\Big|Q(P)\Big\rangle. \quad (4.58)$$

Notice that, just like in the case of the quark and gluon PDF, the theta field PDF has been supplied with a gauge link such as that the bilocal operator defining the PDF is gauge-invariant. The following theta-field PDF contribution is obtained:

$$x f_{\theta/Q}(x) = g^2 C_F\, 8 m_g^2 (1-x)^2\, I_3\big(W_g(x)\big)\,. \quad (4.59)$$

Since the theta field is interpreted as an instanton in the gluon field [44], $f_{\theta/Q}(x)$ should be considered a contribution to the gluon PDF. Therefore, the full gluon PDF with the Cornwall mass term is given by the sum of $f^{\text{naive}}_{g/Q}(x;m_g)$ and $f_{\theta/Q}(x;m_g)$, and reads

$$f_{g/Q}(x;m_g) = f_{g/Q}(x) - 4\, g^2 C_F\, m_g^2\, x\,(1-x)\, I_3\big(w_g(x)\big). \quad (4.60)$$

With the introduction of the θ-field, one now observes that

$$\begin{aligned} f_{q/Q}(x;m_g) &= f^{\text{naive}}_{g/Q}(1-x;m_g) + f_{\theta/Q}(1-x;m_g) \\ &\equiv f_{g/Q}(1-x;m_g)\,, \end{aligned} \quad (4.61)$$

meaning that the expected symmetry relation indeed holds and the momentum sum rule is satisfied. However, the theta-field contribution to the gluon PDF must be accounted for to ensure observance of the momentum sum rule.

4.4 Pion PDFs

We now consider how to incorporate the QTM results derived above into existing results for hadron PDFs from low-energy effective models. In particular, we consider the pion as a concrete example, due to its prominent place in QCD as the Nambu-Goldstone boson of chiral symmetry breaking and because of the existence of both experimental data [2] and phenomenological PDF parametrizations [1] to compare against. The pion can be pictured as a bound state of two constituent quarks. These constituent —dressed quarks, on the other hand, are not structureless, they are composed of yet more "elementary" particles, the current quarks and gluons. Because PDFs are defined in terms of current fields, one needs to uncover the dressing layer of the dressed pion, which will reveal the dressed pion substructure. Therefore, a dressed quark can be described in terms of its substructure. One can address this by combining the dressed pion PDF (we shall refer as body-pion PDF), obtained from a low-energy model of QCD, with the QTM PDFs using a convolution formula. We shall refer to the resulting PDFs as QTM-modified pion PDF.

The QTM-modified pion PDF is obtained by taking a convolution of the model pion PDF $f_{Q/\pi}(x)$ obtained from a low-energy effetive model that only contains quark degrees of freedom, *e.g.* the NJL model, with the quark target model PDFs $f_{q,g/Q}(x)$ obtained in the previous sections, Eqs. (4.35),(4.37) and (4.60). In particular, the quark target is identified with the effective theory's quark degree of freedom—both denotes Q here. This gives us the convolution equation that gives the complete quark and gluon PDFs in the pion:

$$f_{q/\pi}(x) = \sum_{Q} \iint_0^1 \mathrm{d}z\, \mathrm{d}y\, \delta(x - yz)\, f_{q/Q}(y)\, f_{Q/\pi}(z). \tag{4.62}$$

$$f_{g/\pi}(x) = \sum_{Q} \iint_0^1 \mathrm{d}z\, \mathrm{d}y\, \delta(x - yz)\, f_{g/Q}(y)\, f_{Q/\pi}(z). \tag{4.63}$$

The above formulas amounts to describing the dressed pion in terms of its current quark and gluon substructure. We note that since the QTM PDFs satisfy the baryon number and momentum sum rules, this convolution guarantees the sum rules to be satisfied for $f_{q,g/\pi}(x)$ as long as the "body PDFs" $f_{Q/\pi}(x)$ also obey these sum rules. For a concrete example, we consider the PDF of a charged pion in the NJL model, which is calculated via:

$$f_{Q/\pi}(x) = -\frac{Z_\pi}{2P\cdot n}\int \frac{\mathrm{d}^4k}{(2\pi)^4}\delta\left(x-\frac{k\cdot n}{P\cdot n}\right)\mathrm{Tr}\left[\gamma_5\tau_- iS(k)\not{n}\frac{1}{2}(1\pm\tau_3)iS(k)\gamma_5\tau_+ iS(k-p)\right] \tag{4.64}$$

where the trace is over color, flavor and Dirac indices. The result is found to be [40]:

$$f_{Q/\pi}(x) = 3Z_\pi\left[-4I_2(\Delta_\pi(x)) + 8x(1-x)m_\pi^2\right] \tag{4.65}$$

for $Q = U, \bar{D}$, where

$$\Delta_\pi(x) = M_q^2 - x(1-x)m_\pi^2. \tag{4.66}$$

As discussed in Sec 2.4, the pion as a bound state of dressed quarks is a solution of the Bethe-Salpeter equation and can be fully characterized by the parameters introduced therein. We note that the QTM just developed should be applicable to other models closely related to the NJL model, like instanton liquid models [107, 108] which, besides realizing DCSB through a running quark mass function, includes explicit gluonic degrees of freedom.

Having introduced the analytical results, in the next Chapter we shall present the numerical results for the QTM PDFs and the quark and gluon distributions in the pion.

Chapter 5

Numerical Results

In this Chapter we present numerical results for the quark and gluon PDFs in the quark target model [33]. The quark target model PDFs contain UV divergences arising from loop integrals that must be regularized. Thus the numerical results are regularization scheme dependent. We employ proper time regularization with both UV and IR regulators [34–36] to obtain the numerical results presented here, but other schemes such as dimensional regularization (with MS or $\overline{\text{MS}}$ subtraction of the ϵ^{-1}divergences) can be used instead. In Appendix A.5 one can find a dictionary to translate the PDFs expressions in this work into other regularization schemes. For the results in this Chapter, we specifically use $\Lambda_{\text{UV}} = 645$ MeV and $\Lambda_{\text{IR}} = 240$ MeV as discussed in the context of the NJL model in Chapter 2, which are standard values that are used [36]. In the last part, the QTM PDFs are combined in the convolution formalism which was just presented in the last Chapter to obtain the quark and gluon PDFs in the pion. The PDFs are then evolved using the DGLAP equation to be compared to available experimental data and parametrization.

5.1 Quark Target Model

Results for the quark and gluon QTM PDFs at different values of the coupling strength $\alpha_s = g^2/(4\pi)$ are shown in Fig. 5.1. We remark that since $\delta(1-x)$ cannot be plotted, terms containing the delta function are not included in the plot. At large x the quark PDF is dominated by the $1/(1-x)$ term coming from the Wilson line in covariant gauges or the triangle diagram in light cone gauge. This behavior is in contrast to the familar quark PDFs inside hadrons and reflects that this quantity is a quark PDF inside itself. The gluon PDF is positive definite and, aside from the $\delta(1-x)$ term, the quark PDF is also positive-definite. Since the PDFs are linearly proportional to α_s, we observe that the curves within each panel of Fig. 5.1 merely differ by an overall factor.

Information about the dependence of the PDFs on the quark mass M_q is shown in Figs. 5.2 and 5.3. The quark PDF has little relative dependence on the quark mass, with the non-delta contributions being suppressed at larger quark masses. The gluon PDF is likewise suppressed at larger quark masses, and accordingly the gluon carries less momentum for larger quark masses.

We turn our attention to another relevant feature of the quark target model. In Tab. **5.1**, we present the Mellin moments of the quark and gluon QTM PDFs. In order to observe specifically the importance of the Wilson line in obeying the momentum sum rule, we split the quark PDF into two terms: one containing the Z_2 and triangle diagram contributions, and the other containing the Wilson line contributions. These are shown respectively in the second and third columns, with the fourth column containing the total quark Mellin moment and the last column containing the gluon Mellin moments. The first thing to be observed is that the Wilson line indeed does not contribute to the quark number sum rule as demonstrated analytically in the last subsection — Quark number sum rule is satisfied regardless. This can be read off the Tab. **5.1** for $s = 1$.

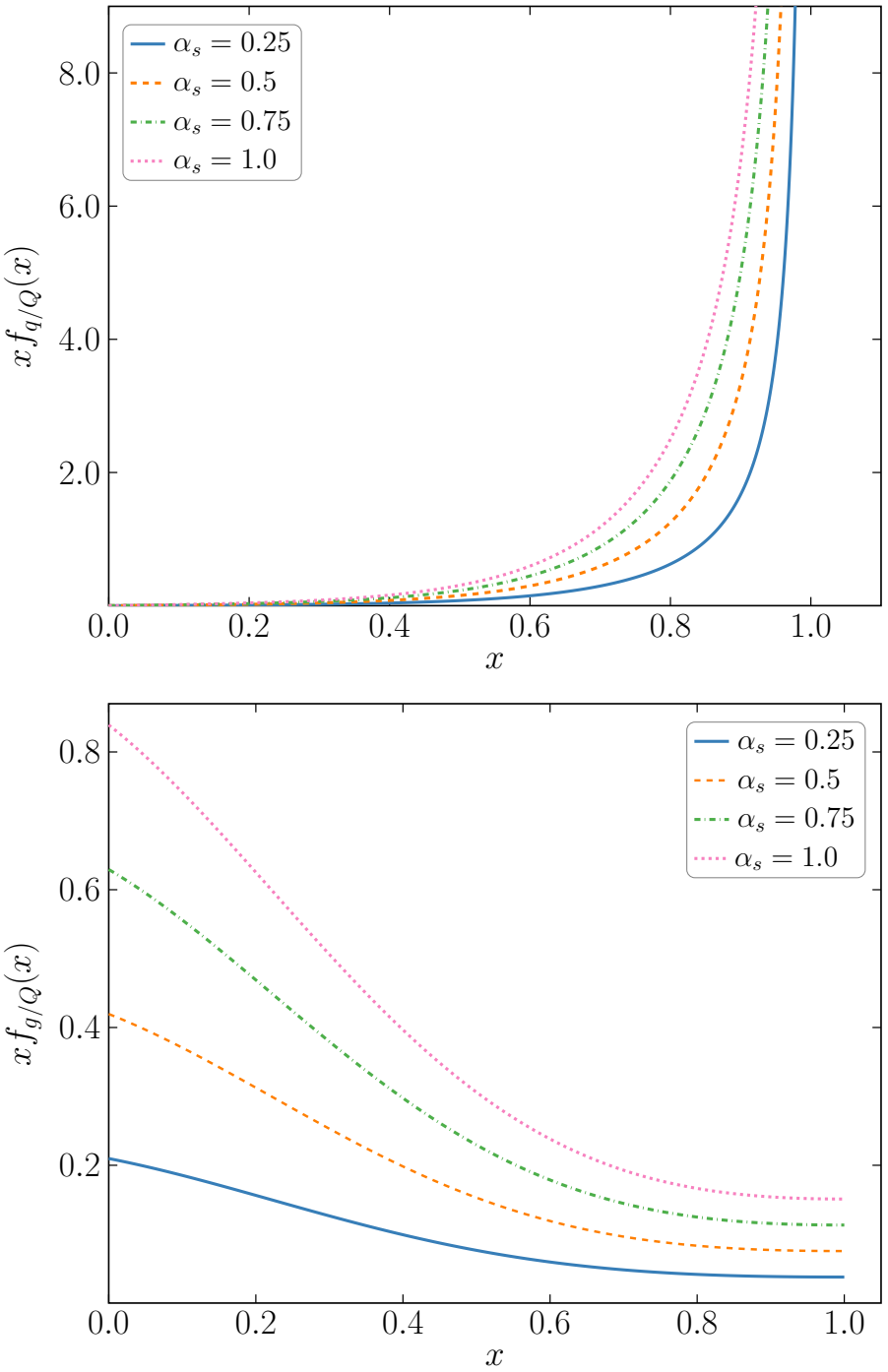

FIGURE 5.1 — Results for the quark and gluon momentum distributions for several values of α_s and fixed quark mass $M_q = 400$ MeV. A tilde in the quark PDF is used to indicate that the delta terms in Eq. (4.2) are not included.

The momentum sum rule, however, is oversaturated without the negative contribution from the Wilson line as it can be seen for $s = 2$. With $M_q = 400\,\text{MeV}$ and $\alpha_s = 0.5$ we find that the quarks carry about 81% of the total light cone momentum and gluons carry about 19%. The Wilson line contribution to the momentum sum rule is -0.1775, which is the same in all covariant gauges, because we are working at one-loop in the on-shell remormalization scheme. This result explicitly illustrates that Wilson line contributions can be large in covariant gauges.

The fact that the Wilson line can make sizeable contributions to the PDFs has important implications for model calculations in covariant gauges that do not explicitly include gauge link contributions to quantum correlation functions. For example, if one were to calculate only quark local operators, and infer the momentum fraction carried by gluons by imposing the momentum sum rule, then one must include Wilson line

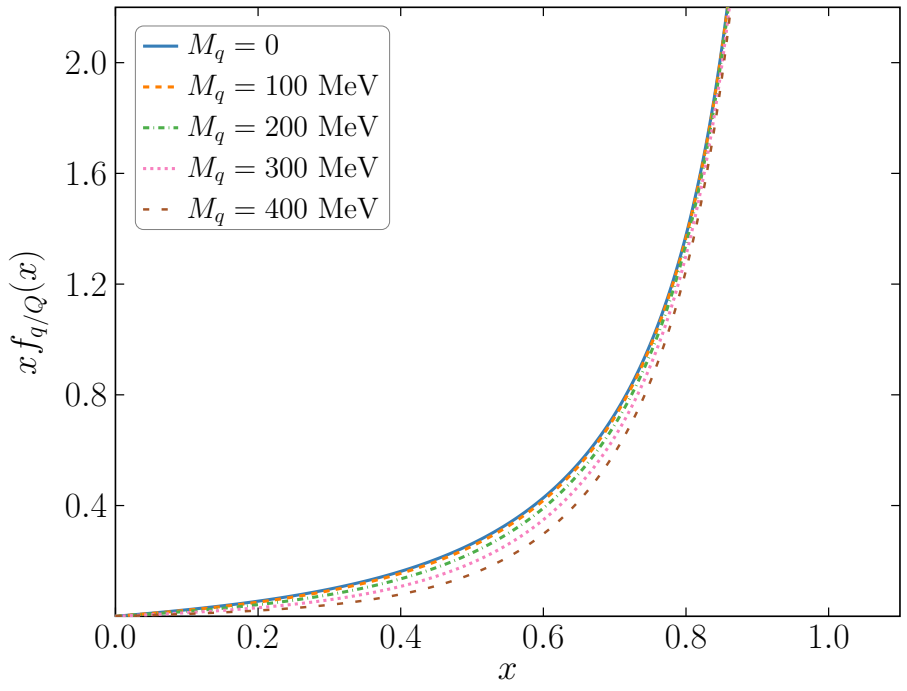

FIGURE 5.2 — Results for the QTM quark PDF for several values of M_q at fixed coupling strength $\alpha_s = 0.5$. Note that the quark PDF also has delta function contributions at $x = 1$ which are not shown.

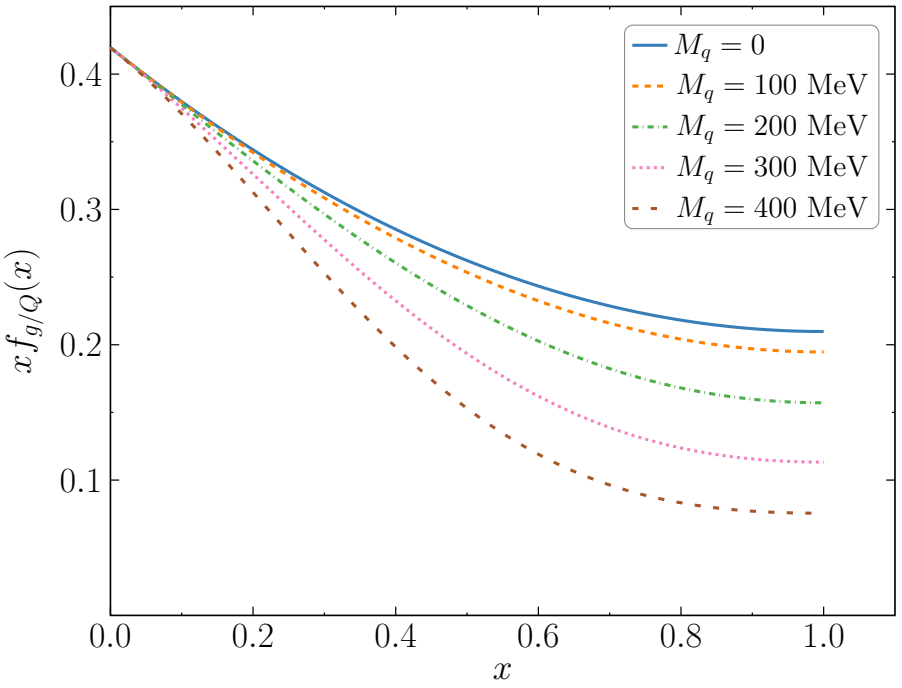

FIGURE 5.3 — Results of the gluon PDF for several values of M_q at fixed coupling strength $\alpha_s = 0.5$.

contributions in order to obtain the correct gluon momentum fraction. Had we not accounted for the Wilson line in this calculation, for instance, and had inferred gluon momentum by what was missing from the momentum sum rule, we would have underestimated the gluon momentum fraction by 0.1775, that is, obtaining $\langle x \rangle_g = 0.0133$ instead of the correct value of $\langle x \rangle_g = 0.1907$. This clearly indicates the importance of accounting for the Wilson line contributions.

Another important feature of the QTM is that the Mellin moments of the quark PDF become negative starting at $s = 19$ for the parameters given in Tab. 5.1. As the table illustrates, this occurs in the covariant gauge specifically because of the Wilson line, whose contribution to the total quark momentum becomes increasingly negative with the Mellin moments, and in light cone gauge because of the extra term in the triangle diagram containing $1/(1-x)$ in Eq. (4.40). This has a major implication for applying the quark target model to calculating hadron PDFs: if a convolution equation

TABLE 5.1 — Results for the s Mellin moments $\langle x^{s-1}\rangle = \int_0^1 dx\, x^{s-1} f(x)$ of the quark and gluon PDFs. In the second and third columns the quark PDF is split according to Eq. (4.35). The fourth and fifth columns give the total quark and gluon moments. For these results the quark mass is set to $M_q = 400\,\text{MeV}$ and the coupling strength to $\alpha_s = 0.5$, which gives $Z_2 = 0.9933$ in a general covariant gauge at one loop.

s	$Z_2 + \langle x^{s-1}\rangle_q^{\text{tri}}$	$\langle x^{s-1}\rangle_q^W$	$\langle x^{s-1}\rangle_q$	$\langle x^{s-1}\rangle_g$
1	1	0	1	-
2	0.9867	-0.1775	0.8093	0.1907
3	0.9866	-0.3034	0.6832	0.0647
4	0.9877	-0.4011	0.5867	0.0351
5	0.9888	-0.4807	0.5081	0.0235
6	0.9896	-0.5479	0.4418	0.0176
7	0.9903	-0.6059	0.3843	0.0140
8	0.9908	-0.6571	0.3337	0.0118
9	0.9912	-0.7027	0.2884	0.0101
10	0.9915	-0.7440	0.2475	0.0088
		⋮		
18	0.9926	-0.9791	0.0135	0.0045
19	0.9927	-1.0010	-0.0084	0.0043
20	0.9927	-1.0219	-0.0292	0.0040

is used in the impulse approximation, and the hadron's body PDF is positive definite, then the hadron's quark PDF will become negative at $x \sim 1$. This indicates that in this region the probabilistic interpretation of the PDF is lost. We illustrate this numerically for the pion in Sec. 4.4.

In Table 5.2, the second Mellin moment is shown to illustrate how the distribution of momentum is affected by a change in the coupling strength. The momentum fraction

TABLE 5.2 — Results for the second Mellin moment $\langle x \rangle = \int_0^1 dx\, x f(x)$ of the quark target model PDFs for several values of the coupling strength α_s, given at a fixed quark mass $M_q = 400$ MeV. In the second and third columns the quark PDF is split according to Eq. (4.35). The fourth and fifth columns give the total quark and gluon moments.

α_s	$Z_2 + \langle x \rangle_q^{\text{tri}}$	$\langle x \rangle_q^W$	$\langle x \rangle_q$	$\langle x \rangle_g$
0.25	0.9934	-0.0887	0.9046	0.0954
0.5	0.9867	-0.1775	0.8093	0.1907
0.75	0.9800	-0.2662	0.7139	0.2861
1	0.9735	-0.3549	0.6185	0.3815

carried by the gluons increases with the coupling strength, and its worth highlighting that the gluon is responsible for carrying $\sim 28\%$ of the quark target momentum at $\alpha_s = 0.75$. This is approximately equal to the fraction of the pion's momentum carried by gluons [1]. The QTM can therefore give a physically reasonable value for the gluon momentum fraction for realistic values of α_s.

5.2 Quark Target Model with a Gluon Mass

In Fig. 5.4, we present results for the quark and gluon PDFs with a gluon mass (with the latter including theta-field contribution) at several values of the gluon mass. The plotted quark PDF excludes $\delta(1-x)$ terms which contribute to the quark number and momentum sum rules. The introduction of a gluon mass suppresses both PDFs, with the quark number and momentum sum rules preserved specifically by an increase in the $\delta(1-x)$ terms excluded from the plots. As the gluon gets massive, it becomes more costly to radiate a gluon. Thus, with all other parameters equal, a larger gluon mass results in gluons carrying a smaller fraction of the dressed quark target's momentum. On the other hand, once a gluon is radiated, it is more likely to carry a large quantity

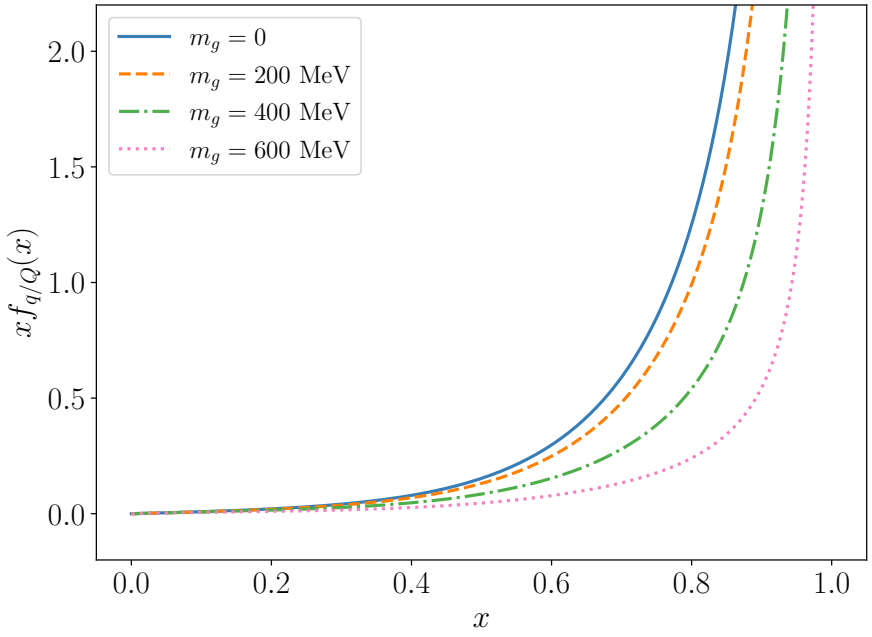

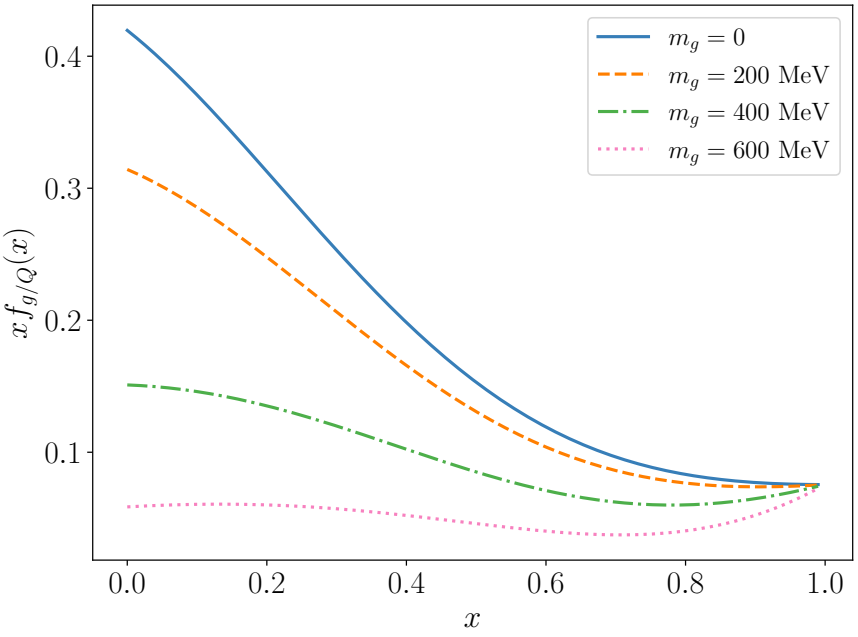

FIGURE 5.4 — Quark and gluon PDFs in the quark target model for several values of m_g, with the gluon PDF defined to include the theta-field contribution. $\alpha_s = 0.5$ and $M_q = 400$ MeV were used in these calculations. The plotted quark PDF does not include $\delta(1-x)$ terms.

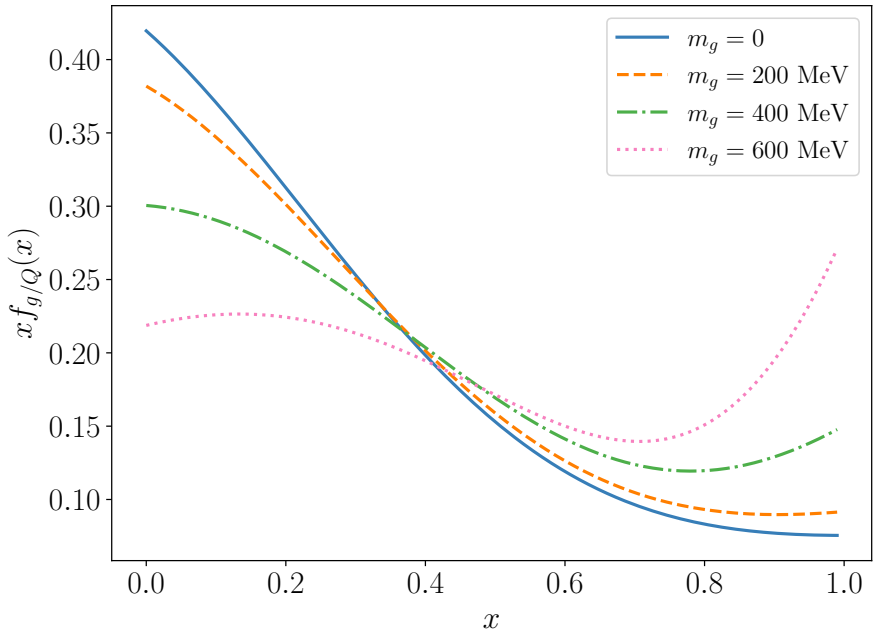

FIGURE 5.5 — Gluon PDFs in the quark target model for several values of m_g, with the gluon PDF defined to include the theta-field contribution. Here, α_s is different for each m_g value, and is chosen to give $\langle x \rangle_g = 0.1907$, and $M_q = 400$ MeV. The specific α_s values used are 0, 0.6077, 0.9951, and 1.8661 for $m_g = 0$, 200 MeV, 400 MeV, and 600 MeV respectively.

of momentum owing to its mass. This has the effect of reshaping the gluon PDF so that it falls less steeply in the intermediate-x region, and even grows at large x. This is illustrated in Fig. 5.5, where α_s has been changed for each m_g value so that the momentum fraction carried by the gluons remains at 0.1907. This can also be observed in the shapes of the curves in the lower panel of Fig. 5.4, although there this behavior is softer.

To acknowledge the relative importance of the theta-field contribution to the total gluon PDF and momentum fraction, in Tab. 5.3, we separate the gluon momentum fraction into two terms: One containing the naive contribution, and the other containing the theta field contribution. The last column is the total gluon momentum (sum of naive and theta). For $m_g = 0$, the QTM PDFs obtained in Sec. 4.1 are recovered as

it should be the case. It seems that up to a certain value of gluon mass, most of the gluon's light cone momentum is contained in the traditional gluon PDF. However, by crossing this gluon mass value this behavior changes and a significant portion of the gluon's light cone momentum is contained in the theta-field PDF, rather than in the traditional gluon PDF. In fact, for $m_g = 600$ MeV, the theta-field carries about 90% of the gluon's light cone momentum.

TABLE 5.3 — Contributions to the quark and gluon momentum fractions for various values of the Cornwall gluon mass (in MeV). The quark momentum fractions are separated according to Eq. (4.35) and the gluon momentum fractions are separated into naive and theta-field contributions. The other parameters are $\alpha_s = 0.5$ and $M_q = 400\,\text{MeV}$.

m_g	$Z_2 + \langle x\rangle_q^{\text{tri}}$	$\langle x\rangle_q^W$	$\langle x\rangle_q$	$\langle x\rangle_g^{\text{naive}}$	$\langle x\rangle_\theta$	$\langle x\rangle_g$
0	0.9867	-0.1775	0.8093	0.1907	0	0.1907
200	0.09885	-0.454	0.8431	0.1293	0.0276	0.1569
400	0.9920	-0.0878	0.9042	0.0434	0.0524	0.0958
600	0.9951	-0.0462	0.9489	0.0045	0.0466	0.0511

In Fig. 5.6, we separate the gluon PDF into naive and theta-field contributions. The value $m_g = 600$ MeV is used for the gluon mass to illustrate an extreme case. In general, the naive diagram makes more significant positive contributions at large x, while the theta-field dominates at small x. For especially large values of the gluon mass, the triangle diagram fails to be positive-definite, and in Fig. 5.6 goes negative at small x. However, the sum of both contributions remains positive definite.

We therefore observe through these numerical examples that the theta-field is necessary to account for massive gluons, both because it contains a significant portion of the gluons light cone momentum, and because—for especially large gluon masses—is necessary to guarantee that the gluon PDF be positive-definite.

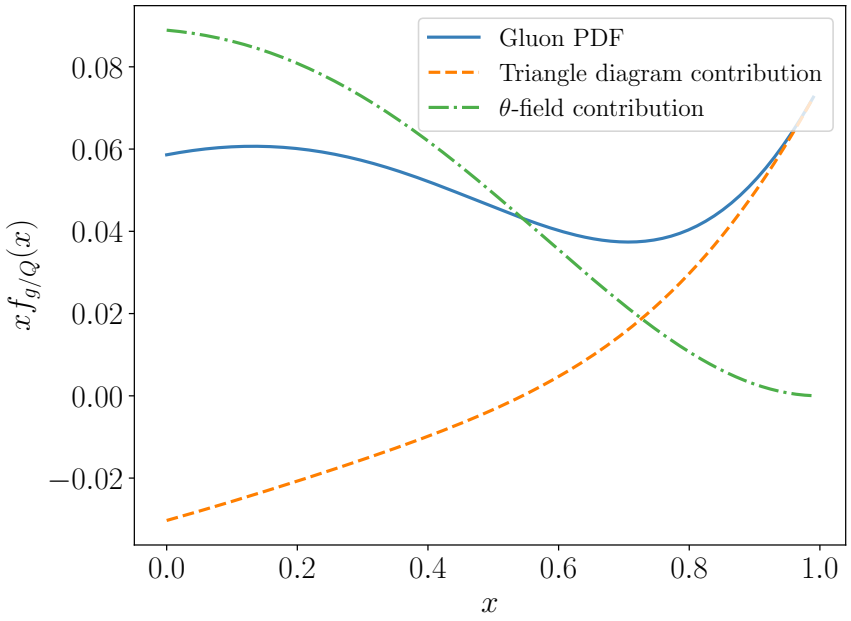

FIGURE 5.6 — Gluon PDFs in the quark target model, separated into naive and theta-field contributions. We use $\alpha_s = 0.5$, $M_q = 400$ MeV, and $m_g = 600\,\text{MeV}$.

5.3 Pion PDF

In order to fully define the model, it is necessary to determine a value for α_s to use both in the QTM calculations and in the DGLAP evolution equations to connect the low-energy effective theory to large-Q^2 — The PDFs at the model scale will provide the initial conditions for the QCD evolution. The way the model scale is usually determined is by fitting to empirical results. We follow this approach and determine the model scale by matching the pion's gluon momentum fraction to that found by the JAM analysis of Ref. [1] after NLO DGLAP evolution. At the charm threshold gluon carries around 30% of the pion's momentum. Furthermore, it is also necessary to pick a value for m_g. We consider both the cases of zero gluon mass, $m_g = 0$, and a finite gluon mass (within the gauge invariant Cornwall formalism), $m_g = 400\,\text{MeV}$. To obtain the evolved PDFs, we summarize the procedure as follows:

1. Determine the model scale Q_0^2 by requiring that the pion's gluon momentum fraction match that found by the JAM.

2. Use NLO DGLAP evolution to evolve the PDFs from the model scale Q_0^2 to the relevant Q^2.

For the $m_g = 0$ case this gives

$$\alpha_{s0} = 0.579, \qquad Q_0^2 = 0.82 \text{ GeV}^2 \tag{5.1}$$

where the NLO equation (Eq. (3.42)) have been used for $\alpha_s(Q^2)$. Similarly, for $m_g = 400$ MeV we find

$$\alpha_{s0} = 0.775, \qquad Q_0^2 = 0.58 \text{ GeV}^2 \tag{5.2}$$

It is worthwhile to mention that, already at the model scale for $m_g = 0$, gluons carry 22% of pion's light cone momentum and the corresponding model scale is much larger than typically used in models with only dressed quarks [37, 109] (in which $Q_0^2 \sim 0.16$ GeV^2). With $m_g = 400$ MeV the gluon light cone momentum fraction is 7% at the corresponding model scale.

In order to get a sense of how the PDF results depend on the model's body pion PDF, we also consider a naive body pion PDF $f_{Q/\pi}(x) = 30x^2(1-x)^2$ as a reference for comparison [110]. The results using both body PDFs are presented in Fig. (5.7). For shortening the notation, there we have defined $\bar{x} = 1 - x$ such that the reference body-pion PDF is written as $f_{Q/\pi}(x) = 30x^2\bar{x}^2$. Increasing the gluon mass, the gluon momentum fraction saturates at a smaller value compared to the massless gluon case. Regarding the quark PDF, as anticipated earlier in Sec. 5.1, it becomes negative at $x \sim 1$. This negativity occurs regardless of the pion body PDF used and as such this feature can be attributed to the combination of the QTM with the impulse

approximation used. Also, the reference body PDF actually presents worse behavior in this regard than the NJL model, as the full quark PDF becomes negative at smaller values of x in this case. If positivity is used to determine the domain of validity for the QTM, then the QTM has a larger domain of validity when paired with the NJL model than when paired with the naive reference body PDF.

That impulse approximation PDFs are negative at large x is inevitable in the quark target model, and can be understood in relation to the DGLAP evolution equations [100]. The DGLAP kernels can be found from the quark target model PDFs by differentiating with respect to the renormalization scale, since DGLAP evolution in effect describes how PDFs evolve with change of scale. In fact, one can see the familiar form of the leading order DGLAP kernels in the factors multiplying $I_2(\Delta_{q/g}(x))$ in Eqs. (4.35), (4.32) and (4.37). The DGLAP kernels, when convoluted with a PDF, result in a function which is negative at x close to 1—which is in fact necessary for the PDF being evolved to decrease with evolution at $x \sim 1$, as is physically expected. It is thus inevitable that the quark target model combined with the impulse approximation will produce a negative PDF for hadrons. One must go beyond the impulse approximation—perhaps by considering kernel diagrams—in order for the PDF to be positive-definite.

To circumvent the negativity of the QTM PDF, positivity is enforced by first setting the negative values of the PDF to zero, and then re-weighting the distributions such as to still satisfy the baryon and momentum sum rules. Because the PDFs in Fig. 5.7 satisfy both sum rules, setting the negative values to zero will spoil the sum rules. Therefore the necessity of re-weighting the PDFs. With positive PDFs in hand, we can now evolve the model PDFs to the empirically relevant scale of $Q^2 = 27$ GeV^2 using NLO DGLAP equations. At this scale, the PDF can be compared to experimental Drell-Yan data from the E615 experiment [2], as well as to the phenomenological parametrization from the JAM analysis [1].

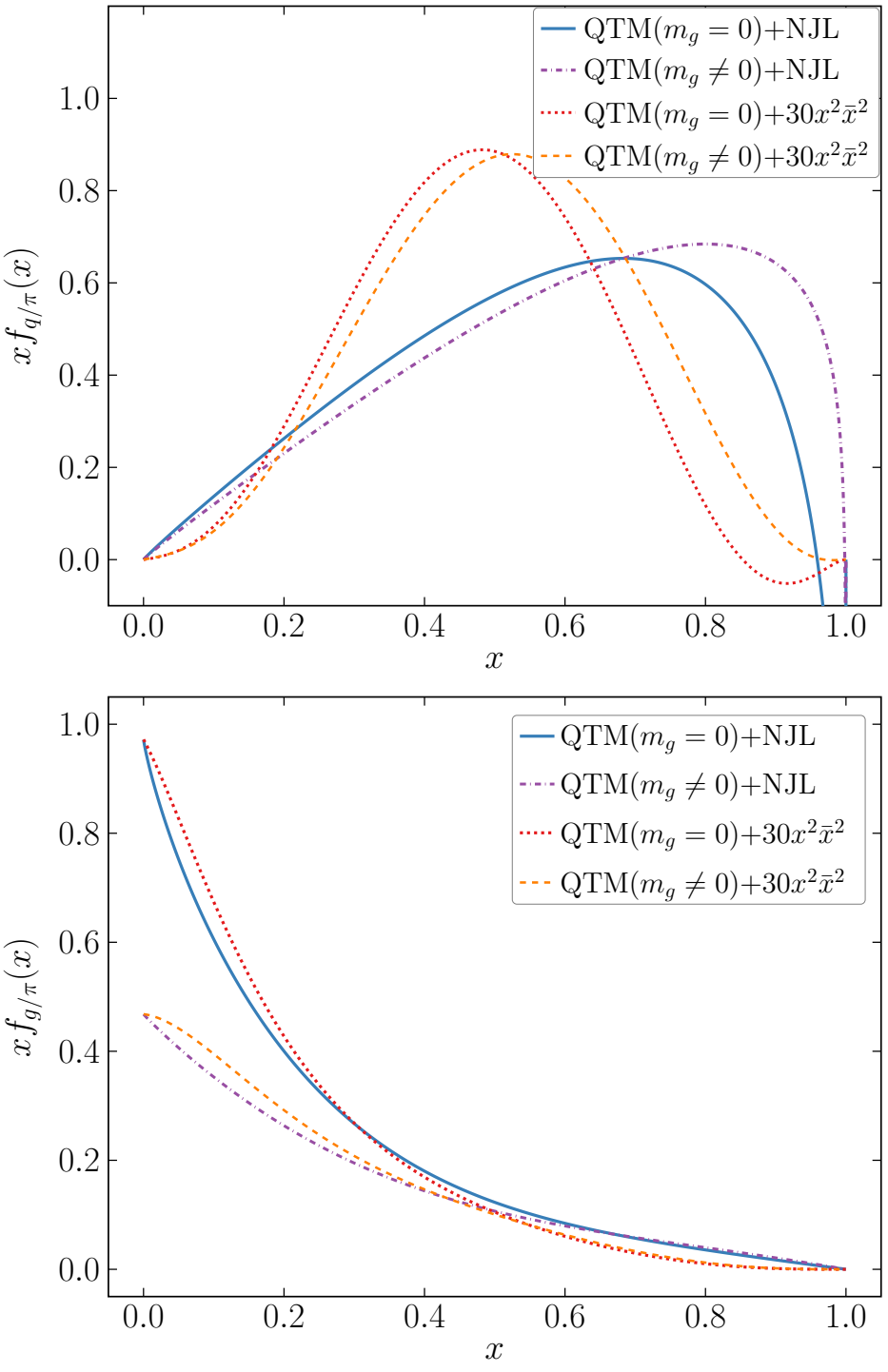

FIGURE 5.7 — Quark (top panel) and gluon (bottom panel) PDFs of the pion at the model scales. For the body PDFs we use the NJL model result and the simple parameterization $30\,x^2\bar{x}^2$, where $\bar{x} = 1 - x$. For the QTM we show results for $m_g = 0$ and $m_g = 400\,\text{MeV}$, which correspond to model scales of $Q_0^2 = 0.82\,\text{GeV}^2$ and $Q_0^2 = 0.58\,\text{GeV}^2$, respectively.

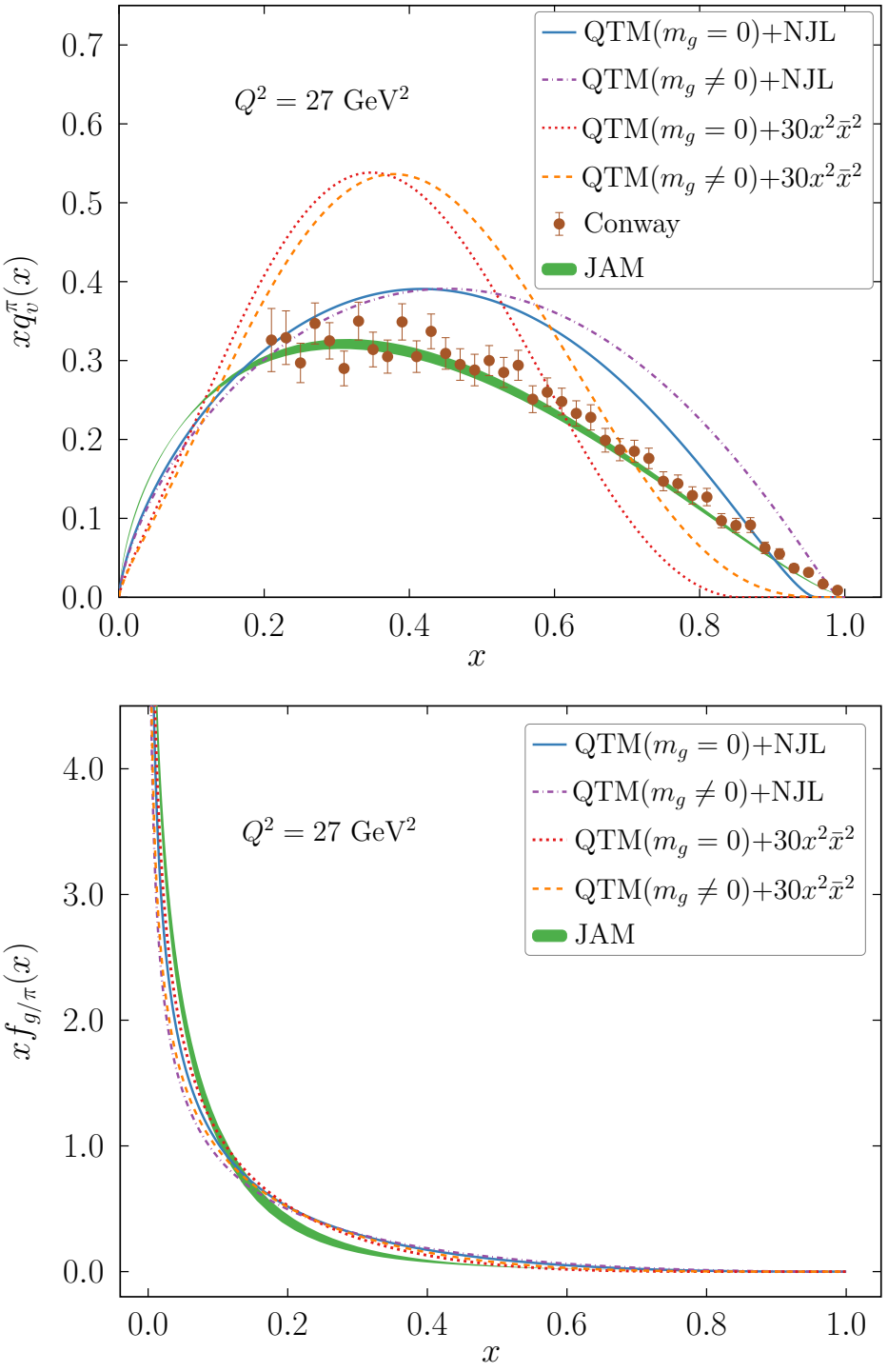

FIGURE 5.8 — The results presented in Fig. 5.7 evolved from the model scale to $Q^2 = 27\,\text{GeV}^2$. These results are contrast with the JAM collaboration results from Ref. [1] and the Conway *et al.* data [2].

Results for the pion's valence quark and gluon distributions at $Q^2 = 27$ GeV^2 obtained via the convolution formula Eqs. (4.62) and (4.63) are presented in Fig. 5.8, along with the foretold comparisons. The first thing to be noticed is that while interesting as a concept to be incorporated at the lagrangian level based on phenomenological ground, we found that a finite gluon mass makes discrepancy with data worse. The gluon PDF has rough agreement with the JAM result, but the pion valence quark PDF disagrees rather badly. The discrepancy from the data is doubtless due in part to the negativity issue—which, even with the workaround, manifests here as zero support for a range of $x < 1$—but likely also stems from the lack of gluon exchange between the dressed quarks in the QTM.

Chapter 6

Conclusions and Outlook

We have constructed a QTM at leading order in the quark-gluon coupling strength. Quark and gluon PDFs of a dressed quark target were calculated directly, including for the first time the Wilson line contributions in covariant gauges. This is completely similar to a one-loop calculation in perturbative QCD. The expected gauge invariance of the results was demonstrated by explicitly calculating the PDFs in both covariant and light-cone gauges. This allows to gain intuition regarding the PDF calculations in both gauges. On the one hand, working in covariant gauges requires the consideration of the Wilson lines, which within the continuum approach of Dyson-Schwinger (DSE) might become quite challenging. On the other hand, working in the light-cone gauge allows us to get rid of the Wilson lines, but the price to pay is to work with a light-cone gauge gluon propagator, whose light-cone singularity structure presents its own challenges within DSE. We envisage progress in this direction by working directly in Minkowski space using light-cone gauge gluon propagators [111] within the framework of the spectral representation of the propagators [6] and the pion Bethe-Salpeter amplitude [112–114].

The first significant finding in this work was that the Wilson line can make

non-trivial, sizeable contributions to the quark PDFs in covariant gauges, providing as much as a 20% correction to the quark momentum fraction. Therefore, approaches that do not include the Wilson lines may be, *a priori*, failing to account for a large contribution to the quark lightcone momentum. DSE calculations, for instance, are generally carried out in Landau gauge. For consistency, these calculations should take into account the Wilson line contributions to the PDF, which have been ignored in PDF calculations so far. However, it is unclear how to incorporate the Wilson line into these calculations. Alternatively, solving the DSE in the lightcone gauge would avoid the need to account for the Wilson line, though both approaches present their own challenges, as mentioned earlier.

Following indications from lattice QCD and Dyson-Schwinger equations that gluons acquire an effective mass at low-momentum, we extended the QTM to incorporate a gluon mass into the model. We explored two different approaches to include an explicit mass into the calculations. Motivated by numerous works that include an explicit mass for the gluon [105, 106], we introduced a naive mass term in the model, knowingly to violate gauge invariance. We also found that such term violates the momentum sum rule, as expected. To circumvent this issue, we studied the gluon mass term proposed by Cornwall [44] which preserves gauge invariance by also introducing an auxiliary theta field. We found that the theta field carries gluon momentum and this fixes the momentum sum rule which were broken by the naive mass term.

Using a convolution formalism the quark target PDFs were then combined with two different dressed quark-antiquark models to calculate the quark and gluon distributions in the pion. The resulting PDFs were evolved from the model scale to higher momentum scales using NLO DGLAP equations and compared to existing empirical and phenomenological results. We found good agreement between the empirical and calculated gluon PDFs, however, the agreement for the quark PDF is less satisfactory. A gluon mass, although reducing the gluon lightcone momentum fraction, including such

a mass term did not provide improved agreement with existing data for the pion PDF. When using the QTM as a method to include intrinsic gluons into low-energy effective theories one shortcoming was identified. This is the unavoidable domain of negative support in the quark PDFs at $x \sim 1$. In covariant gauges this is directly connected to the bilocal operator that defines the PDF and the associated Wilson line contribution. Likely, this can be attributed to the limited way in which gluons were incorporated in the model. For observables defined by local operators this shortcoming will not materialize.

In conclusion, the central challenge remains: how can gluon degrees of freedom be effectively incorporated in low-energy effective models of QCD? In principle, including gluons in a pure quark effective model, even if gluons are only incorporated at leading order, will have effects not only on the inner structure of the dressed quarks, but will also modify the hadron wave functions (e.g., their Bethe-Salpeter amplitudes). After all, introducing a gluon into the model will now make gluon exchange part of the force that binds quarks into hadrons. The QTM+convolution approach taken in this work does not account for gluon exchange between the quarks. Including these effects may provide the necessary ingredients to include intrinsic gluons in effective quark theories and avoid the shortcoming found in this study. This would enable calculations of quantities such as quark and gluon GPDs, TMDs, gravitational form factors, and mass decompositions for the pion and kaon.

Appendix A

Conventions and Notation

In this Appendix, we fix some conventions and notations used throughout this thesis.

A.1 Definitions

1. The metric is $g_{\mu\nu} = diag(1, -1, -1, -1)$.

2. The propagators are defined as

$$\begin{aligned} i\Delta(x-y) &= \langle 0|T\phi(x)\phi(y)|0\rangle \\ &= \int \frac{d^4k}{(2\pi)^4} \frac{i}{k^2 - m^2 + i\eta} e^{-ik(x-y)}, \end{aligned} \tag{A.1}$$

$$\begin{aligned} iS(x-y) &= \langle 0|T\psi(x)\bar{\psi}(y)|0\rangle \\ &= \int \frac{d^4k}{(2\pi)^4} \frac{i}{\not{k} - m + i\eta} e^{-ik(x-y)}. \end{aligned} \tag{A.2}$$

3. The spinors normalization is

$$\bar{u}(p)u(p) = 2m. \tag{A.3}$$

4. The light-cone coordinates are defined as

$$x^{\pm} = \frac{1}{\sqrt{2}}(x^0 \pm x^3), \tag{A.4}$$

such that a 4-vector $x^\mu = (x^0, x^1, x^2, x^3)$ in this coordinate system is

$$x^\mu = (x^+, \mathbf{x}^\perp, x^-), \tag{A.5}$$

where $\mathbf{x}^\perp = (x^1, x^2)$.

5. For two light-cone vectors n^μ and p^μ, the scalar product reads

$$n \cdot p = n_\mu p^\mu = n^0 k^0 - n^3 k^3 - \mathbf{n} \cdot \mathbf{p} = n^+ p^- + n^- p^+ - \mathbf{n}_\perp \cdot \mathbf{p}_\perp, \tag{A.6}$$

and the norm

$$p^2 = 2p^+ p^- - \mathbf{p}_\perp^2. \tag{A.7}$$

6. We define two light-like vectors as

$$p^\mu = \frac{1}{\sqrt{2}}(\Lambda, 0, 0, \Lambda), \tag{A.8}$$

$$n^\mu = \frac{1}{\sqrt{2}}(\Lambda^{-1}, 0, 0, -\Lambda^{-1}), \tag{A.9}$$

for arbitrary Λ. Being light-cone coordinates, they satisfy

$$p^2 = n^2 = 0, \qquad p \cdot n = 1, \qquad n^+ = 0 = p^-. \tag{A.10}$$

Then, in light-cone coordinates, we have

$$p^\mu = (\Lambda, \mathbf{0}_\perp, 0), \tag{A.11}$$

$$n^\mu = (0, \mathbf{0}_\perp, \Lambda^{-1}). \tag{A.12}$$

An arbitrary vector can be parametrized (known as Sudakov decomposition) as

$$A^\mu = \alpha p^\mu + \beta n^\mu + A^{\perp\mu} \tag{A.13}$$

$$= (A \cdot n)p^\mu + A^{\perp\mu} + (A \cdot p)n^\mu, \tag{A.14}$$

with $A^{\perp\mu} = (0, \mathbf{A}^\perp, 0)$.

A.2 Matrix Elements

The matrix elements between the spinors $\bar{u}(P)$ and $u(P)$ needed for calculating the unpolarized quark and gluon distributions are given by:

$$\begin{gathered}
\langle\gamma^\mu\rangle = 2P^\mu \qquad \langle\gamma^+\gamma^-\gamma^1\rangle = 2m \qquad \langle\gamma^+\gamma^-\gamma^2\rangle = -2(p_2 - ip_1) \\
\langle\gamma^+\gamma^-\rangle = 2m \qquad \langle\gamma^+\gamma^1\rangle = 0 \qquad \langle\gamma^+\gamma^2\rangle = 0 \\
\langle\gamma^+(\not{p} - \not{k})\rangle = 2m(p^+ - k^+)
\end{gathered} \tag{A.15}$$

where $\langle\Gamma\rangle = \bar{u}(P)\Gamma u(P)$.

A.3 Proper Time Regularization

$$\frac{1}{A^n} = \frac{1}{(n-1)!}\int_0^\infty d\tau\, e^{-\tau\Delta} \longrightarrow \frac{1}{(n-1)!}\int_{1/{\Lambda_{\mathrm{UV}}}^2}^{1/{\Lambda_{\mathrm{IR}}}^2} d\tau\, \tau^{n-1}\, e^{\tau\Delta} \tag{A.16}$$

A.4 Useful Relation

$$\left(\frac{k\cdot n + xP\cdot n}{P\cdot n}\right)^{s-1} = x^{s-1} + \left(\frac{k\cdot n}{P\cdot n}\right)\frac{\mathrm{d}}{\mathrm{d}x}x^{s-1} + \cdots$$

A.5 Regularized Integrals

The following notation for basic regularized integrals that appear throughout this thesis is used:

$$I_n(\Delta) \equiv i\int \frac{\mathrm{d}^4k}{(2\pi)^4}\,\frac{1}{(k^2-\Delta+i\epsilon)^n}, \tag{A.17}$$

to keep the results general and avoid committing to a particular regularization scheme. The specific values of $n = 2$ and $n = 3$ appear, where the former is logarithmically divergent and the latter convergent. Results in the proper-time and dimensional regularization scheme follow below.

In the proper time regularization scheme these are given by:

$$I_2(\Delta) = -\frac{1}{16\pi^2}\int \mathrm{d}\tau\,\frac{1}{\tau}\,e^{-\tau\Delta}, \tag{A.18}$$

$$I_3(\Delta) = \frac{1}{16\pi^2}\int \mathrm{d}\tau\,\frac{1}{2}\,e^{-\tau\Delta}\,. \tag{A.19}$$

In the proper time regularization scheme these basic integrals become:

$$I_2(\Delta) = -\frac{1}{16\pi^2}\,\Gamma\left(0, \Delta/\Lambda^2_{\mathrm{UV}}, \Delta/\Lambda^2_{\mathrm{IR}}\right), \tag{A.20}$$

$$I_3(\Delta) = \frac{1}{32\pi^2}\frac{1}{\Delta}\left(e^{-\Delta/\Lambda^2_{\mathrm{UV}}} - e^{-\Delta/\Lambda^2_{\mathrm{IR}}}\right), \tag{A.21}$$

where $\Gamma(s,a,b) = \int_a^b \mathrm{d}t\, t^{s-1}\, e^{-t}$ is the generalized incomplete gamma function.
In dimensional regularization the basic integral is given by:

$$I_n(\Delta) = \frac{(-1)^n\,(i^2)}{(4\pi)^{d/2}} \frac{\Gamma(n-d/2)}{\Gamma(n)} \left(\frac{1}{\Delta}\right)^{2-d/2}. \tag{A.22}$$

When using dimensional regularization it is generally important to work in $d = 4-2\epsilon$ dimensions from the outset, however, for these simple calculations we can make the replacements

$$I_2(\Delta) = -\frac{1}{16\pi^2}\left[\epsilon^{-1} + \log\left(\mu^2/\Delta\right) + \log(4\pi) - \gamma_E\right], \tag{A.23}$$

$$I_3(\Delta) = \frac{1}{32\pi^2}\frac{1}{\Delta}, \tag{A.24}$$

to obtain results in dimensional regularization. The terms $(\epsilon^{-1} + \log(4\pi) - \gamma_E)$ can be removed from $I_2(\Delta)$ by the common $\overline{\mathrm{MS}}$ subtraction scheme.

Appendix B

Derivation of the QTM PDFs

B.1 Quark PDF

The quark unpolarized quark PDF is defined by:

$$f_{q/Q}(x) = \frac{1}{2}\int \frac{\mathrm{d}\,\lambda}{2\,\pi}\, e^{ix\lambda\, P\cdot n}\, \langle \mathrm{Q}(P)|\, \hat{O}_q(0,n\lambda)\, |\mathrm{Q}(P)\rangle_c, \tag{B.1}$$

where $\hat{O}_q(0,n\lambda)$ is the operator

$$\hat{O}_q(0,n\lambda) = \bar{\psi}_q(0)\, \not{n}\, W(0,n\lambda)\, \psi_q(n\lambda)\rangle, \tag{B.2}$$

and

$$W(0,n\lambda) = \mathrm{P}\, e^{-ig\int_\lambda^0 \mathrm{d}\xi\ n\cdot A(n\xi)}, \tag{B.3}$$

is the Wilson line operator necessary to have a color gauge invariant PDF definition, with P denoting the path-ordering operator. In order to derive the corrections to the quark PDF, we start from the off-diagonal matrix element

$$\langle \mathrm{Q}(p_2)|\, \hat{O}_q(y,z)\, |\mathrm{Q}(p_1)\rangle_c, \tag{B.4}$$

where at the end we take $p_1 = p_2 = P$, $y = 0$ and $z = n\lambda$. The Lehmann, Symanzik and Zimmermann (LSZ) formalism is used to write the transition amplitude in terms of time-ordered products of the interacting theory

$$\langle \mathrm{Q}(p_2)|\, \hat{O}_{q/g}(y,z)\, |\mathrm{Q}(p_1)\rangle_c = (-i)^2 \int \mathrm{d}^4x_1 \int \mathrm{d}^4x_2\, e^{ip_2x_2}\, \bar{u}(p_2)\, [i\overrightarrow{\not\partial}_{x_2} - m] \\ \times \langle \Omega|\, T\left[\psi(x_2)\hat{O}_{q/g}(y,z)\bar{\psi}(x_1)\right]|\,\Omega\rangle [-i\overleftarrow{\not\partial}_{x_1} - m]\, u(p_1)\, e^{-ip_1x_1}, \quad \text{(B.5)}$$

where the vacuum expectation value is:

$$\langle \Omega|\, T\left[\psi(x_2)\hat{O}_{q/g}(y,z)\bar{\psi}(x_1)\right]|\,\Omega\rangle = \langle 0|\, T\left[\psi(x_2)\hat{O}_{q/g}(y,z)\bar{\psi}(x_1)\, e^{i\mathcal{S}_{\mathrm{int}}}\right]|\,0\rangle \\ = \langle 0|\, T\left[\psi(x_2)\hat{O}_q(y,z)\bar{\psi}(x_1)\Big(1 + i\mathcal{S}_{\mathrm{int}} + \frac{1}{2!}\,(i\mathcal{S}_{\mathrm{int}})\,(i\mathcal{S}_{\mathrm{int}}) + \cdots\Big)\right]|\,0\rangle \quad \text{(B.6)}$$

and

$$\mathcal{S}_{\mathrm{int}} = -g \int \mathrm{d}^4x\ \bar{\psi}(x)\gamma^\mu\psi(x)A_\mu(x) \quad \text{(B.7)}$$

is the interaction action and $\hat{O}_{q/g}$ can be either the quark or gluon bilocal operators defining the PDFs. Notice that the Wilson line should also be expanded in powers of the coupling "g".

B.1.1 Zeroth-order Contribution

The first term in Eq. (B.6) gives the vacuum expectation value at zeroth order in the strong coupling:

$$\langle \Omega|\, T\left[\psi(x_2)\hat{O}_q(y,z)\bar{\psi}(x_1)\right]|\,\Omega\rangle^{(0)} = iS(x_2 - y)\not{n}\, iS(z - x_1).$$

Using the Fourier transform of the propagator and acting with the Dirac operator, one finds

$$[i\overrightarrow{\not\partial}_{x_2} - m]i\,S(x_2-y) = \int \frac{\mathrm{d}^4k_2}{(2\pi)^4}\,[\not k_2 - m]\,iS(k_2)e^{-ik_2(x_2-y)} = i\delta^{(4)}(x_2-y)\mathbf{1}_{4\times4}$$
$$i\,S(z-x_1)[-i\overleftarrow{\not\partial}_{x_1} - m] = \int \frac{\mathrm{d}^4k_1}{(2\pi)^4}\,[\not k_1 - m]\,iS(k_1)e^{-ik_1(y-x_1)} = i\delta^{(4)}(z-x_1)\mathbf{1}_{4\times4}.$$

Inserting these in Eq. (B.5), gives:

$$\langle \mathrm{Q}(p_2)|\,\hat{O}_q(y,z)|\,\mathrm{Q}(p_1)\rangle_c = e^{ip_2y}\,e^{-ip_1z}\,\bar{u}(p_2)\not n\,u(p_1).$$

Taking $p_1 = p_2 = P$, $y = 0$, $z = n\lambda$ and plugging this result in Eq. (B.1), gives the zeroth-order in g contribution of the quark PDF

$$f^{(0)}_{q/Q}(x) = \delta(1-x), \tag{B.8}$$

where the matrix elements in Appendix A.2 have been used.

B.1.2 One-loop Contribution

B.1.2.1 Wilson Line

The next non-vanishing contribution to the quark PDF comes from the first order expansion in the interaction, i.e., the second term in the r.h.s of Eq. (B.6). The Wilson line gives a non-trivial contribution coming from its expansion to first order in "g". To account for its contribution, it is convenient to split the Wilson line into a Wilson line going to infinity and then back to the endpoint

$$W(y,z) = W(y,+\infty)W(+\infty,z) = [W(+\infty,y)]^\dagger\,W(+\infty,z). \tag{B.9}$$

We expand each of the Wilson lines in Eq. (B.9) to first order in g and discard terms $O(g^2)$ when taking the product of them since this will only contribute at higher orders once the interaction is considered. This means taking

$$[W(+\infty, y)]^\dagger W(+\infty, z) \to 1 + ig \int_y^\infty \mathrm{d}\eta \; n \cdot A(\eta) - ig \int_z^\infty \mathrm{d}\eta \; n \cdot A(\eta), \tag{B.10}$$

where $n = (0, 1, \mathbf{0}_\perp)$ is a light-cone vector. In the forthcoming discussion, let us consider first the contribution of the last term on the r.h.s. of Eq. (B.10). The vacuum expectation value gives:

$$\begin{aligned}\langle \Omega | \, T \left[\psi(x_2) \hat{O}_q(y, z) \bar{\psi}(x_1) \right] | \, \Omega \rangle &= \langle 0 | \, T \left[\psi(x_2) \bar{\psi}(y) \not{n} \, [W(+\infty, y)]^\dagger \right. \\ &\qquad \left. \times W(+\infty, z) \psi(z) \bar{\psi}(x_1) i S_{int} \right] | \, 0 \rangle \\ &= -ig \int_z^\infty \mathrm{d}\eta \; \langle 0 | \, T \left[\psi(x_2) \bar{\psi}(y) \not{n} \, n \cdot A(\eta) \psi(z) \bar{\psi}(x_1) \, i S_{int} \right] | \, 0 \rangle. \end{aligned} \tag{B.11}$$

Using the interaction Eq. (B.7), and writing the indices explictly, we have

$$\begin{aligned}&\langle \Omega | \, T \left[\psi(x_2) \hat{O}_q(y, z) \bar{\psi}(x_1) \right] | \, \Omega \rangle = n^\nu (-ig) \int_z^\infty \mathrm{d}\eta \int \mathrm{d}^4 x_3 \, \langle 0 | \, T \big[\psi^{i_2 f_2}_{\alpha_2}(x_2) \bar{\psi}^{f' i'}_{\alpha}(y) (\not{n})_{\alpha\beta} \\ &\times A^{a_2}_\nu(\eta) (t^{a_2})^{i' j'} \psi^{f' j'}_\beta(z) \bar{\psi}^{f_1 i_1}_{\alpha_1}(x_1) \bar{\psi}^{f_3 i_3}_{\alpha_3}(x_3) (-ig) (\gamma^\mu)_{\alpha_3 \beta_3} \psi^{j_3 f_3}_{\beta_3}(x_3) (t^{a_3})^{i_3 j_3} A^{a_3}_\mu(x_3) \big] | \, 0 \rangle \end{aligned}$$

The time-ordering operator allows us to express the vacuum expectation value in terms of propagators by taking the Wick contractions of the fields. This leads to

$$\begin{aligned}\langle \Omega | \, T \left[\psi(x_2) \hat{O}_q(y, z) \bar{\psi}(x_1) \right] | \, \Omega \rangle &= n^\nu (-ig) \, C_F \int_z^\infty \mathrm{d}\eta \int \mathrm{d}^4 x_3 \, S(x_2 - x_3) (-ig) \gamma^\mu \\ &\qquad \times \; S(x_3 - y) \not{n} \, S(z - x_1) D_{\mu\nu}(x_3 - \eta), \end{aligned} \tag{B.12}$$

where we have used

$$(t^a)^{i_2 i} (t^a)^{i i_1} = (t^a)^{i_2 i_1} = (t^a)^2 \delta^{i_1 i_2} = C_F \delta^{i_1 i_2}, \tag{B.13}$$

with $C_F = (N_c - 1)/2N_c$ being the Casimir invariant in the fundamental representation. As in Subsec. (B.1.1), the propagators are written using its Fourier transform and inserted in and Eq. (B.12) is inserted back in Eq. (B.5) The propagators are written using its Fourier transform and this expression is inserted back in Eq. (B.5), leading to:

$$\langle \mathrm{Q}(p_2)|\, \hat{O}_q(y,z)|\, \mathrm{Q}(p_1)\rangle_c = (ig)n^\nu C_F \int \frac{\mathrm{d}^4k_1}{(2\pi)^4} \int \frac{\mathrm{d}^4k_2}{(2\pi)^4} \int \mathrm{d}^4x\, e^{ix(p_2-k_1-k_2)} \int_z^\infty d\eta\, e^{ik_2\eta} \times e^{-ip_1 z} \bar{u}(p_2)(-ig)\gamma^\mu S(k_1)\, \not{n}\, D_{\mu\nu}(k_2) u(p_1) e^{ik_1 y}. \quad \text{(B.14)}$$

Integrating over the delta function after using

$$\int \mathrm{d}^4x\, e^{i(k-k')x} = (2\pi)^4 \delta^4(k-k'),$$

and noticing that

$$\int_z^\infty d\eta\, e^{i(p_2-k)\eta} = \frac{i}{p_2 - k + i0} e^{i(p_2-k)z},$$

one finds

$$\langle \mathrm{Q}(p_2)|\, \hat{O}_q(y,z)|\, \mathrm{Q}(p_1)\rangle_c = (ig)n^\nu C_F \int \frac{\mathrm{d}^4k}{(2\pi)^4} \frac{i}{p_2 - k + i0} e^{i(p_2-p_1-k)z} e^{ik_1 y} \times \bar{u}(p_2)(-ig)\gamma^\mu S(k) \not{n}\, D_{\mu\nu}(p-k) u(p_1). \quad \text{(B.15)}$$

In order to obtain the Wilson line contribution to the quark pdf, one still has to take $p_1 = p_2 = P, y = 0, z = n\lambda$ and the light-cone Fourier transform of Eq. (B.15) as in Eq. (B.1), resulting in

$$f_{q/Q}^{W_1}(x) = \frac{g^2 C_F}{2} n^\nu \int \frac{\mathrm{d}^4k}{(2\pi)^4}\, \delta\big[n\cdot(xP-k)\big]\, \bar{u}(P) \frac{i}{n\cdot(P-k)} \gamma^\mu S(k) \not{n} D_{\mu\nu}(P-k) u(P). \quad \text{(B.16)}$$

The contribution of the second term in the r.h.s. of Eq. (B.10) is obtained in an analagous way and will only differ in the last step when taking $y = 0$ and $z = n\lambda$. One finds that

$$f_{q/Q}^{W_2}(x) = -\frac{g^2 C_F}{2(n\cdot P)} n^\nu \delta(1-x) \int \frac{\mathrm{d}^4 k}{(2\pi)^4}\, \bar{u}(P) \frac{i}{n\cdot(P-k)+i0} \gamma^\mu S(k) \not{n} D_{\mu\nu}(P-k) u(P).$$

B.1.2.2 Triangle Diagram

The triangle diagram comes from expanding the interacting vacuum to second order in the strong coupling g:

$$\langle\Omega|\, T\left[\psi(x_2)\hat{O}_q(y,z)\bar{\psi}(x_1)\right]|\,\Omega\rangle^{(2)} = \frac{1}{2!}\langle 0|\, T\left[\psi(x_2)\hat{O}_q(y,z)\bar{\psi}(x_1)(i\mathcal{S}_{\mathrm{int}})(i\mathcal{S}_{\mathrm{int}})\right]|\,0\rangle$$

Writing all indices explicitly, the vacuum expectation value at order g^2 gives

$$\begin{aligned}\langle\Omega|T\left[\psi(x_2)\hat{O}_q(y,z)\bar{\psi}(x_1)\right]|\Omega\rangle^{(2)} = \frac{1}{2!}\int \mathrm{d}x_3 \int \mathrm{d}x_4\, \langle 0|T\Big[&\psi_{\alpha_2}^{q_2 i_2}(x_2)\bar{\psi}_{\alpha}^{q\, i}(y)(\not{n})_{\alpha\beta}\psi_{\beta}^{q\, i}(z) \\ &\times \bar{\psi}_{\alpha_1}^{q_1 i_1}(x_1)(-ig)\bar{\psi}_{\alpha_3}^{q_3 i_3}(x_3)(\gamma^{\mu_3})_{\alpha_3\beta_3}\psi_{\beta_3}^{q_3 j_3}(x_3)A_{\mu_3}^{a_3}(x_3)(t^{a_3})^{i_3 j_3} \\ &\times (-ig)\bar{\psi}_{\alpha_4}^{q_4 i_4}(x_4)(\gamma^{\mu_4})_{\alpha_4\beta_4}\psi_{\beta_4}^{q_4 j_4}(x_4)A_{\mu_4}^{a_4}(x_4)(t^{a_4})^{i_4 j_4}\Big]|\,0\rangle,\end{aligned}$$

and after applying Wick's theorem, it becomes

$$\begin{aligned}\langle\Omega|\, T\left[\psi(x_2)\hat{O}_q(y,z)\bar{\psi}(x_1)\right]|\,\Omega\rangle^{(2)} = C_F \int dx_3 \int dx_4\ &[-iS(x_2-x_3)]\,\gamma^\mu\,[-iS(x_3-y)] \\ &\times(-ig)\not{n}\,[-iS(z-x_4)]\,\gamma^\nu(-ig)\,[-iS(x_4-x_1)]\,[iD_{\mu\nu}(x_3-x_4)]\,. \qquad \text{(B.17)}\end{aligned}$$

Inserting this result back in Eq. (B.5), gives:

$$\begin{aligned}\langle \mathrm{Q}(p_2)|\,\tilde{O}_q(y,z)|\,\mathrm{Q}(p_1)\rangle = ig^2 C_F \int \frac{\mathrm{d}^4 k}{(2\pi)^4} e^{ik_1 y} e^{-i(p_1-p_2+k_1)z} \\ \times \bar{u}(p_2)\gamma^\mu S(k_1)\not{n} S(p_1-p_2+k_1)\gamma^\nu D_{\mu\nu}(p_2-k_1)u(p_1). \qquad \text{(B.18)}\end{aligned}$$

As before, the appropriate substitutions $p_1 = p_2 = p$, $y = 0$ and $z = n\lambda$ are made and the light-cone Fourier transform is taken to obtain the corresponding contribution to the quark PDF. This gives

$$f_{q/Q}^{\text{tri}}(x) = \frac{ig^2}{2}\frac{C_F}{P\cdot n}\int \frac{\mathrm{d}^4k}{(2\pi)^4}\,\delta\left(x - \frac{k\cdot n}{P\cdot n}\right)\bar{u}(P)\,\gamma^\mu\,S(k)\,\not{n}\,S(k)\,\gamma^\nu\,D_{\mu\nu}(P-k)\,u(P). \tag{B.19}$$

B.2 Gluon PDF

The unpolarized gluon distribution is defined by

$$x f_{g/Q}(x) = \frac{1}{P\cdot n}\int \frac{\mathrm{d}\lambda}{2\pi}\,e^{ix\lambda\,P\cdot n}\langle \mathrm{Q}(P)|\,\hat{O}_g(0,n\lambda)|\,\mathrm{Q}(P)\rangle, \tag{B.20}$$

where $\hat{O}_g(0,n\lambda)$ is the operator

$$\hat{O}_g(0,n\lambda) = G^n_\mu(0)\,W_A(0,n\lambda)\,G^{\mu n}(n\lambda) \tag{B.21}$$

and $W_A(0,n\lambda)$ is a Wilson line in the adjoint representation whose color indices are contracted to those of $G_{\mu\nu} = t^a G^a_{\mu\nu} = t^a\left(\partial_\mu A^a_\nu - \partial_\nu A^a_\mu - g f^{abc} A^b_\mu A^c_\nu\right)$. Following the same steps as before, we first calculate the general matrix element

$$\langle \mathrm{Q}(p_2)|\,\hat{O}_g(y,z)|\,\mathrm{Q}(p_1)\rangle \tag{B.22}$$

where at the end we take the limit of equal moments $p_1 = p_2 = P$ and $y = 0, z = n\lambda$. Expanding the Wilson line to zeroth order and the interaction to second order in the coupling, we have for the vacuum expectation value

$$\langle\Omega|\,T\big[\psi(x_2)\hat{O}_g(y,z)\bar{\psi}(x_1)\big]\,|\,\Omega\rangle^{(2)} = \frac{1}{2!}\langle 0|\,T\big[\psi(x_2)\hat{O}_g(y,z)\bar{\psi}(x_1)iS_{int}iS_{int}\big]\,|\,0\rangle.$$

with S_{int} as given in Eq. (B.7). Writing all the Dirac, color and flavor indices, we have

$$\langle\Omega|\,T\big[\psi(x_2)\hat{O}_g(y,z)\bar{\psi}(x_1)\big]\,|\,\Omega\rangle^{(2)} = (-ig)^2\frac{1}{2!}\int \mathrm{d}^4x_3\int \mathrm{d}^4x_4$$
$$\times\,\langle 0|\,T\big[\psi^{i_2f_2}_{\alpha_2}(x_2)G^n_{\ \mu}(y)G^\mu_{\ n}(z)\bar{\psi}^{i_1f_1}_{\alpha_1}(x_1)\bar{\psi}^{i_3f_3}_{\alpha_3}(x_3)(\gamma^{\mu_3})_{\alpha_3\beta_3}A^{a_3}_{\mu_3}(x_3)(t^{a_3})^{i_3j_3}\psi^{j_3f_3}_{\beta_3}(x_3)$$
$$\times\,\bar{\psi}^{i_4f_4}_{\alpha_4}(x_4)(\gamma^{\mu_4})_{\alpha_4\beta_4}A^{a_4}_{\mu_4}(x_4)(t^{a_4})^{i_4j_4}\psi^{j_4f_4}_{\beta_4}(x_4)\big]\,|\,0\rangle. \quad \text{(B.23)}$$

First, let us look separately at the gluon field contractions. Only the derivative terms in the gauge field-strength tensor will contribute at one-loop level:

$$\begin{aligned} G^n_{\ \mu}(y)A^{a_3}_{\mu_3}(x_3) &= t^{a_2}\left[\left(n\partial_{(y)}\right)A^{a_2}_{\mu}(y) - \partial^{(y)}_{\mu}\left(nA^{a_2}\right)(y)\right]A^{a_3}_{\mu_3}(x_3) \\ \overbrace{G^\nu_{\ \mu}(y)A^{a_3}_{\mu_3}}(x_3) &= it^{a_2}\left[(n\partial_{(y)})D^{a_2a_3}_{\mu\mu_3}(y-x_3) - \partial^{(y)}_{\mu}n^\nu D^{a_2a_3}_{\nu\mu_3}(y-x_3)\right]\delta^{a_2a_3}. \end{aligned}$$

The same follows to the other term,

$$\begin{aligned} G^\mu_{\ n}(z)A^{a_4}_{\mu_4}(x_4) &= t^{a_1}\left[\partial^{\mu}_{(z)}(nA^{a_1})(z) - (n\partial^{(z)})A^{\mu,a_1}(z)\right]A^{a_4}_{\mu_4}(x_4) \\ \overbrace{G^\mu_{\ \alpha}(z)A^{a_4}_{\mu_4}}(x_4) &= it^{a_1}\left[\partial^{\mu}_{(z)}n^\alpha D^{a_1a_4}_{\alpha\mu_4}(z-x_4) - (n\partial^{(z)})D^{\mu,a_1a_4}_{\ \ \mu_4}(z-x_4)\right]\delta^{a_1a_4}. \end{aligned}$$

Making all the contractions, the vacuum expectation value turns out to be:

$$\langle\Omega|\,T\big[\psi(x_2)\hat{O}_g(y,z)\bar{\psi}(x_1)\big]\,|\,\Omega\rangle^{(2)} = (-ig)^2\frac{1}{2!}C_F\int \mathrm{d}^4x_3\int \mathrm{d}^4x_4\,[-iS(x_2-x_3)]\,\gamma^{\mu_3}$$
$$\times\,[iS(x_3-x_4)]\gamma^{\mu_4}[-iS(x_4-x_1)]i\left[(n\partial_{(y)})D_{\mu\mu_3}(y-x_3) - \partial^{(y)}_{\mu}n^\nu D_{\nu\mu_3}(y-x_3)\right]$$
$$\times\,i[\partial^{\mu}_{(z)}n^\alpha D_{\alpha\mu_4}(z-x_4) - (n\partial^{(z)})D^{\mu}_{\ \ \mu_4}(z-x_4)] + (x_3\leftrightarrow x_4)\,. \quad \text{(B.24)}$$

This expression is inserted in Eq. (B.5), giving the following transition amplitude:

$$\langle \mathrm{Q}(p_2)|\,\hat{O}_g(y,z)\,|\,\mathrm{Q}(p_1)\rangle_c = -ig^2C_F\int\frac{\mathrm{d}^4x}{(2\,\pi)^4}\,e^{iy(-p_1+p_2+k)}\,e^{-ikz}$$
$$\times\,\bar{u}(p_2)\gamma^{\mu_3}S(p_2-k)\gamma^{\mu_4}u(p_1)D_{\nu\mu_3}(k-p_1+p_2)D_{\alpha\mu_4}(k)$$
$$\times\left[n\cdot(k-p_1+p_2)g^\nu_\mu - (k-p_1+p_2)_\mu\,n^\nu\right]\left[(n\cdot k)g^{\mu\alpha} - k^\mu\,n^\alpha\right]. \quad \text{(B.25)}$$

Finally, taking the appropriate limits $p_1 = p_2 = P$, $y = 0$ and $z = n = n\lambda$ and inserting it in the definition of the gluon PDF Eq. (B.20) gives

$$x\, f_{g/Q}(x) = -i\, g^2\, \frac{C_F}{P \cdot n} \int \frac{\mathrm{d}^4 k}{(2\pi)^4}\; \bar{u}(P)\, \gamma^{\mu_3}\, S(P-k)\, \gamma^{\mu_4}\, u(P)\, \delta\left(n\,[xP - k]\right) \\ \times \left[(n\cdot k) g_\mu^\nu - k_\mu\, n^\nu\right] \left[(n\cdot k) g^{\mu\alpha} - k^\mu n^\alpha\right] D_{\nu\mu_3}(k) D_{\alpha\mu_4}(k). \qquad \text{(B.26)}$$

Appendix C

Explicit Calculation of the PDFs

C.1 Quark PDF

C.1.1 Triangle Diagram

In this section we are considering the Feynman gauge, $\xi = 0$. We evaluate the moments where

$$\left\langle x^{s-1}\right\rangle_q^{\text{tri}} = \int \mathrm{d}x\, x^{s-1} f_{q/Q}(x), \tag{C.1}$$

so that we have

$$\left\langle x^{s-1}\right\rangle_q^{\text{tri}} = \frac{-ig^2 C_F}{2(P\cdot n)} \int \frac{\mathrm{d}^4k}{(2\pi)^4} \left(\frac{k\cdot n}{P\cdot n}\right)^{s-1} \frac{\bar{u}(P)\gamma^\mu(\not{k}+M_q)\not{n}(\not{k}+M_q)\gamma_\mu u(P)}{(k^2-M_q^2+i\epsilon)^2[(P-k)^2-m_g^2+i\epsilon]}. \tag{C.2}$$

The algebra of the numerator gives

$$\bar{u}(P)\gamma^\mu(\not{k}+M_q)\not{n}(\not{k}+M_q)\gamma_\mu = 8(k\cdot n)\left(2M_q^2 - k\cdot P\right) + 4\left(k^2-M_q^2\right)(n\cdot P) \tag{C.3}$$

Feynman parametrization is employed to combine the product of propagators into a single fraction, so that the denominator can be written as

$$\frac{1}{(k^2-M_q^2+i\epsilon)^2[(P-k)^2-m_g^2+i\epsilon]} = \int_0^1 \mathrm{d}x\, 2(1-x) \times \frac{1}{[(k-Px)^2-x(x-1)P^2-m_g^2x-M_q^2(1-x)+i\epsilon]^3} \overset{k\to k+xP}{\longrightarrow} \int \mathrm{d}x\, \frac{2(1-x)}{(k^2-\Delta_1+i\epsilon)^3}, \tag{C.4}$$

where

$$\Delta_q(x) \equiv x(x-1)P^2 + M_q^2(1-x) + m_g^2x \tag{C.5}$$

with $P^2 = M_q^2$. Therefore,

$$\left\langle x^{s-1}\right\rangle_q^{\mathrm{tri}} = \frac{-ig^2C_F}{2(P\cdot n)}\int_0^1 \mathrm{d}x\, 2(1-x)\int \frac{d^4k}{(2\pi)^4}\left(\frac{k\cdot n + x\,P\cdot n}{P\cdot n}\right)^{s-1}\frac{1}{(k^2-\Delta_q(x)+i\epsilon)^3} \times (-4)\Big\{(n\cdot P)\left[M_q^2\left(x^2-4x+1\right)-k^2\right]+2(k\cdot n)\left[k\cdot P+M_q^2(x-2)\right]\Big\}. \tag{C.6}$$

The only terms which will contribute to the integral are those even in k, therefore using the expansion

$$\left(\frac{k\cdot n + xP\cdot n}{P\cdot n}\right)^{s-1} = x^{s-1} + \left(\frac{k\cdot n}{P\cdot n}\right)\frac{\mathrm{d}}{\mathrm{d}x}x^{s-1} + \cdots$$

gives

$$\left\langle x^{s-1}\right\rangle_q^{\mathrm{tri}} = \frac{-ig^2C_F}{(P\cdot n)}\int_0^1 \mathrm{d}x\, x^{s-1}(1-x)\int \frac{d^4k}{(2\pi)^4}\left(\frac{k\cdot n}{P\cdot n}\right)^{s-1}\frac{1}{(k^2-\Delta_q(x)+i\epsilon)^3} \times \left[4k^2(n\cdot P)-8(k\cdot n)(k\cdot P)-4(n\cdot P)(1-4x+x^2)M_q^2\right], \tag{C.7}$$

and using the definition of the moments in Eq. (C.1) we can readily read off the triangle diagram contribution of the quark PDF

$$f_{q/Q}^{\rm tri}(x) = \frac{-ig^2 C_F(1-x)}{(P\cdot n)}\int\frac{{\rm d}^4k}{(2\pi)^4}\frac{1}{(k^2-\Delta_q(x)+i\epsilon)^3} \times\left[4k^2(n\cdot P)-8(k\cdot n)(k\cdot P)-4(n\cdot P)(1-4x+x^2)M_q^2\right], \tag{C.8}$$

which in terms of the basic integrals given in Sec. (A.5) becomes

$$f_{q/Q}^{\rm tri}(x) = -2\,g^2C_F\Big[(1-x)\,I_2(\Delta_q(x))+4\,M_q^2\,x(1-x)\,I_3(\Delta_q(x))+2m_g^2x\,I_3(\Delta_q(x)).\Big] \tag{C.9}$$

C.1.2 Self-Energy

We now calculate the one-loop contribution to the residue which is obtained by differentiating the one loop self-energy with respect to $\not{p}$ and then setting $\not{p}=m$. The one loop quark self-energy is given by

$$\Sigma^{(1)}(p) = ig^2C_F\int\frac{{\rm d}^4k}{(2\pi)^4}\gamma_\mu S(p-k)\gamma^\nu D_{\mu\nu}(k).$$

In Feynman gauge, one obtains

$$\Sigma^{(1)}(p) \;=\; -ig^2C_F\int\frac{{\rm d}^4k}{(2\pi)^4}\frac{4M_q-2(\not{p}-\not{k})}{[(p-k)^2-M_q^2+i\epsilon][k^2-m_g^2+i\epsilon]}. \tag{C.10}$$

Using Feynman parametrization and then shifting the momentum to $k\to k+(1-x)p$ we can drop the linear term in k so that we are left with

$$\Sigma^{(1)}(p) = -2g^2C_F\int_0^1{\rm d}x\,\left[2M_q-x\not{p}\right]\,I_2(\Delta_q(x)) \tag{C.11}$$

with $\Delta_q(x)$ as given in eq. (C.5). For the residue, we obtain

$$\begin{aligned} Z_q &= 1 + \left(\frac{\mathrm{d}}{\mathrm{d}\not{p}}\Sigma^{(1)}(p)\right)_{\not{p}=M_q} \\ &= 1 + 2g^2 C_F \int_0^1 \mathrm{d}x \left[x I_2(\Delta_q(x)) + 4M_q^2(x-2)(x-1)x I_3(\Delta_q(x))\right]. \end{aligned} \tag{C.12}$$

C.1.3 Wilson Line Contribution

Each of the Wilson lines is given by:

$$f_{q/Q}^W(x) = g^2 \frac{C_F}{2(P\cdot n)} n^\nu \int \frac{\mathrm{d}^4k}{(2\pi)^4}\left[\delta\left(x - \frac{k\cdot n}{P\cdot n}\right) - \delta(1-x)\right] \frac{i}{n\cdot(P-k)+i0} \times \bar{u}(P)\,\gamma^\mu\, S(k)\,\not{n}\, D_{\mu\nu}(P-k)\,u(p). \tag{C.13}$$

We start by evaluating the first term. For our purposes we consider here only the Feynman gauge. We find

$$f_{q/Q}^{W_1}(x) = \frac{g^2 C_F}{(P\cdot n)} \frac{2}{1-x}\, g(x, P, M_q, m_g), \tag{C.14}$$

where

$$g(x, P, M_q, m_g) = i \int \frac{\mathrm{d}^4k}{(2\pi)^4}\,\delta\left(x - \frac{k\cdot n}{P\cdot n}\right) \frac{k\cdot n}{(k^2 - M_q^2 + i\epsilon)[(P-k)^2 - m_g^2 + i\epsilon]}. \tag{C.15}$$

We evaluate the moments

$$\left\langle x^{s-1}\right\rangle_q^{\mathrm{W_1}} = i\int_0^1 \mathrm{d}x\, x^{s-1} g(x, p, M_q, m_g) \tag{C.16}$$

to find

$$\begin{aligned}\left\langle x^{s-1}\right\rangle_q^{\mathrm{W}_1} &= i\int\frac{\mathrm{d}^4k}{(2\pi)^4}\left(\frac{k\cdot n}{P\cdot n}\right)^{s-1}\frac{k\cdot n}{(k^2-M_q^2+i\epsilon)[(P-k)^2-m_g^2+i\epsilon]}\\ &= i\int_0^1\mathrm{d}x\int\frac{\mathrm{d}^4k}{(2\pi)^4}\left(\frac{k\cdot n+xP\cdot n}{P\cdot n}\right)^{s-1}\frac{k\cdot n+xP\cdot n}{(k^2-\Delta_q(x)+i\epsilon)^2}.\end{aligned}\tag{C.17}$$

The only non-vanishing term which will contribute to the integral is

$$\left\langle x^{s-1}\right\rangle_q^{\mathrm{W}_1} = i\int_0^1\mathrm{d}x\,x^{s-1}\int\frac{\mathrm{d}^4k}{(2\pi)^4}\frac{x\,P\cdot n}{(k^2-\Delta_q(x)+i\epsilon)^2}.$$

Therefore, we find

$$g(x,P,M_q,m_g) = x(P\cdot n)\,I_2(\Delta_q(x)),\tag{C.18}$$

so that

$$f_{q/Q}^{W_1}(x) = g^2C_F\frac{2x}{1-x}\,I_2(\Delta_q(x)).\tag{C.19}$$

For the second term on the R.H.S. of Eq. (C.13), one has

$$\begin{aligned}f_{q/Q}^{W_2}(x) &= -2\,i\,g^2\,C_F\,\delta(1-x)\\ &\quad\times\int\frac{\mathrm{d}^4k}{(2\pi)^4}\frac{k\cdot n}{[n\cdot(P-k)+i\epsilon](k^2-M_q^2+i\epsilon)[(P-k)^2-m_g^2+i\epsilon]}.\end{aligned}\tag{C.20}$$

We use Feynman parametrization only for the quark and gluon propagators denominators, leading to

$$\begin{aligned}f_{q/Q}^{W_2}(x) &= \frac{-2ig^2C_F}{n\cdot P}\delta(1-x)\int_0^1\mathrm{d}y\frac{1}{1-y}\\ &\quad\times\int\frac{d^4k}{(2\pi)^4}\frac{k\cdot n+y\,n\cdot P}{(k^2-\Delta_q(x)+i\epsilon)^2}\frac{1}{\left[1-\dfrac{k\cdot n}{(1-y)(n\cdot P)}\right]}.\end{aligned}\tag{C.21}$$

Now, by noting that

$$\frac{1}{\left[1-\dfrac{k\cdot n}{(1-y)(n\cdot P)}\right]}=\sum_{\alpha=0}^{k}\left(\frac{k\cdot n}{(1-y)n\cdot P}\right)^{\alpha}, \tag{C.22}$$

the only term which will contribute in the geometric expansion is the $\alpha = 0$ term. The linear term in k is also dropped since it will not contribute to the quadratic integral. Therefore, we obtain

$$f_{q/Q}^{W_2}(x)=-g^2C_F\,\delta(1-x)\int_0^1 \mathrm{d}y\frac{2y}{1-y}\,I_2(\Delta_q(x)). \tag{C.23}$$

It is worth pointing out that although $\dfrac{k\cdot n}{(1-y)n\cdot P}$ is not necessarily less than 1 and in fact can acquire high values, it is still reasonable to assume the series convergence. The result we obtain for the Wilson line on these grounds agrees to the expected Wilson line behavior and gives the right result for the sum rules.

C.2 Gluon PDF

As in the last section, we evaluate the distribution using the moments where

$$\left\langle x^{s-1}\right\rangle=\int_0^1 \mathrm{d}x\,x^{s-1}f_{g/Q}(x), \tag{C.24}$$

with

$$\begin{aligned} x\,f_{g/Q}(x)=-i\,g^2\,\frac{C_F}{P\cdot n}\int\frac{\mathrm{d}^4k}{(2\pi)^4}\;\bar{u}(P)\,\gamma^{\mu_3}\,S(P-k)\,\gamma^{\mu_4}\,u(P)\,\delta\left(n\left[xP-k\right]\right)\\ \times\left[(n\cdot k)g_{\mu}^{\nu}-k_{\mu}\,n^{\nu}\right]\left[(n\cdot k)g^{\mu\alpha}-k^{\mu}n^{\alpha}\right]D_{\nu\mu_3}(k)D_{\alpha\mu_4}(k). \end{aligned} \tag{C.25}$$

Therefore,

$$\left\langle x^{s-1}\right\rangle = -i\,g^2\,\frac{C_F}{(P\cdot n)^2}\int\frac{\mathrm{d}^4k}{(2\pi)^4}\,\left(\frac{k\cdot n}{P\cdot n}\right)^{n-2}\,\bar{u}(P)\,\gamma^{\mu_3}\,S(P-k)\,\gamma^{\mu_4}\,u(P)$$
$$\times\left[(n\cdot k)g^{\nu}_{\mu}-k_\mu\,n^\nu\right]\left[(n\cdot k)g^{\mu\alpha}-k^\mu n^\alpha\right]D_{\nu\mu_3}(k)D_{\alpha\mu_4}(k). \tag{C.26}$$

Here the gluon propagator is in an arbitrary gauge and has the form

$$D_{\nu\mu}(k)=\left[-g_{\mu\nu}+(1-\xi)\frac{k_\mu k_\nu}{k^2}\right]\frac{1}{k^2-m_g^2}.$$

It is easily seen that the terms which goes with $\sim(1-\xi)$ will cancel out, so that the only terms which will contribute are the metric terms of the gluon propagator. Therefore, the algebra of the numerator gives

$$\bar{u}(P)\,\gamma^{\mu_3}\,(\not{P}-\not{k}+M_q)\,\gamma^{\mu_4}\,u(P)\left[(n\cdot k)g^{\nu}_{\mu}-k_\mu\,n^\nu\right]\left[(n\cdot k)g^{\mu\alpha}-k^\mu n^\alpha\right]g_{\nu\mu_3}\,g_{\alpha\mu_4}$$
$$=-4\left\{(k\cdot n)^2\left[M_q^2+(k\cdot P)\right]-2(n\cdot k)(k\cdot P)(n\cdot P)+k^2(n\cdot P)^2\right\}. \tag{C.27}$$

Using Feynman parametrization to write the denominator as

$$\frac{1}{(k^2-M_q^2+i\epsilon)^2[(p-k)^2-m_g^2+i\epsilon]}\overset{k\to k+xp}{=}\int\mathrm{d}x\,\frac{2(1-x)}{(k^2-\Delta_g(x)+i\epsilon)^3}, \tag{C.28}$$

where $\Delta_g(x)=M_q^2x^2-m_g^2(x-1)$, we obtain

$$\left\langle x^{s-1}\right\rangle = -i\,g^2\,\frac{C_F}{(P\cdot n)^2}\int_0^1\mathrm{d}x\,2(1-x)$$
$$\times\int\frac{\mathrm{d}^4k}{(2\pi)^4}\,\left(\frac{k\cdot n+x\,P\cdot n}{P\cdot n}\right)^{n-2}\,\frac{N^{\left\langle x^{s-1}\right\rangle}}{(k^2-\Delta_g(x)+i\epsilon)^3}, \tag{C.29}$$

where

$$N^{\left\langle x^{s-1}\right\rangle}=\left(\frac{k\cdot n+x\,P\cdot n}{P\cdot n}\right)^{s-2}(-4)\Big\{\,[n\cdot(k+xP)]^2\left(M_q^2+(k\cdot P)+M_q^2x\right)$$
$$-2[n\cdot(k+xP)](k\cdot P+M_q^2x)(n\cdot P)+(k+xP)^2(n\cdot P)^2\Big\}. \tag{C.30}$$

The only terms which will contribute to the quadratic integral are those which are even powers of k:

$$N^{\langle x^{s-1}\rangle} = x^{s-2}\Big\{ -4\left[(n\cdot P)^2k^2 + 2(x-1)(n\cdot P)(k\cdot n)(k\cdot P) + (n\cdot P)^2M_q^2x^3\right]\Big\} \\ -4\left(\frac{k\cdot n}{P\cdot n}\right)\frac{\mathrm{d}}{\mathrm{d}x}x^{s-2}x^2(k\cdot P)(n\cdot P)^2. \qquad \text{(C.31)}$$

This result is then inserted back in Eq. (C.29) and the derivative term is dealt with using integrating by parts. This allows to factorize x^{s-2} in such a way that is straightforward to read off the PDF out of the moments $\langle x^{s-1}\rangle$:

$$N^{\langle x^{s-1}\rangle} = \frac{-8ig^2C_F}{(P\cdot n)^2}\int_0^1 \mathrm{d}x\, x^{s-1}\frac{1}{x}\int\frac{\mathrm{d}^4k}{(2\pi)^4}\frac{1}{(k^2-\Delta_g(x)+i\epsilon)} \\ \Big\{(1-x)(n\cdot P)^2\left[k^2+M_q^2x^3\right] - 2(1-x)(n\cdot P)(k\cdot n)(k\cdot P) \\ + x^2\left[1-(1-x)\frac{\mathrm{d}}{\mathrm{d}x}\right](n\cdot P)(k\cdot n)(k\cdot P)\Big\}. \qquad \text{(C.32)}$$

Therefore, the gluon PDF is

$$f_{g/Q}(x) = \frac{-8ig^2C_F}{x(P\cdot n)^2}\int\frac{\mathrm{d}^4k}{(2\pi)^4}\Big\{(1-x)(n\cdot P)^2(k^2+M_q^2x^3) \\ -2(1-x)(n\cdot P)(k\cdot n)(k\cdot P) \\ + x^2\left[1-(1-x)\frac{\mathrm{d}}{\mathrm{d}x}\right](n\cdot P)(k\cdot n)(k\cdot P)\Big\}\frac{1}{(k^2-\Delta_g(x)+i\epsilon)}. \qquad \text{(C.33)}$$

With the basic integrals as given in Sec. (A.5), we obtain for the gluon PDF:

$$f_{g/Q}(x) = -2g^2C_F\Big[\left[1+(1-x)^2\right]I_2(\Delta_g(x)) + 4M_q^2x^2(1-x)I_3(\Delta_g(x)) \\ + 2m_g^2(1-x)(x^2-2x+2)I_3(\Delta_g(x))\Big]. \qquad \text{(C.34)}$$

Bibliography

[1] P. Barry, N. Sato, W. Melnitchouk, and C.-R. Ji, "First Monte Carlo Global QCD Analysis of Pion Parton Distributions," *Phys. Rev. Lett.* **121** (2018) no. 15, 152001, arXiv:1804.01965 [hep-ph].

[2] J. Conway *et al.*, "Experimental Study of Muon Pairs Produced by 252-GeV Pions on Tungsten," *Phys. Rev. D* **39** (1989) 92–122.

[3] M. Breidenbach, J. I. Friedman, H. W. Kendall, E. D. Bloom, D. H. Coward, H. C. DeStaebler, J. Drees, L. W. Mo, and R. E. Taylor, "Observed behavior of highly inelastic electron-proton scattering," *Phys. Rev. Lett.* **23** (1969) 935–939.

[4] E. D. Bloom *et al.*, "High-Energy Inelastic e p Scattering at 6-Degrees and 10-Degrees," *Phys. Rev. Lett.* **23** (1969) 930–934.

[5] G. Krein, C. D. Roberts, and A. G. Williams, "On the implications of confinement," *Int. J. Mod. Phys. A* **7** (1992) 5607–5624.

[6] E. L. Solis, C. S. R. Costa, V. V. Luiz, and G. Krein, "Quark propagator in Minkowski space," *Few Body Syst.* **60** (2019) no. 3, 49, arXiv:1905.08710 [hep-ph].

[7] V. Sauli, "Implications of analyticity to solution of Schwinger-Dyson equations in Minkowski space," *Few Body Syst.* **39** (2006) 45, arXiv:hep-ph/0412188 [hep-ph].

[8] V. Sauli, J. Adam, Jr., and P. Bicudo, "Dynamical chiral symmetry breaking with integral Minkowski representations," *Phys. Rev.* **D75** (2007) 087701, arXiv:hep-ph/0607196 [hep-ph].

[9] E. P. Biernat, F. Gross, T. Peña, A. Stadler, and S. Leitão, "Quark mass functions and pion structure in the Covariant Spectator Theory," *Few Body Syst.* **59** (2018) no. 5, 80, arXiv:1802.00266 [hep-ph].

[10] F. Siringo, "Analytic structure of QCD propagators in Minkowski space," *Phys. Rev.* **D94** (2016) no. 11, 114036, arXiv:1605.07357 [hep-ph].

[11] B. El-Bennich, G. a. Krein, E. Rojas, and F. E. Serna, "Excited hadrons and the analytical structure of bound-state interaction kernels," *Few Body Syst.* **57** (2016) no. 10, 955–963, arXiv:1602.06761 [nucl-th].

[12] A. Castro, E. Ydrefors, W. De Paula, T. Frederico, J. H. De Alvarenga Nogueira, and P. Maris, "The Bethe-Salpeter approach to bound states: from Euclidean to Minkowski space," *J. Phys. Conf. Ser.* **1291** (2019) no. 1, 012006, arXiv:1901.04266 [hep-ph].

[13] D. J. Gross and F. Wilczek, "Ultraviolet Behavior of Nonabelian Gauge Theories," *Phys. Rev. Lett.* **30** (1973) 1343–1346.

[14] H. D. Politzer, "Reliable Perturbative Results for Strong Interactions?," *Phys. Rev. Lett.* **30** (1973) 1346–1349.

[15] K. G. Wilson, "Confinement of Quarks," *Phys. Rev. D* **10** (1974) 2445–2459.

[16] J. Smit, *Introduction to quantum fields on a lattice: A robust mate*, vol. 15. Cambridge University Press, 1, 2011.

[17] W. Detmold, W. Melnitchouk, and A. W. Thomas, "Extraction of parton distributions from lattice QCD," *Mod. Phys. Lett. A* **18** (2003) 2681–2698, arXiv:hep-lat/0310003.

[18] X. Ji, "Parton Physics on a Euclidean Lattice," *Phys. Rev. Lett.* **110** (2013) 262002, arXiv:1305.1539 [hep-ph].

[19] A. V. Radyushkin, "Quasi-parton distribution functions, momentum distributions, and pseudo-parton distribution functions," *Phys. Rev. D* **96** (2017) no. 3, 034025, arXiv:1705.01488 [hep-ph].

[20] Y.-Q. Ma and J.-W. Qiu, "Exploring Partonic Structure of Hadrons Using ab initio Lattice QCD Calculations," *Phys. Rev. Lett.* **120** (2018) no. 2, 022003, arXiv:1709.03018 [hep-ph].

[21] T. Izubuchi, X. Ji, L. Jin, I. W. Stewart, and Y. Zhao, "Factorization Theorem Relating Euclidean and Light-Cone Parton Distributions," *Phys. Rev. D* **98** (2018) no. 5, 056004, arXiv:1801.03917 [hep-ph].

[22] R. S. Sufian, C. Egerer, J. Karpie, R. G. Edwards, B. Joó, Y.-Q. Ma, K. Orginos, J.-W. Qiu, and D. G. Richards, "Pion Valence Quark Distribution from Current-Current Correlation in Lattice QCD," *Phys. Rev. D* **102** (2020) no. 5, 054508, arXiv:2001.04960 [hep-lat].

[23] B. Joó, J. Karpie, K. Orginos, A. V. Radyushkin, D. G. Richards, and S. Zafeiropoulos, "Parton Distribution Functions from Ioffe Time Pseudodistributions from Lattice Calculations: Approaching the Physical Point," *Phys. Rev. Lett.* **125** (2020) no. 23, 232003, arXiv:2004.01687 [hep-lat].

[24] X. Gao, L. Jin, C. Kallidonis, N. Karthik, S. Mukherjee, P. Petreczky, C. Shugert, S. Syritsyn, and Y. Zhao, "Valence parton distribution of the pion from lattice QCD: Approaching the continuum limit," *Phys. Rev. D* **102** (2020) no. 9, 094513, arXiv:2007.06590 [hep-lat].

[25] Z. Fan and H.-W. Lin, "Gluon Parton Distribution of the Pion from Lattice QCD," arXiv:2104.06372 [hep-lat].

[26] R. Alkofer and L. von Smekal, "The Infrared behavior of QCD Green's functions: Confinement dynamical symmetry breaking, and hadrons as relativistic bound states," *Phys. Rept.* **353** (2001) 281, arXiv:hep-ph/0007355.

[27] I. C. Cloët and C. D. Roberts, "Explanation and Prediction of Observables using Continuum Strong QCD," *Prog. Part. Nucl. Phys.* **77** (2014) 1–69, arXiv:1310.2651 [nucl-th].

[28] K. D. Bednar, I. C. Cloët, and P. C. Tandy, "Distinguishing Quarks and Gluons in Pion and Kaon Parton Distribution Functions," *Phys. Rev. Lett.* **124** (2020) no. 4, 042002, arXiv:1811.12310 [nucl-th].

[29] C. Shi, K. Bednar, I. C. Cloët, and A. Freese, "Spatial and Momentum Imaging of the Pion and Kaon," *Phys. Rev. D* **101** (2020) no. 7, 074014, arXiv:2003.03037 [hep-ph].

[30] Z.-F. Cui, M. Ding, F. Gao, K. Raya, D. Binosi, L. Chang, C. D. Roberts, J. Rodríguez-Quintero, and S. M. Schmidt, "Kaon and pion parton distributions," *Eur. Phys. J. C* **80** (2020) no. 11, 1064.

[31] A. Freese, I. C. Cloët, and P. C. Tandy, "Gluon PDF from Quark dressing in the Nucleon and Pion," arXiv:2103.05839 [hep-ph].

[32] A. Accardi *et al.*, "Electron Ion Collider: The Next QCD Frontier: Understanding the glue that binds us all," *Eur. Phys. J. A* **52** (2016) no. 9, 268, arXiv:1212.1701 [nucl-ex].

[33] C. S. R. Costa, A. Freese, I. C. Cloët, B. El-Bennich, G. Krein, and P. C. Tandy, "Intrinsic Glue and Wilson lines within Dressed Quarks," arXiv:2103.17163 [hep-ph].

[34] D. Ebert, T. Feldmann, and H. Reinhardt, "Extended NJL model for light and heavy mesons without q - anti-q thresholds," *Phys. Lett. B* **388** (1996) 154–160, arXiv:hep-ph/9608223.

[35] G. Hellstern, R. Alkofer, and H. Reinhardt, "Diquark confinement in an extended NJL model," *Nucl. Phys.* **A625** (1997) 697–712, arXiv:hep-ph/9706551 [hep-ph].

[36] I. C. Cloët, W. Bentz, and A. W. Thomas, "Role of diquark correlations and the pion cloud in nucleon elastic form factors," *Phys. Rev.* **C90** (2014) 045202, arXiv:1405.5542 [nucl-th].

[37] I. C. Cloët, W. Bentz, and A. W. Thomas, "Transversity quark distributions in a covariant quark-diquark model," *Phys. Lett.* **B659** (2008) 214–220, arXiv:0708.3246 [hep-ph].

[38] I. C. Cloët, W. Bentz, and A. W. Thomas, "Nucleon quark distributions in a covariant quark-diquark model," *Phys. Lett.* **B621** (2005) 246–252, arXiv:0504229 [hep-ph].

[39] P. T. P. Hutauruk, J. J. Cobos-Martínez, Y. Oh, and K. Tsushima, "Valence-quark distributions of pions and kaons in a nuclear medium," *Phys. Rev. D* **100** (2019) no. 9, 094011, arXiv:1908.02406 [hep-ph].

[40] P. T. P. Hutauruk, W. Bentz, I. C. Cloët, and A. W. Thomas, "Charge Symmetry Breaking Effects in Pion and Kaon Structure," *Phys. Rev.* **C97** (2018) no. 5, 055210, arXiv:1802.05511 [nucl-th].

[41] A. Freese and I. C. Cloët, "Impact of dynamical chiral symmetry breaking and dynamical diquark correlations on proton generalized parton distributions," *Phys. Rev. C* **101** (2020) no. 3, 035203, arXiv:1907.08256 [nucl-th].

[42] A. Freese and I. C. Cloët, "Quark spin and orbital angular momentum from proton GPDs," arXiv:2005.10286 [nucl-th].

[43] A. C. Aguilar, D. Binosi, and J. Papavassiliou, "The Gluon Mass Generation Mechanism: A Concise Primer," *Front. Phys. (Beijing)* **11** (2016) no. 2, 111203, arXiv:1511.08361 [hep-ph].

[44] J. M. Cornwall, "Dynamical Mass Generation in Continuum QCD," *Phys. Rev.* **D26** (1982) 1453.

[45] **UKQCD** Collaboration, D. B. Leinweber, J. I. Skullerud, A. G. Williams, and C. Parrinello, "Asymptotic scaling and infrared behavior of the gluon propagator," *Phys. Rev. D* **60** (1999) 094507, arXiv:hep-lat/9811027. [Erratum: Phys.Rev.D 61, 079901 (2000)].

[46] O. Oliveira and P. Bicudo, "Running Gluon Mass from Landau Gauge Lattice QCD Propagator," *J. Phys. G* **38** (2011) 045003, arXiv:1002.4151 [hep-lat].

[47] A. G. Duarte, O. Oliveira, and P. J. Silva, "Lattice Gluon and Ghost Propagators, and the Strong Coupling in Pure SU(3) Yang-Mills Theory: Finite Lattice Spacing and Volume Effects," *Phys. Rev. D* **94** (2016) no. 1, 014502, arXiv:1605.00594 [hep-lat].

[48] M. Bhagwat, M. Pichowsky, C. Roberts, and P. Tandy, "Analysis of a quenched lattice QCD dressed quark propagator," *Phys. Rev. C* **68** (2003) 015203, arXiv:nucl-th/0304003.

[49] M. Bhagwat and P. Tandy, "Analysis of full-QCD and quenched-QCD lattice propagators," *AIP Conf. Proc.* **842** (2006) no. 1, 225–227, arXiv:nucl-th/0601020.

[50] A. Aguilar, D. Binosi, and J. Papavassiliou, "The dynamical equation of the effective gluon mass," *Phys. Rev. D* **84** (2011) 085026, arXiv:1107.3968 [hep-ph].

[51] L. D. Faddeev and V. N. Popov, "Feynman Diagrams for the Yang-Mills Field," *Phys. Lett. B* **25** (1967) 29–30.

[52] S. Pokorski, *GAUGE FIELD THEORIES*. Cambridge University Press, 1, 2005.

[53] G. Curci, W. Furmanski, and R. Petronzio, "Evolution of Parton Densities Beyond Leading Order: The Nonsinglet Case," *Nucl. Phys. B* **175** (1980) 27–92.

[54] G. Leibbrandt, "The Light Cone Gauge in Yang-Mills Theory," *Phys. Rev. D* **29** (1984) 1699.

[55] S. Mandelstam, "Light Cone Superspace and the Ultraviolet Finiteness of the N=4 Model," *Nucl. Phys. B* **213** (1983) 149–168.

[56] A. Cucchieri, T. Mendes, and E. M. S. Santos, "Covariant gauge on the lattice: A New implementation," *Phys. Rev. Lett.* **103** (2009) 141602, arXiv:0907.4138 [hep-lat].

[57] F. C. Khanna, A. P. C. Malbouisson, J. M. C. Malbouisson, and A. R. Santana, *Thermal quantum field theory - Algebraic aspects and applications*. 2009.

[58] C. D. Roberts and A. G. Williams, "Dyson-Schwinger equations and their application to hadronic physics," *Prog. Part. Nucl. Phys.* **33** (1994) 477–575, arXiv:hep-ph/9403224.

[59] J. Collins, *Foundations of perturbative QCD*. Cambridge University Press, 2013. http://www.cambridge.org/de/knowledge/isbn/item5756723.

[60] T. Muta, *Foundations of quantum chromodynamics: An Introduction to perturbative methods in gauge theories*, vol. 5. 1987.

[61] M. E. Peskin and D. V. Schroeder, *An Introduction to quantum field theory*. Addison-Wesley, Reading, USA, 1995. http://www.slac.stanford.edu/~mpeskin/QFT.html.

[62] S. Weinberg, *The quantum theory of fields. Vol. 2: Modern applications*. Cambridge University Press, 8, 2013.

[63] T. P. Cheng and L. F. Li, *GAUGE THEORY OF ELEMENTARY PARTICLE PHYSICS*. 1984.

[64] M. D. Schwartz, *Quantum Field Theory and the Standard Model*. Cambridge University Press, 2014.

[65] Y. Nambu and G. Jona-Lasinio, "Dynamical Model of Elementary Particles Based on an Analogy with Superconductivity. 1.," *Phys. Rev.* **122** (1961) 345–358.

[66] Y. Nambu and G. Jona-Lasinio, "DYNAMICAL MODEL OF ELEMENTARY PARTICLES BASED ON AN ANALOGY WITH SUPERCONDUCTIVITY. II," *Phys. Rev.* **124** (1961) 246–254.

[67] U. Vogl and W. Weise, "The Nambu and Jona Lasinio model: Its implications for hadrons and nuclei," *Prog. Part. Nucl. Phys.* **27** (1991) 195–272.

[68] S. P. Klevansky, "The Nambu–Jona-Lasinio Model of Quantum Chromodynamics," *Rev. Mod. Phys.* **64** (1992) 649–708.

[69] T. Hatsuda and T. Kunihiro, "QCD phenomenology based on a chiral effective Lagrangian," *Phys. Rept.* **247** (1994) 221–367, arXiv:hep-ph/9401310.

[70] M. Buballa, "NJL model analysis of quark matter at large density," *Phys. Rept.* **407** (2005) 205–376, arXiv:hep-ph/0402234.

[71] L. M. Abreu, F. C. Khanna, A. P. C. Malbouisson, J. M. C. Malbouisson, and A. E. Santana, "Finite-size effects on the phase transition in a four- and six-fermion interaction model," *Phys. Lett. A* **378** (2014) 2597–2602, arXiv:1409.0842 [hep-th].

[72] E. B. S. Corrêa, C. A. Linhares, A. P. C. Malbouisson, J. M. C. Malbouisson, and A. E. Santana, "Finite-size, chemical-potential and magnetic effects on the phase transition in a four-fermion interacting model," *Eur. Phys. J. C* **77** (2017) no. 4, 261.

[73] F. Serna, *Symmetry-preserving contact interaction model for hadron structure and quark matter*. PhD thesis, Instituto de Física Teórica (UNESP), 10, 2017.

[74] F. E. Serna, B. El-Bennich, and G. a. Krein, "Charmed mesons with a symmetry-preserving contact interaction," *Phys. Rev. D* **96** (2017) no. 1, 014013, arXiv:1703.09181 [hep-ph].

[75] M. A. Bedolla, J. J. Cobos-Martínez, and A. Bashir, "Charmonia in a contact interaction," *Phys. Rev. D* **92** (2015) no. 5, 054031, arXiv:1601.05639 [hep-ph].

[76] J. O. Andersen, W. R. Naylor, and A. Tranberg, "Phase diagram of QCD in a magnetic field: A review," *Rev. Mod. Phys.* **88** (2016) 025001, arXiv:1411.7176 [hep-ph].

[77] M. E. Carrillo-Serrano, W. Bentz, I. C. Cloët, and A. W. Thomas, "ρ meson form factors in a confining Nambu–Jona-Lasinio model," *Phys. Rev. C* **92** (2015) no. 1, 015212, arXiv:1504.08119 [nucl-th].

[78] W. Bentz and A. W. Thomas, "The Stability of nuclear matter in the Nambu-Jona-Lasinio model," *Nucl. Phys. A* **696** (2001) 138–172, arXiv:nucl-th/0105022.

[79] N. Nakanishi, "A General survey of the theory of the Bethe-Salpeter equation," *Prog. Theor. Phys. Suppl.* **43** (1969) 1–81.

[80] C. Itzykson and J. B. Zuber, *Quantum Field Theory*. International Series In Pure and Applied Physics. McGraw-Hill, New York, 1980. http://dx.doi.org/10.1063/1.2916419.

[81] N. Ishii, W. Bentz, and K. Yazaki, "Baryons in the NJL model as solutions of the relativistic Faddeev equation," *Nucl. Phys. A* **587** (1995) 617–656.

[82] **TASSO** Collaboration, R. Brandelik *et al.*, "Evidence for Planar Events in e+ e- Annihilation at High-Energies," *Phys. Lett. B* **86** (1979) 243–249.

[83] D. P. Barber *et al.*, "Discovery of Three Jet Events and a Test of Quantum Chromodynamics at PETRA Energies," *Phys. Rev. Lett.* **43** (1979) 830.

[84] **PLUTO** Collaboration, C. Berger *et al.*, "Evidence for Gluon Bremsstrahlung in e+ e- Annihilations at High-Energies," *Phys. Lett. B* **86** (1979) 418–425.

[85] **JADE** Collaboration, W. Bartel *et al.*, "Observation of Planar Three Jet Events in e+ e- Annihilation and Evidence for Gluon Bremsstrahlung," *Phys. Lett. B* **91** (1980) 142–147.

[86] J. D. Bjorken, "Asymptotic Sum Rules at Infinite Momentum," *Phys. Rev.* **179** (1969) 1547–1553.

[87] W. K. H. Panofsky, "Low q electrodynamics, elastic and inelastic electron (and muon) scattering," in *14th International Conference on High Energy Physics*, pp. 23–42. 1968.

[88] R. E. Taylor, "Inelastic electron - proton scattering in the deep continuum region," *Conf. Proc. C* **690914** (1969) 251–260.

[89] R. E. Taylor, "Deep inelastic scattering: The Early years," *Rev. Mod. Phys.* **63** (1991) 573–595.

[90] H. W. Kendall, "Deep inelastic scattering: Experiments on the proton and the observation of scaling," *Rev. Mod. Phys.* **63** (1991) 597–614.

[91] J. I. Friedman, "Deep inelastic scattering: Comparisons with the quark model," *Rev. Mod. Phys.* **63** (1991) 615–629.

[92] R. P. Feynman, "Very high-energy collisions of hadrons," *Phys. Rev. Lett.* **23** (1969) 1415–1417.

[93] R. P. Feynman, "Photon-hadron interactions,".

[94] C. G. Callan, Jr. and D. J. Gross, "High-energy electroproduction and the constitution of the electric current," *Phys. Rev. Lett.* **22** (1969) 156–159.

[95] F. Halzen and A. D. Martin, *QUARKS AND LEPTONS: AN INTRODUCTORY COURSE IN MODERN PARTICLE PHYSICS*. 1984.

[96] R. L. Jaffe, "Spin, twist and hadron structure in deep inelastic processes," in *Ettore Majorana International School of Nucleon Structure: 1st Course: The Spin Structure of the Nucleon*, pp. 42–129. 1, 1996. arXiv:hep-ph/9602236.

[97] E. Leader and E. Predazzi, *An Introduction to gauge theories and modern particle physics. Vol. 1: Electroweak interactions, the new particles and the parton model*. Cambridge University Press, 4, 2011.

[98] Y. L. Dokshitzer, "Calculation of the Structure Functions for Deep Inelastic Scattering and e+ e- Annihilation by Perturbation Theory in Quantum Chromodynamics.," *Sov. Phys. JETP* **46** (1977) 641–653.

[99] V. N. Gribov and L. N. Lipatov, "Deep inelastic electron scattering in perturbation theory," *Phys. Lett. B* **37** (1971) 78–80.

[100] G. Altarelli and G. Parisi, "Asymptotic Freedom in Parton Language," *Nucl. Phys. B* **126** (1977) 298–318.

[101] **Particle Data Group** Collaboration, M. Tanabashi *et al.*, "Review of Particle Physics," *Phys. Rev. D* **98** (2018) no. 3, 030001.

[102] M. Miyama and S. Kumano, "Numerical solution of Q**2 evolution equations in a brute force method," *Comput. Phys. Commun.* **94** (1996) 185–215, arXiv:hep-ph/9508246.

[103] A. Grozin, *Lectures on QED and QCD*. 8, 2005. arXiv:hep-ph/0508242.

[104] C. Itzykson and J. B. Zuber, *Quantum Field Theory*. International Series In Pure and Applied Physics. McGraw-Hill, New York, 1980.

[105] M. Tissier and N. Wschebor, "Infrared propagators of Yang-Mills theory from perturbation theory," *Phys. Rev. D* **82** (2010) 101701, arXiv:1004.1607 [hep-ph].

[106] P. Dall'Olio and A. Weber, "Exploiting the scheme dependence of the renormalization group improvement in infrared Yang-Mills theory," arXiv:2012.02389 [hep-th].

[107] E. V. Shuryak and T. Schäfer, "The QCD vacuum as an instanton liquid," *Ann. Rev. Nucl. Part. Sci.* **47** (1997) 359–394.

[108] A. E. Dorokhov and L. Tomio, "Pion structure function within the instanton model," *Phys. Rev. D* **62** (2000) 014016.

[109] Y. Ninomiya, W. Bentz, and I. C. Cloët, "Transverse-momentum-dependent quark distribution functions of spin-one targets: Formalism and covariant calculations," *Phys. Rev.* **C96** (2017) no. 4, 045206, arXiv:1707.03787 [nucl-th].

[110] L. Chang, C. Mezrag, H. Moutarde, C. D. Roberts, J. Rodríguez-Quintero, and P. C. Tandy, "Basic features of the pion valence-quark distribution function," *Phys. Lett. B* **737** (2014) 23–29, arXiv:1406.5450 [nucl-th].

[111] C. S. R. Costa and G. Krein, "Minkowski space quark propagator in the light-cone gauge," *Work in progress* (2021) .

[112] V. Sauli, "Confined gluon from Minkowski space continuation of PT-BFM SDE solution," *J. Phys.* **G39** (2012) 035003, arXiv:1102.5765 [hep-lat].

[113] J. P. B. C. de Melo, R. M. Moita, and T. Frederico, "Pion observables with the Minkowski Space Pion Model," *PoS* **LC2019** (2019) 037, arXiv:1912.07459 [hep-ph].

[114] W. de Paula, E. Ydrefors, J. H. Alvarenga Nogueira, T. Frederico, and G. Salmè, "Observing the Minkowskian dynamics of the pion on the null-plane," *Phys. Rev. D* **103** (2021) no. 1, 014002, arXiv:2012.04973 [hep-ph].